AN ABSTRACT OF THE THESIS OF

Michael J. Britch for the degree of Master of Science in Civil Engineering presented on July 24, 1990.

Title: Watershed Modeling at Yucca Mountain, Nevada

Abstract Approved: Redacted for Privacy

Jonathan D. Istok

Studies are currently underway to determine the suitability of Yucca Mountain in Nevada as the nation's first high-level nuclear waste repository. Values of net infiltration are required to determine pre-waste emplacement groundwater travel times and the performance of the repository as a waste containment system. The objective of this study was to develop a numerical model to perform water balance calculations and predict rates of net infiltration for the site. The model included processes of precipitation, runoff, evapotranspiration, infiltration, and redistribution of water within a soil profile. The watershed was divided into 477 grid cells 75.7 x 75.7 m. The elevation, slope, aspect, and hydrologic properties were assumed to be constant within a grid cell but varied from one cell to the next. Water balance calculations were performed for each cell using a one-dimensional form of Richards equation. The solution was obtained using the finite difference method with Newton-Raphson iteration.

The model was calibrated using water content data obtained from neutron-moisture meter measurements in boreholes located in Pagany Wash Watershed. Measurements were made in channel and terrace alluvium and in tuffs. Computer simulations reproduced water content data for a major precipitation event that occurred in 1984. Simulations verified the importance of antecedent soil water content in controlling the occurrence of runoff. Sensitivity analysis indicated that the soil and alluvium grain-size distributions, which are used to calculate unsaturated hydraulic conductivity, can greatly affect predicted rates of water movement.

Watershed Modeling at Yucca Mountain, Nevada

by

Michael J. Britch

A THESIS

submitted to

Oregon State University

in partial fulfillment of
the requirements for the
degree of

Master of Science

Completed July 24, 1990

Commencement June 1991

APPROVED:

Redacted for Privacy

Associate Professor of Civil Engineering in charge of major

Redacted for Privacy

Chairman of Civil Engineering Department

Redacted for Privacy

Dean of Graduate School

Date thesis is presented July 24, 1990

Typed by Ann Daggett for Michael J. Britch

TABLE OF CONTENTS

LIST OF FIGURES

LIST OF TABLES

WATERSHED MODELING AT YUCCA MOUNTAIN, NEVADA

INTRODUCTION

High-level radioactive waste is accumulating in the United States. In 1983, there were about 4,600 m^3 (160,000 ft^3) of spent fuel from commercial nuclear power plants in the United States. It is estimated that this volume will increase to over 19,000 m^3 (670,000 ft^3) by the year 2000 and to over 33,000 m^3 (1,200,000 ft^3) by the year 2010 (Weber and Wiltshire, 1985). In 1982, Congress passed the Nuclear Waste Policy Act. This legislation authorized the Department of Energy (DOE) to investigate several sites for possible use as deep geologic repositories. In addition, the DOE was to oversee design, construction, and operation of two repositories. Out of nine sites initially selected, three were nominated by the DOE for further site characterization. These included a site in Deaf Smith County on the Texas panhandle, the Hanford site in Washington, and Yucca Mountain in Nevada. In 1987, as part of amendments to the Nuclear Waste Policy Act, site characterization was limited to Yucca Mountain.

At Yucca Mountain, the potential repository host rock is in the Topopah Spring member of the Paint Brush tuff formation, a densely welded and fractured volcanic tuff. The water table is about 510 m (1,700 ft) below the land surface. The proposed location of the repository is in the unsaturated zone about 300 m (1,000 ft) beneath the land surface. Initially, the repository was to be located in the saturated zone. However, due to potential difficulties arising from retrieval of radioactive wastes and the desire to limit radionuclide contact with regional groundwater among other issues, the proposed repository horizon was moved to the unsaturated zone (Roseboom, 1983).

As part of the licensing process, the DOE must project the performance of the repository for 10,000 years considering the full range of environmental conditions that may affect the repository during that time (Justus and Stablein, 1987). To attain safe storage, the design relies on the site's natural processes to isolate the waste. Assuming a release of the radioactive material from the waste canisters to have occurred, one possible mechanism for radionuclide transport is advection by the unsaturated flow of water. To evaluate and quantify the significance of radionuclide transport through the tuff, knowledge of the boundary conditions in the unsaturated zone is required. The lower boundary condition is controlled by the elevation of the regional water table. The

upper boundary condition is controlled by the rate of recharge (net infiltration) of water at the soil surface.

Several estimates of net infiltration have been suggested for Yucca Mountain and the vicinity. Winograd and Thordarson (1975) used measurements of discharge from springs at Ash Meadows (south of Yucca Mountain near the Nevada-California border) to estimate net infiltration for the lower carbonate aquifer. They estimated that about 3 percent of the precipitation falling on carbonate-rock uplands within the boundaries of the Ash Meadows basin becomes net infiltration. Watson et al. (1976) investigated the Maxey-Eakin method (Maxey and Eakin, 1949) of estimating net infiltration to groundwater basins in Nevada. With the Maxey-Eakin method, average annual precipitation (AAP) is used to classify areas of a basin into five zones. Estimates of annual net infiltration for each zone were obtained by applying a scaling factor to AAP (Table 1).

Table 1. Predicted values of net infiltration by Maxey-Eakin method.

Average annual precipitation (cm)	Average annual precipitation (in)	Predicted Net Infiltration (% of AAP)
>50.8	>20.0	25
38.1-50.8	15.0-20.0	15
30.5-38.1	12.0-15.0	7
20.3-30.5	8.0-12.0	3
<20.3	<8.0	0

Czarnecki (1984), in a study of the effects of possible increases in net infiltration on the groundwater flow system at Yucca Mountain and vicinity, used estimates of net infiltration based on the Maxey-Eakin method. Czarnecki separated the area into three zones based on values of AAP. Estimated rates of net infiltration ranged between 0 and 2.0 mm/yr (0 and 0.08 in/yr). Rush (1970) also used this method to estimate net infiltration for the western two-thirds of Jackass Flats (about 6.5 km east of Yucca Mountain) to be about 1.5 mm/yr (0.059 in/yr).

Assuming steady-state conditions, Winograd (1981) estimated net infiltration through the unsaturated valley fill at Sedan Crater, about 48 km (30 miles) northeast of Yucca Mountain, to be about of 2 mm/yr (0.08 in/yr).

Scott et al. (1983) developed a conceptual hydrologic model of Yucca Mountain. They estimated net infiltration to be 6 mm/yr (0.2 in/yr); 3 percent of an AAP value of 20 cm/yr (8 in/yr). Montazer and Wilson (1984) developed a conceptual hydrologic model similar to Scott et al. (1983). In their model, they also assumed 3 percent of the precipitation as net infiltration but used different values for AAP. They suggested 4.5 mm/yr (0.18 in/yr) as a upper estimate on net infiltration at Yucca Mountain.

Net infiltration estimates for basins in Nevada have also been obtained using chloride-balance calculations. Dettinger (1989) applied this method to sixteen basins in Nevada. His estimates compared closely to those obtained using the Maxey-Eakin method and water balance calculations. Dettinger (1989) states that the chloride-balance method is practical, at a reconnaissance level, for estimating average rates of net infiltration for many desert basins of the western United States.

An alternative approach for estimating net infiltration is to perform water balance calculations. Nichols (1987) used a numerical model to perform water balance calculations for the unsaturated zone at a burial site for low-level radioactive waste near Beatty, Nevada. His model was used to determine under what conditions net infiltration might have occurred during a 15 year study period. Nichols (1987) estimated a rate of net infiltration of 0.04 mm/yr (0.002 in/yr). Additionally, experiments at Jackass Flats suggested that downward movement of water below the upper 0.5 m (1.7 ft) did not occur until the soil reached a saturation of about 50 percent (Nichols, 1987).

To obtain rates of net infiltration using water balance calculations requires hydrologic data, an understanding of the processes involved, numerical models for each of these processes, and the ability to link these processes together and keep mass balance errors within desired tolerances. The processes include precipitation, evapotranspiration, runoff, and infiltration and redistribution of the soil moisture. It is also important to consider the variability of these processes in space and time.

The objective of this study was to develop and calibrate a numerical model based on textural parameters to perform water balance calculations for Yucca Mountain. A sensitivity analysis is performed to determine the sensitivity of water balance calculations to variation in model parameters. In a future study the calibrated model will be used to predict rates of net infiltration for Yucca Mountain.

STUDY AREA

Yucca Mountain is located in Nye County, Nevada about 160 km (100 miles) northwest of Las Vegas, Nevada. Yucca Mountain lies within the Upper Amargosa River Watershed (UARW) (Figure 1). The study area is Pagany Wash Watershed, located east of Yucca Mountain's ridge line (Figures 2 and 3). Pagany Wash Watershed is representative of Yucca Mountain. Pagany Wash Watershed is a small (about 2.7 km^2 or 1.1 mi^2), narrow watershed, that descends towards the southeast. It contains a channel bed that extends about 3.6 km (2.3 miles) up from the watershed outlet. For the purposes of this study, the outlet of the watershed was located at an elevation of 1151 m (3800 ft) (Figure 2). Near the watershed outlet, the watershed widens, creating terrace areas adjacent to the channel. About 2.7 km (1.7 miles) up from the outlet the channel forks to the west. The side slopes adjacent to the channel are typically steep, with slopes greater than 20 degrees. Slopes along the channel and above the steep sides are generally much less.

Climate

Weather patterns within the study area vary seasonally. Average monthly precipitation (1978 - 1988) for three selected weather stations show the trends (Figure 4). Most precipitation occur from July to September and from November to April; the maximum amount occurs in March.

Summer precipitation primarily comes from the south and southeast. The southerly winds carrying the summer precipitation tend to curve east over southern Nevada (French, 1983). Below 38°30'N latitude, southern Nevada can be divided into deficit and excess zones of precipitation with an indefinite transition zone which covers the Nevada Test Site (NTS) and Yucca Mountain (French, 1983). Generally, stations east of longitude 115°45'W receive from 1.5 to 2.5 times more precipitation than stations at similar altitudes located west of longitude 116°45'W (Winograd and Thordarson, 1975).

Average annual precipitation (AAP) varies considerably throughout the study area. AAP for the Death Valley, California, weather station is 5.99 cm (2.36 in). AAP for the Beatty, Nevada, station is 16.6 cm (6.52 in). The most recent estimate of AAP at Yucca Mountain is 15.1 cm (5.94 in) (Hevesi, 1990). The Spring Mountains in the southeast of the study area are an exception to the region's typically arid climate; precipitation here generally ranges from 25 cm (10 in) at lower elevations to 76 cm (30

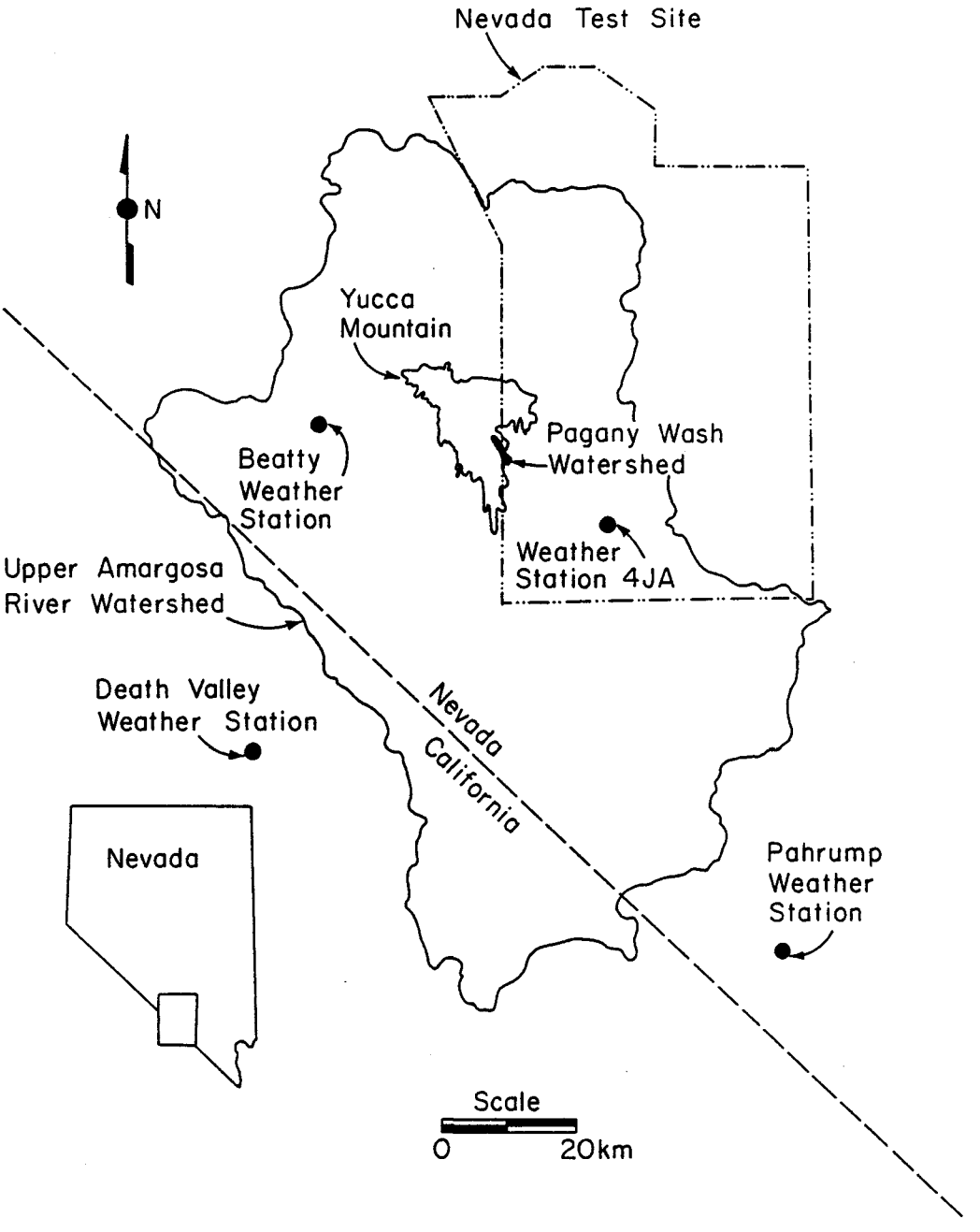

Figure 1. Location of study area

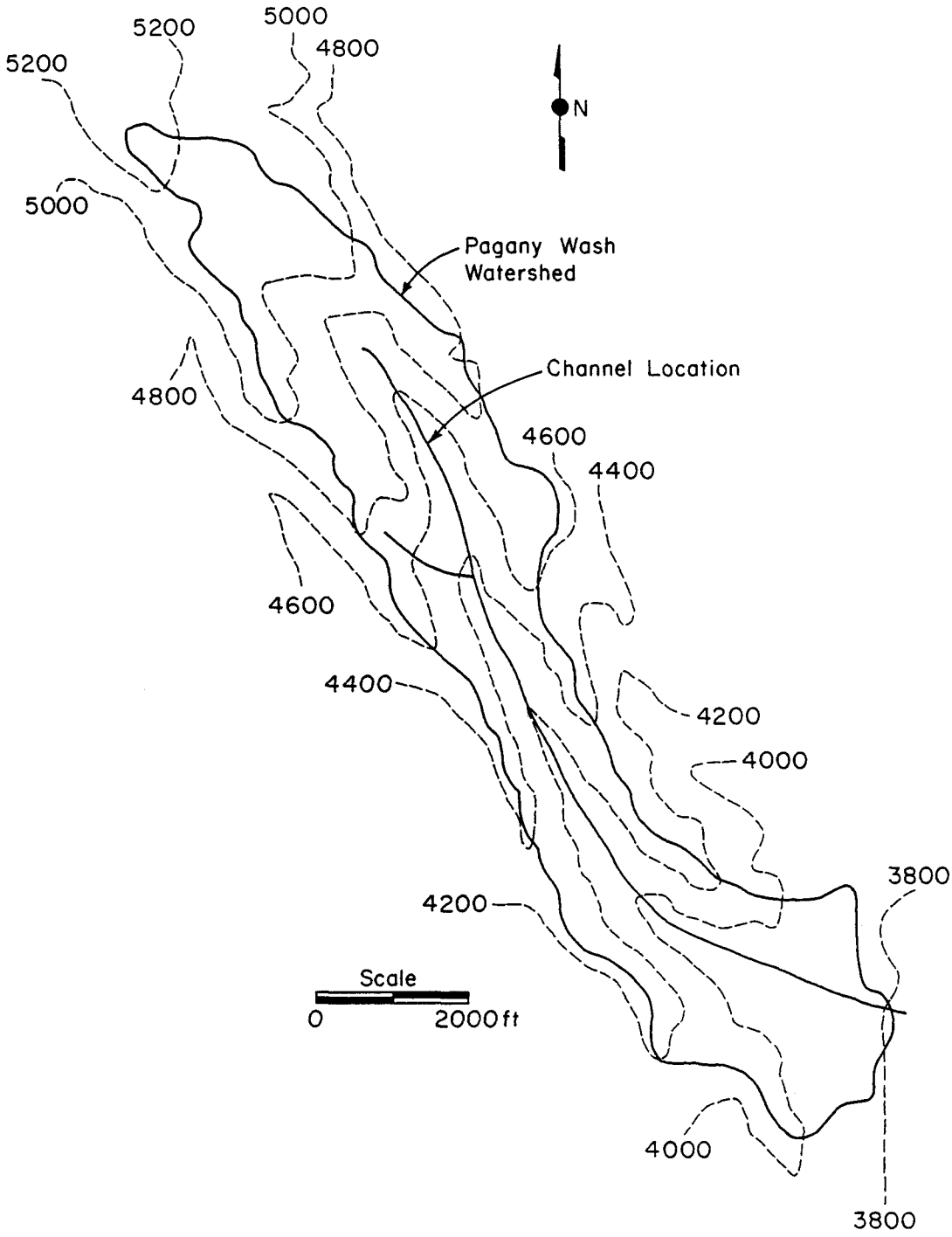

Figure 2. Pagany Wash Watershed

Figure 3a. Pagany Wash Watershed; looking upstream near watershed outlet

Figure 3b. Pagany Wash Watershed; view of channel in lower portion of watershed

Figure 3c. Pagany Wash Watershed; looking upstream near neutron-access hole N-1

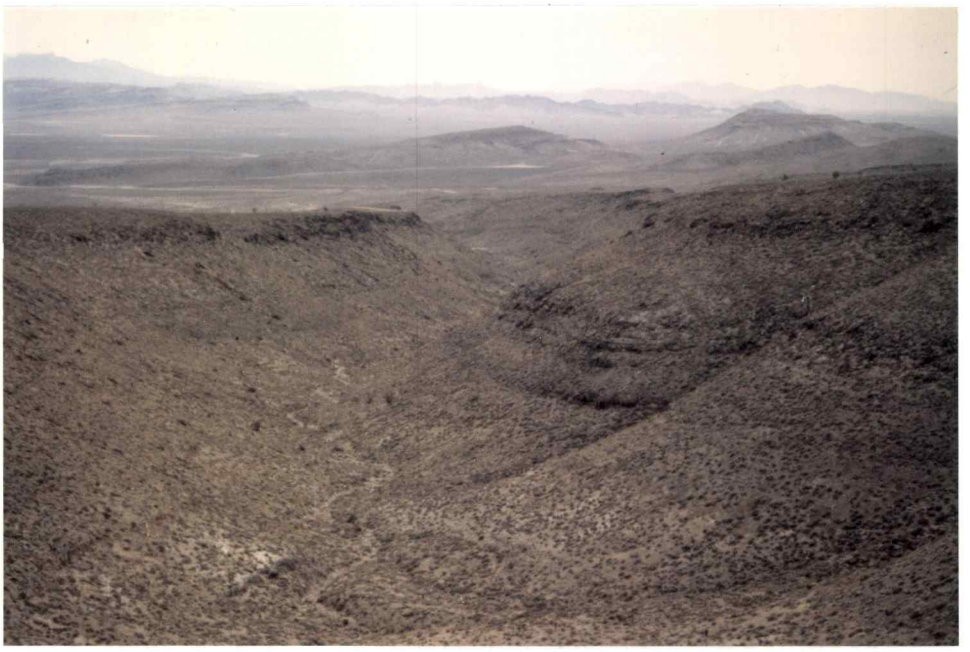

Figure 3d. Pagany Wash Watershed; looking downstream from watershed boundary

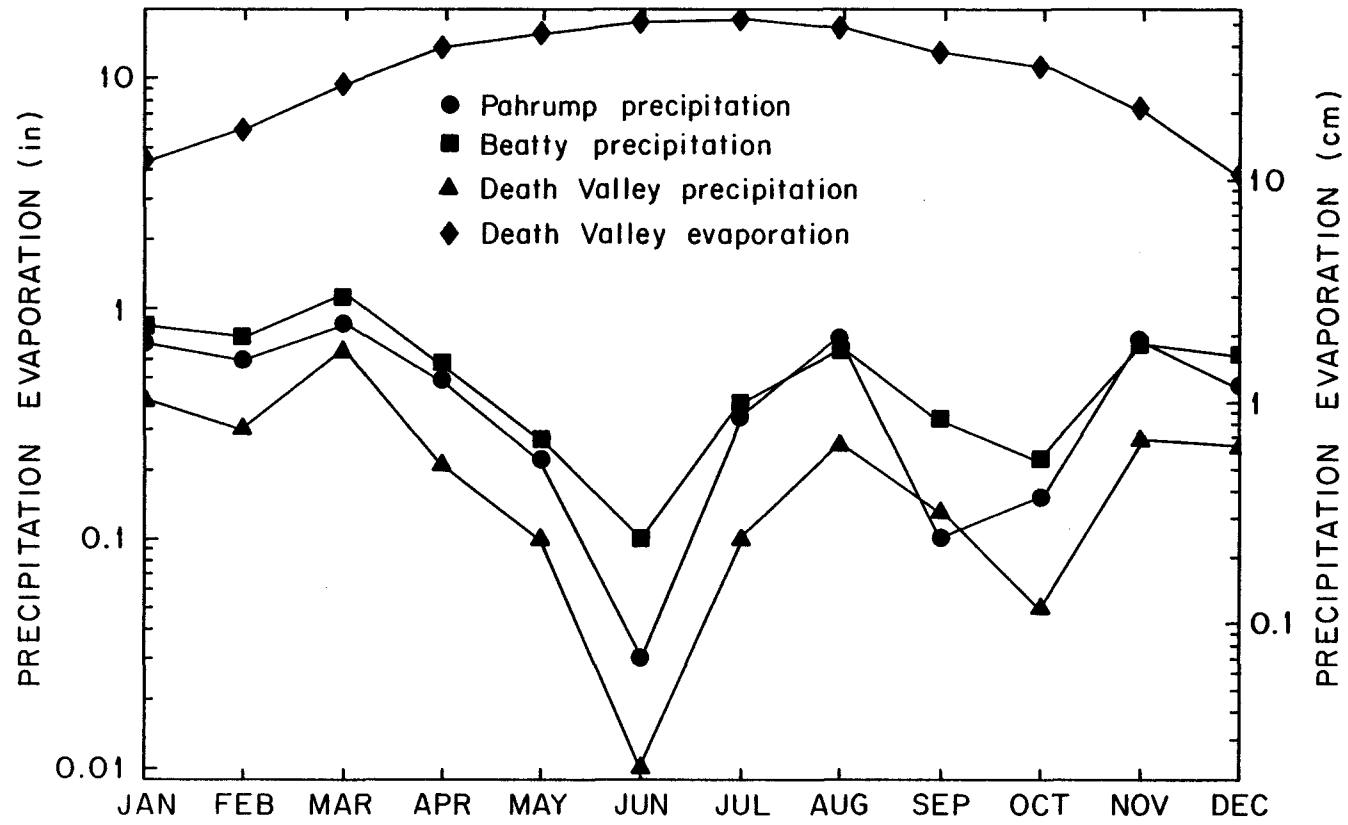

Figure 4. Average monthly precipitation and evaporation

in) on the highest peaks where as much as one-third of AAP occurs as snowfall (Winograd and Thordarson, 1975).

Monthly pan evaporation rates are very large; exceeding monthly precipitation rates (Figure 4). The average annual pan evaporation at Death Valley is 341 cm (134 in). Average monthly temperatures (AMTs) for the study area are high (Figure 5), generally highest during July and lowest in December.

Soils

For the purposes of this study, the soils in the watershed were classified into two groups: upland soils and alluvium. The upland soils cover about 90 percent of the watershed including the steep side slopes, plateau areas at the top of the steep side slopes, and the valley floor above about the lower 1.6 km (1 mile) of channel. Alluvium occurs in the lower portion of the watershed.

Schmidt (1988) further classified the upland soils into four mapping units based on geomorphic characteristics and soil physical properties. Schmidt described the upland soils as gravelly to very gravelly sandy loam with loamy skeletal inclusions. Organic matter contents are low (0.39 to 1.68%). Schmidt recorded volumetric rock contents generally above the limit for skeletal soils (35%), and as high as 59.6%. Measured total soil thicknesses were between 0.10 and 2.4 meters (0.33 and 7.9 ft). Using a method based on textural analysis, Schmidt estimated saturated hydraulic conductivities of the soils in the four units to range between 1.93 and 2.11 cm/hr (0.76 and 0.83 in/hr). Due to the similarities in hydraulic conductivities, Schmidt postulated that upland soils would behave similarly with respect to infiltration.

Grain-size analysis data from Schmidt (1988) were used to obtain the hydraulic properties for upland soils for use in the computer model (Figure 6). Grain-size distributions were also used to estimate the hydraulic properties of the alluvium. Alluvium samples weighing between 8 and 10 kg (18 and 22 lb) were obtained from the channel and adjacent terrace area using a shovel. The samples were oven-dried and sieved using a mechanical shaker. The proportion of silt and clay were determined using the hydrometer method (Gee and Bauder, 1986).

Surface Tuff

Tuff underlies the surface soils and also occurs at the surface in numerous outcrops. The tuff is characterized as either the bedded unit, the Tiva Canyon welded unit, the Tiva Canyon nonwelded unit, or the Timber Mountain nonwelded unit (Scott and Bonk, 1984). The depth of the tuff-alluvium contact ranges from zero to about

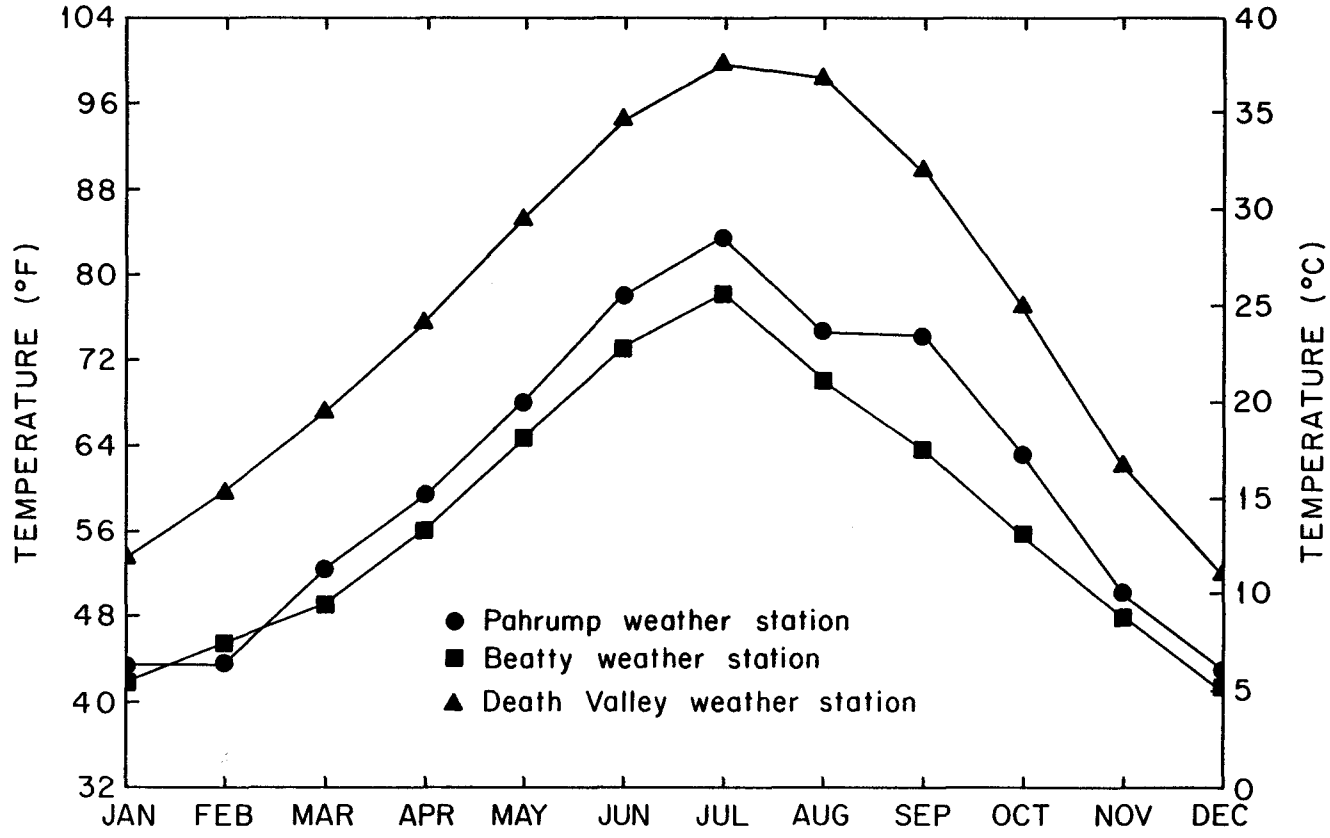

Figure 5. Average monthly temperature

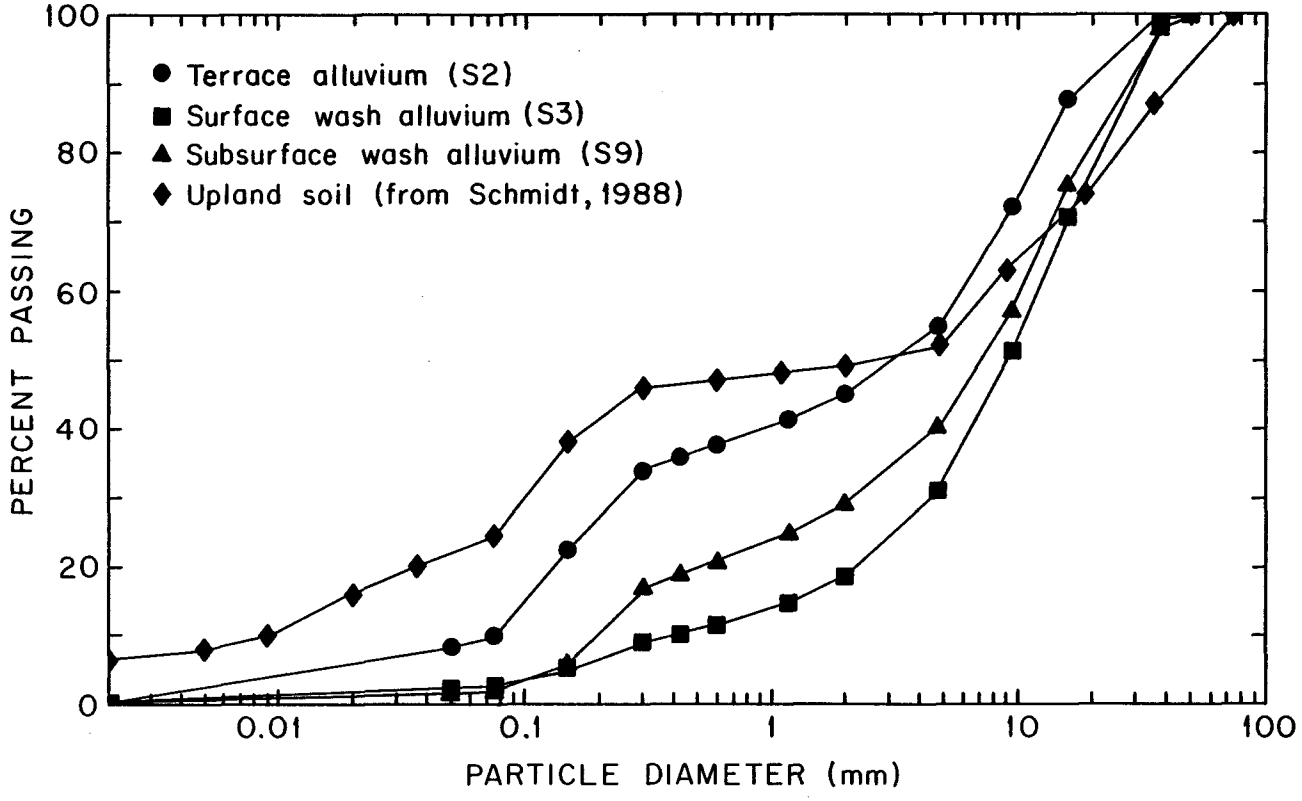

Figure 6. Grain-size distributions for upland soils and alluvium

13.6 m (45.0 ft). Hydraulic properties for the tuff were obtained from Flint and Flint (1990). Saturated hydraulic conductivities ranged from 1.8×10^{-6} cm/hr (7.1×10^{-7} in/hr) in the Tiva Canyon welded unit to 0.17 cm/hr (6.7×10^{-2} in/hr) for the Tiva Canyon nonwelded unit.

CONCEPTUAL MODEL OF PROCESSES

Hydrologic System

This study is concerned with the near-surface (from the surface to a depth of about 15 m or 50 ft) hydrologic system at Pagany Wash Watershed. The processes considered include precipitation, evapotranspiration, runoff and channel flow, infiltration, and redistribution of the water in the near-surface unsaturated zone.

Precipitation

During the summer, precipitation frequently occurs as thunderstorms with short durations and high intensities. Precipitation usually occurs in the mid-afternoon, the time of maximum solar heating (Dale Ambos, U.S. Geological Survey, personal communication, 1990). In August of 1984, Pagany Wash experienced two important precipitation events separated by a few days; both events resulted in runoff and channel flow. Precipitation data from the nearest weather station with complete records (4JA, see Figure 1) were used for this study.

Evapotranspiration

Evaporation is the transfer of water from the liquid phase to the vapor phase. Transpiration is the process by which plants remove liquid water from the soil and release it to the air as vapor (Linsley and Franzini, 1979). Evaporation and transpiration can remove large amounts of water from the soil in desert environments. These two processes are often combined into a single term (evapotranspiration or ET) for analysis.

The rate of ET is controlled by meteorological factors, surface characteristics, and soil water status. Meteorological factors include solar radiation, air temperature, vapor pressure, wind, and to a minimal extent atmospheric pressure (Linsley et al., 1982). Solar radiation and air temperature are the important factors controlling rates of ET in the study area. Important surface characteristics include ground slope, aspect, and effects of shading due to blocking ridges.

Soil water status often controls the rate of ET. Water within the soil is transferred to the surface by both liquid and vapor flow. As the surface soil dries, its ability to supply liquid water to the surface decreases in response to the soil's decreasing hydraulic conductivity. Water vapor flow is controlled by the soil's conductivity to vapor and by vapor density and thermal gradients. Thermal gradients are also a factor in liquid flow because of the dependence of liquid water properties on

temperature. Soil temperature fluctuates like air temperature except that the depth of diurnal temperature change is lower in soil because soil has a larger heat capacity than air. During the day when surface temperatures are high, vapor would be expected to move into the soil. During the night when the surface cools, vapor flow moves to the soil surface, where it condense and replenishing the liquid water removed by ET during the previous day.

Runoff and Channel Flow

Runoff (overland flow) and channel flow are important processes for moving water at Pagany Wash Watershed. Runoff and channel flow occur only when precipitation intensity is high and/or the antecedent (prior to the storm) water content of the soils on the watershed is large. A large antecedent water content increases the potential for runoff and overland flow due to a decrease in the soil's water storage capacity. A small soil depth also increases the potential for runoff due to a decrease in the soil's water storage capacity. In many areas along the soil depth is zero and the surface consists entirely of tuff. Since the tuff's ability to accept water is small due to its very low hydraulic conductivity, it is assumed that overland flow is most likely to occur in these areas.

Infiltration

Infiltration is the movement of water through the soil surface and into the soil (Linsley and Franzini, 1979). The maximum rate at which water can enter the soil is referred to as the soil's infiltration capacity. Many infiltration equations have been developed in an attempt to predict infiltration rates. A comparison of several of these equations are shown in Table 2. Richards equation can also be used to describe the redistribution of water within the soil profile. The upland soils and alluvium have large particle sizes and saturated hydraulic conductivities which result in maximum infiltration rates that exceed precipitation intensities for most precipitation events.

Redistribution

Redistribution of water occurs following precipitation events and in response to diurnal changes in ET. Because the study area is in an arid climate, the soils are almost always unsaturated. Unsaturated flow is difficult to predict and simulate due to the highly nonlinear relationships between matric potential and hydraulic conductivity and between matric potential and volumetric water content. Depending on the soil type,

Table 2. Comparison of infiltration equations*

Equation Name	Requirements	Advantages	Disadvantages
Green-Ampt (1911) $q(t) = K_s(H_o+S_f+L_f)/L_f$	depth of water, H_o wetting front suction, S_f saturated conductivity, K_s	physically based mathematical solution	difficult to determine S_f sharp wetting front not realistic for most soils
Richards (1931)** $\frac{\partial\theta}{\partial t} = \frac{\partial}{\partial z}\left[k(\theta)\left\{ \frac{\partial\psi}{\partial z} + 1 \right\} \right]$	k vs. θ ψ vs. θ	physical basis for infiltration theory	difficult to measure unsaturated properties
Kostiakov (1932) $q(t) = \alpha_1 t^{-\alpha 2}$ (from Haverkamp et al., 1988)	empirical parameters	simple	empirical expression fails as $t \rightarrow \infty$
Horton (1940) $q(t) = \gamma_1 + \gamma_2 \exp(-\gamma_3 t)$ (from Haverkamp et al., 1988)	empirical parameters	simple	empirical expression fails as $t \rightarrow 0$
Philip (1957) $q(t) = 1/2St^{1/2} + A$ (from Haverkamp et al., 1988)	constants S and A	physically based mathematical solution	fails as $t \rightarrow \infty$ ($A \neq K_s$)
Holtan (1961) $q(t) = a(M - I)^n + i_c$ (from Hillel, 1982)	empirical parameters	simple	empirical expression solution not continuous ($q(t) = i_c$ for $I > M$)

*boundary conditions: $\lim_{t \rightarrow 0} I(t) = 0$; $\lim_{t \rightarrow \infty} I(t) = \infty$; $\lim_{t \rightarrow 0} q(t) = \infty$; $\lim_{t \rightarrow \infty} q(t) = \text{constant}$

where I = cumulative volume of water infiltrated; q(t) = dI/dt, surface flux

**solved for vertical flow from Freeze and Cherry (1979)

hysteresis in these relationships can also be important. Hysteresis refers to the observed differences in these relationships for wetting and drying cycles.

Soil Moisture Data

Several neutron-access boreholes were installed in Pagany Wash Watershed beginning in 1984 to measure water content in the alluvium and tuff. Neutron-access holes were located at various sites in the channel, terrace, and adjacent tuff (Figure 7a). At one location, the neutron holes were aligned perpendicular to the channel (Figure 7b). Neutron-access holes N-2 through N-9 comprise the perpendicular section. N-10 roughly marks the upper extent of the alluvium. N-13 and N-14 lie just above the watershed outlet.

Watershed Response to Precipitation Events

Simulations for much of this study were focused on neutron logging data from N-7 located in middle of the channel at the cross-section shown in Figure 7b. Measurements at N-7 were performed several times following the August 1984 precipitation events (Figure 8). To simplify interpretation of the N-7 data, a five point moving average smoothing was performed. To show the response of the soil profile to precipitation events, the water content data are presented as "relative water content". Relative water contents are computed by subtracting water content measurements for July 26, 1984 from the measurements for each subsequent date. The area beneath plots of relative water content represents the amount of water entering (or leaving) the soil profile.

Between August 14 and 16, 2.13 cm (0.84 in) of precipitation occurred. However, analysis of the water content data for N-7 indicated an increase of 5.15 cm (2.03 in) in the amount of water stored in the profile (Figure 8). The additional 3.02 cm (1.19 in) increase in storage is attributed to infiltration of water from the channel. It is believed that channel flow resulted from runoff from the steep side slopes with small or no soil cover.

Similarly, between August 18 and 19, 2.29 cm (0.90 in) of precipitation occurred followed by an increase of 20.15 cm (7.43 in) in the amount of water stored in the profile at N-7 (Figure 8). The additional 17.86 cm (7.03 in) of water is attributed to infiltration of water from the channel. Channel discharge was observed to occur for a period of 30 to 60 minutes during the precipitation event with an estimated peak

discharge of 4.3 m^3/s (150 ft^3/s) (Alan Flint, U.S. Geological Survey, personal communication, 1990).

The relative water content profiles (Figure 9) show a sharp increase at a depth of about 2.2 m (7.3 ft) and it appears that only a small amount of water moved below this depth after August 20. Above the 2.2 m (7.3 ft) depth, it appears that a large decrease in water storage occurs after the August 20 logging due to ET. Based on this analysis, it is believed that the N-7 profile consists of a heterogeneous soil system, with a highly conductive, coarse-textured layer overlying a less conductive layer that retards the movement of water below a depth of about 2.2 m (7.3 ft).

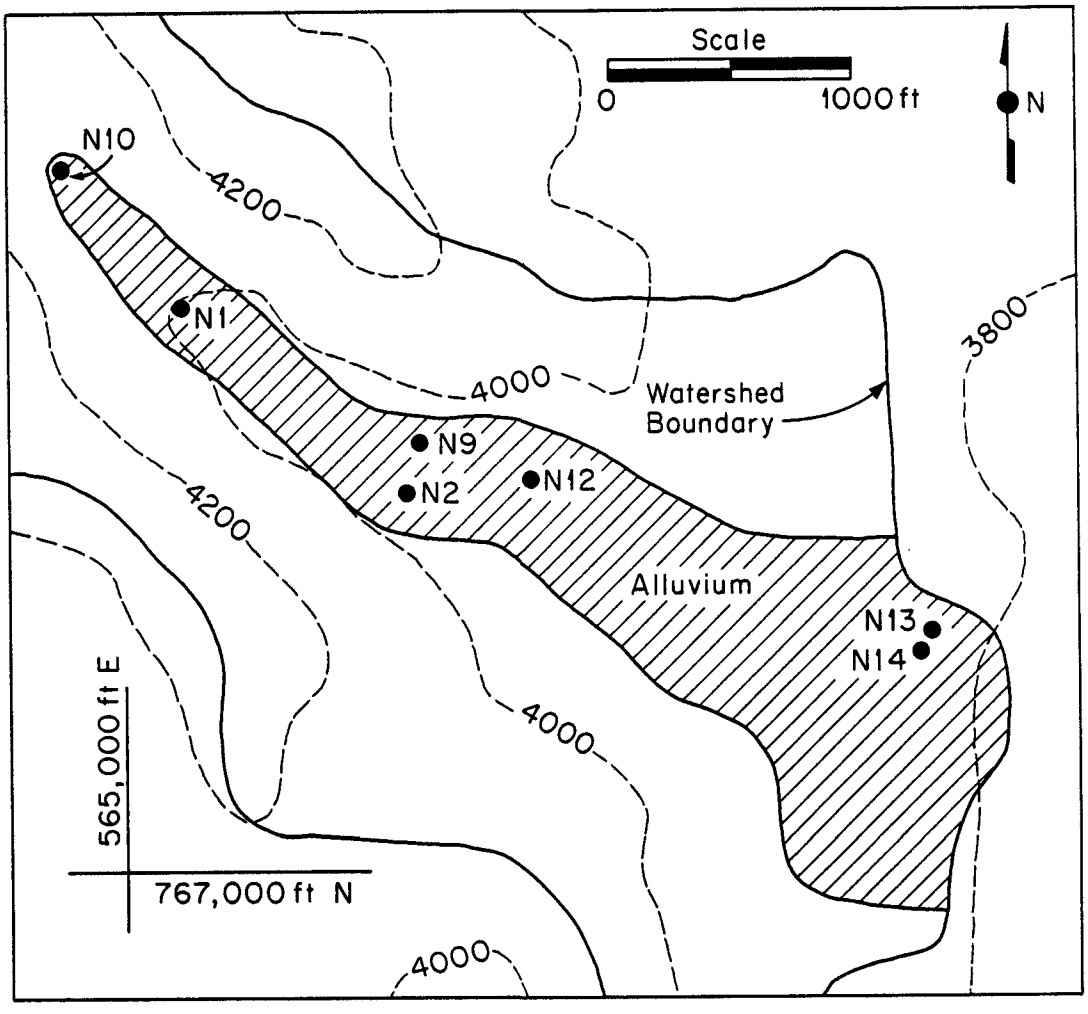

Figure 7a. Location of neutron-access holes

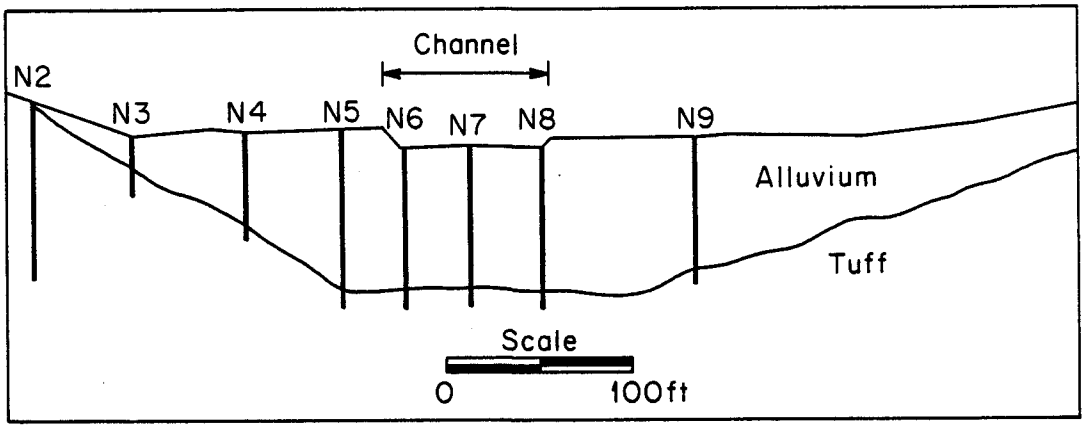

Figure 7b. Cross-section of watershed at location of neutron-access holes N2 to N9

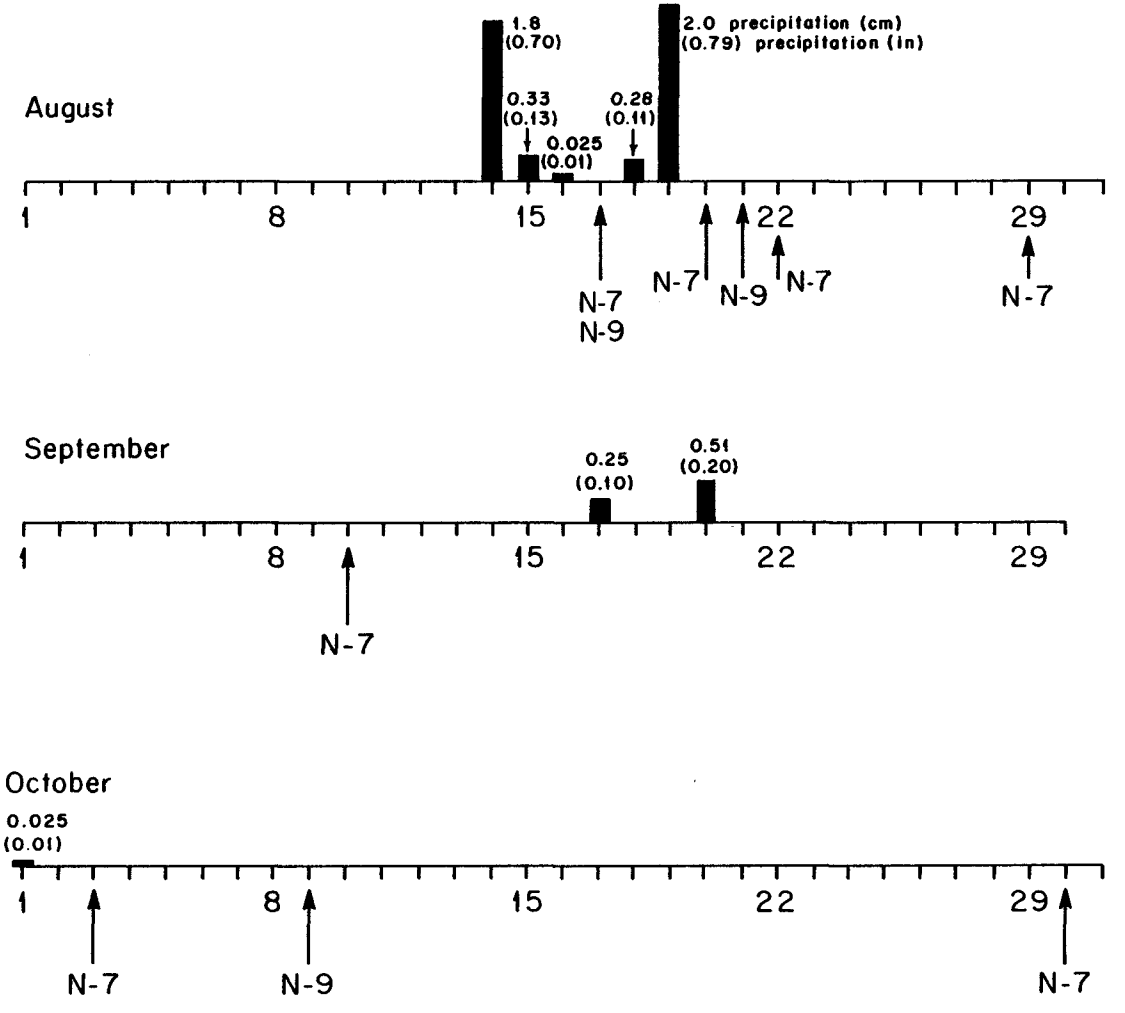

Figure 8. Precipitation data for August to October, 1984

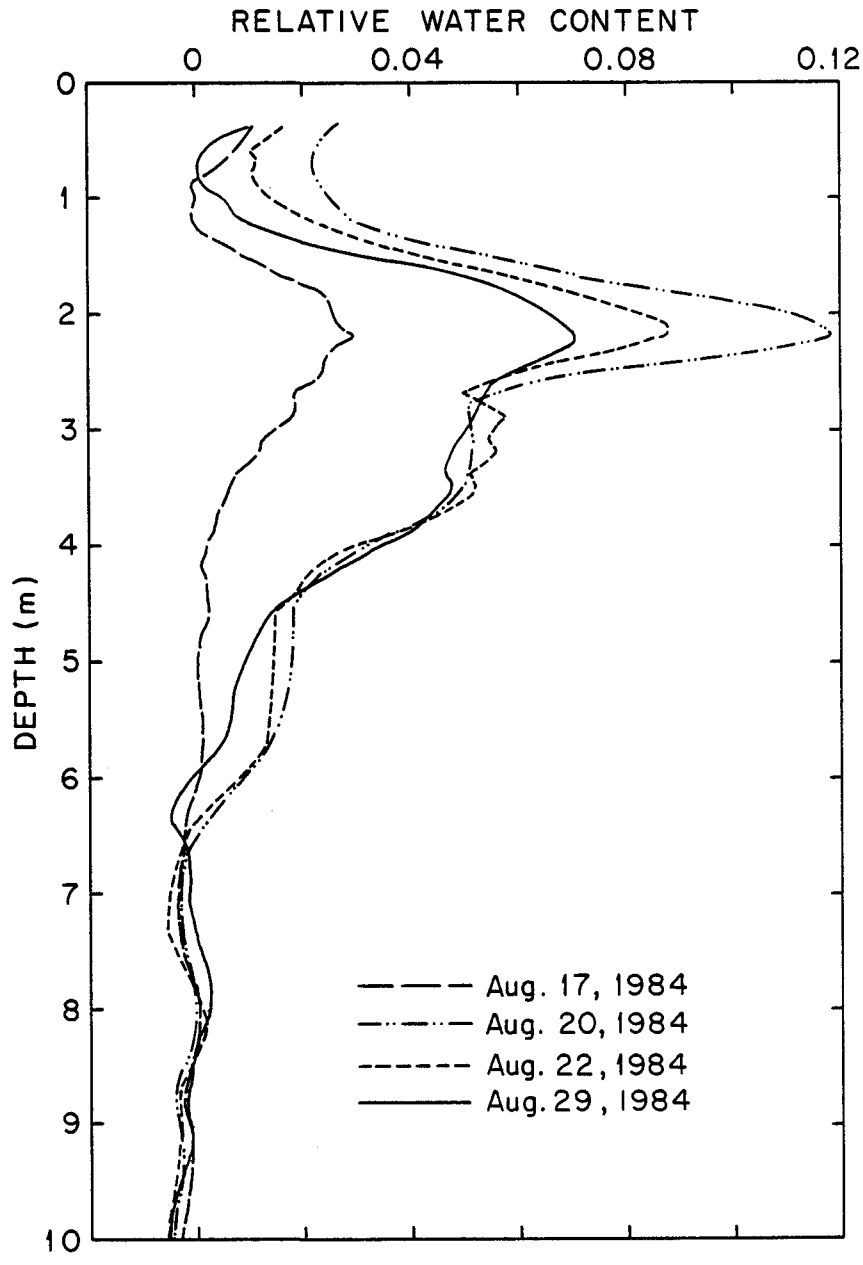

Figure 9. Relative water contents for neutron-access hole N-7

NUMERICAL MODEL

Hydrologic characteristics of the watershed vary spatially. For this reason, the watershed was divided into 477 square panels or grid cells 75.7 x 75.7 m (250 x 250 ft) (Figure 10). Each grid cell is centered on points (grid points) of known elevation. The parameters within a grid cell (elevation, slope, aspect, soil type, and soil depth) are assumed constant, but are allowed to vary from one cell to the next.

The location of a grid point is specified by its easting (east-west position) and northing (north-south position) as given by the Nevada State Central Coordinate System. Elevation data were obtained in digital form for each grid point from Sandia National Laboratories. The precision of the elevation data was 0.3 m (1 ft). These data were verified by visually comparing a topographic map prepared from the digital elevation data with U.S. Geological Survey (USGS) topographic maps of the area (Busted Butte and Topopah Spring NW; 1:24,000 scale, contour interval 6.1 m or 20 ft). The topographic map was prepared using the program SURFER and plotted as a transparent overlay (Golden Graphics, 1989). Although a few isolated point anomalies were observed, topographic maps prepared from the data showed a very good correlation with the USGS topographic maps.

The land surface of each grid cell is assumed to be a plane defined by the elevation at surrounding grid points. The slope and aspect of the surface plane are required to perform ET calculations and to route overland flow. The slope is the acute angle formed by the intersection of the surface plane and the horizon. The aspect is the bearing of a horizontal line in the surface plane. Aspect is orientated in the clockwise direction with 360° corresponding to North 0° East.

To compute slope and aspect of the surface plane for a grid cell, the elevations at the midpoints of each of the sides of the cell were first calculated. The difference between these elevations for a given coordinate direction was used to compute the component of slope for that direction. The resultant slope of a grid cell is calculated by taking the square root of the sum of the squares of the two slope components. The arctangent of the resultant slope gives the slope of the plane.

Precipitation

Daily precipitation was available for station 4JA (Figure 1). All precipitation events were assumed to begin at 15:00. The precipitation was applied at an intensity of 5 cm/hr (2 in/hr).

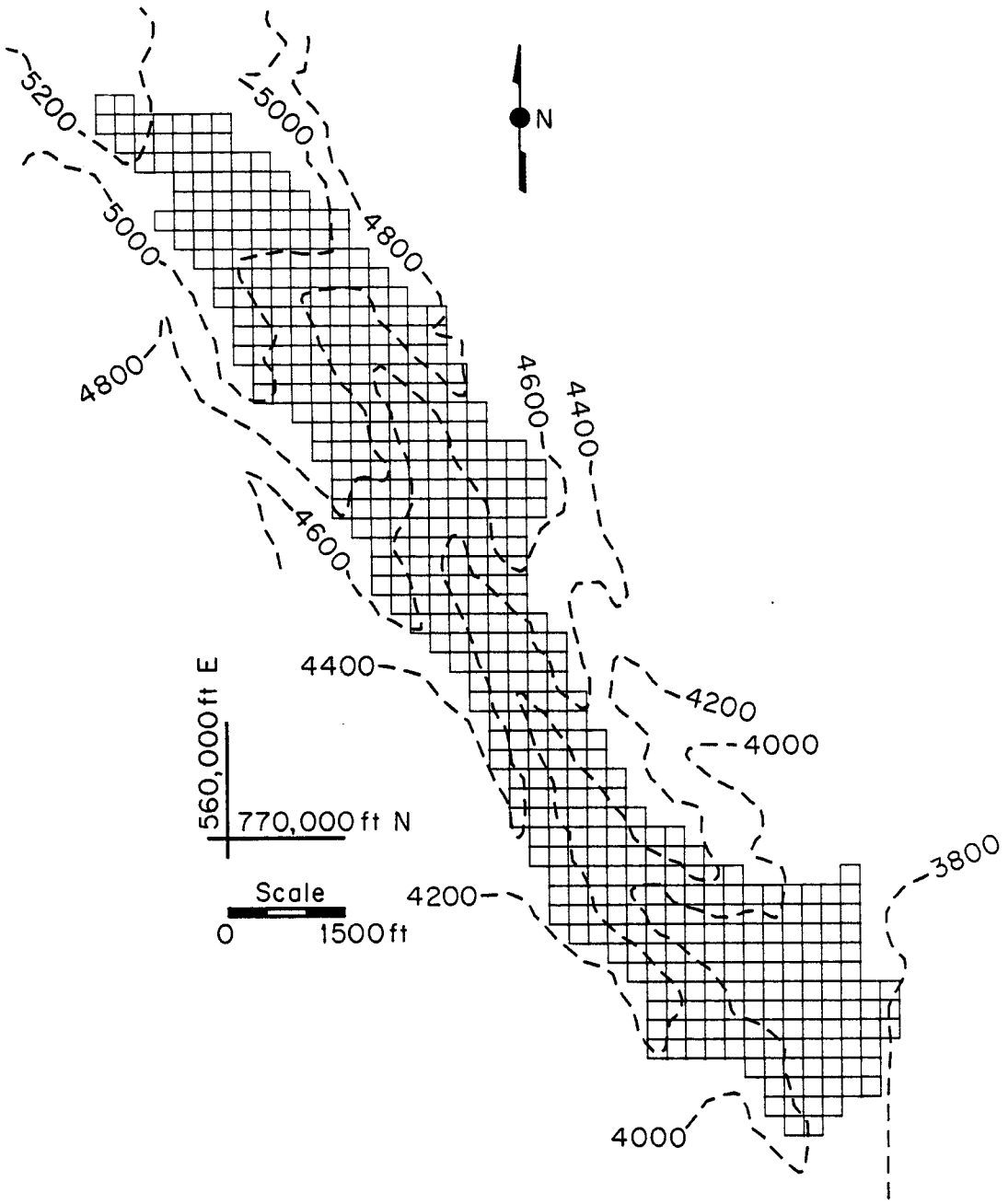

Figure 10. Collection of grid cells used to model hydrologic processes

Evapotranspiration

Daily values of ET were calculated using an equation developed by Priestly and Taylor (1972) where the evaporation rate (E) is given by

$$\lambda E = \alpha\left(\frac{s}{s+\gamma}\right)(R_n - G) \quad (1)$$

where λ is the latent heat of vaporization, α is a model coefficient, s is the slope of the saturation-vapor-density curve, γ is the psychrometric constant, R_n is net radiation, and G is the soil heat flux which is assumed negligible over the diurnal cycle. The Priestly-Taylor coefficient, α, was determined to be 1.26 for freely evaporating surfaces (Priestly and Taylor, 1972). Flint and Childs (1987) redefined α as α', making it a function of soil water content. The new coefficient, α', was found to be also a function of air temperature and water vapor density and is independent of R_n and G. Modifications were made (Alan Flint, U.S. Geological Survey, personal communication, 1990) to formulate α' as

$$\alpha' = A[1 - \exp(B \cdot \chi)] \quad (2)$$

$$\chi = \frac{(\theta - \theta_r)}{(\theta_s - \theta_r)} \quad (3)$$

where A and B are regression coefficients, χ is the relative water saturation, θ is the soil water content, θ_r is the residual soil water content, and θ_s is the soil water content at saturation. The residual soil water content is used to represent the water content in the soil at which no further evaporation can occur. For most simulations in this study, θ_r was set to 0.04.

The $s/(s+\gamma)$ term in equation 1 was solved by using linear regression based on air temperature from Campbell (1977)

$$\frac{s}{s+\gamma} = -44.957 - 0.13318(T + 273.15) + 4.9452(\sqrt{T + 273.15}) \quad (4)$$

where T is of air temperature in degrees Celsius. Air temperature for equation 4 is obtained using another regression equation (Ann Ritcey and Alan Flint, U.S. Geological Survey, personal communication, 1990).

$$T = -0.97292 + 20.980\left(\frac{DN}{360}\pi\right) - 2.0396\left(\left(\frac{DN}{360}\pi\right)^3\right) \quad (5)$$

where DN is the Julian day number (1 to 366) and T is the air temperature in degrees Celsius.

Predicting net radiation using equation 1 required additional regression equations. Flat plate solar radiation data, k↓ (MJ/m^2), were corrected for grid cell slope and aspect using linear regression to give (Ann Ritcey and Alan Flint, U.S. Geological Survey, personal communication, 1990)

$$RC = 8.597 + (0.024 * (k\downarrow)^2) - ((0.001) * SL * RA) \quad (6)$$

$$RA = A - 180^o \quad (7)$$

where RC term is the flat plate radiation (W/m^2) corrected for slope and aspect, SL is the grid cell slope in percent, RA is the relative aspect in degrees, and A is the grid cell aspect in degrees. Net radiation, R_n, was predicted using a regression equation

$$R_n = \left[\left(\frac{RC}{0.0009}\right)(0.58889) - 42.439\right] \text{ x } 0.0009 \quad (8)$$

Finally, daily potential ET (mm) is given by

$$ET = 0.4\left(\frac{s}{s+\gamma}\right)R_n \quad (9)$$

where the 0.4 term is a conversion factor. The rate of ET was computed by distributing daily ET as a sine-wave function

$$ep = 3.1428\left(\frac{ET/1000}{86400}\right)\sin(0.2618(t-6)) \ , \quad 6 \le t \le 18 \quad (10)$$

where t is the clock time in hours. Although the potential ET would most likely peak later than 12:00, it is assumed that the distribution used in this study is close enough for this initial work.

Predicted rates of vapor and liquid flow are based on a solution in Campbell (1985). The liquid flow part is the same for both the evaporation and the redistribution processes. Liquid flow calculations are discussed in the Infiltration/Redistribution section. Vapor flow is given by

$$j_v = -k_v \Delta h \tag{11}$$

where j_v is the vapor flow, h is the relative humidity, and k_v is the soil vapor conductivity. Derivation of k_v is given by Campbell (1985). The relative humidity is given as a function of the soil water potential ψ

$$h = \exp\left(\frac{M_w \cdot \psi}{R \cdot K}\right) \tag{12}$$

where M_w is the mass of a mole of water, R is the gas constant (8.31 J/mole/K), and K is the absolute temperature in degrees Kelvin.

Runoff and Channel Flow

Based on the grid cell elevations the location of channel was defined. For the numerical model, grid cells adjacent to the channel with slopes greater than 20 degrees were assumed to be the source areas for runoff (Figure 11). Assuming 10 mm of surface water is available for overland flow, 80 of the 131 cells shown on Figure 11 would be required to generate the estimated 4.3 m^3/s (150 ft^3/s) for about one hour. Estimated time of concentration for the watershed is approximately 40 minutes.

Infiltration/Redistribution

Rates of infiltration and redistribution are computed using a solution in Campbell (1985). The hydraulic properties of a soil are predicted using the mean particle diameter, dg (mm), and geometric standard deviation of particle sizes, sd (Shirazi and Boersma, 1984). The geometric standard deviation can be used as a measure of the degree of sorting of a soil sample (the spread of the particle-size distribution curve). The required values are the mass percent clay size (< 0.002 mm, 0.00008 in), silt (0.002 to 0.05 mm, 0.00008 to 0.002 in), sand (0.05 to 2.00 mm, 0.002 to 0.0787 in), and gravel (2.00 to 75.0 mm, 0.0787 to 2.95 in). Using these values dg can be computed using

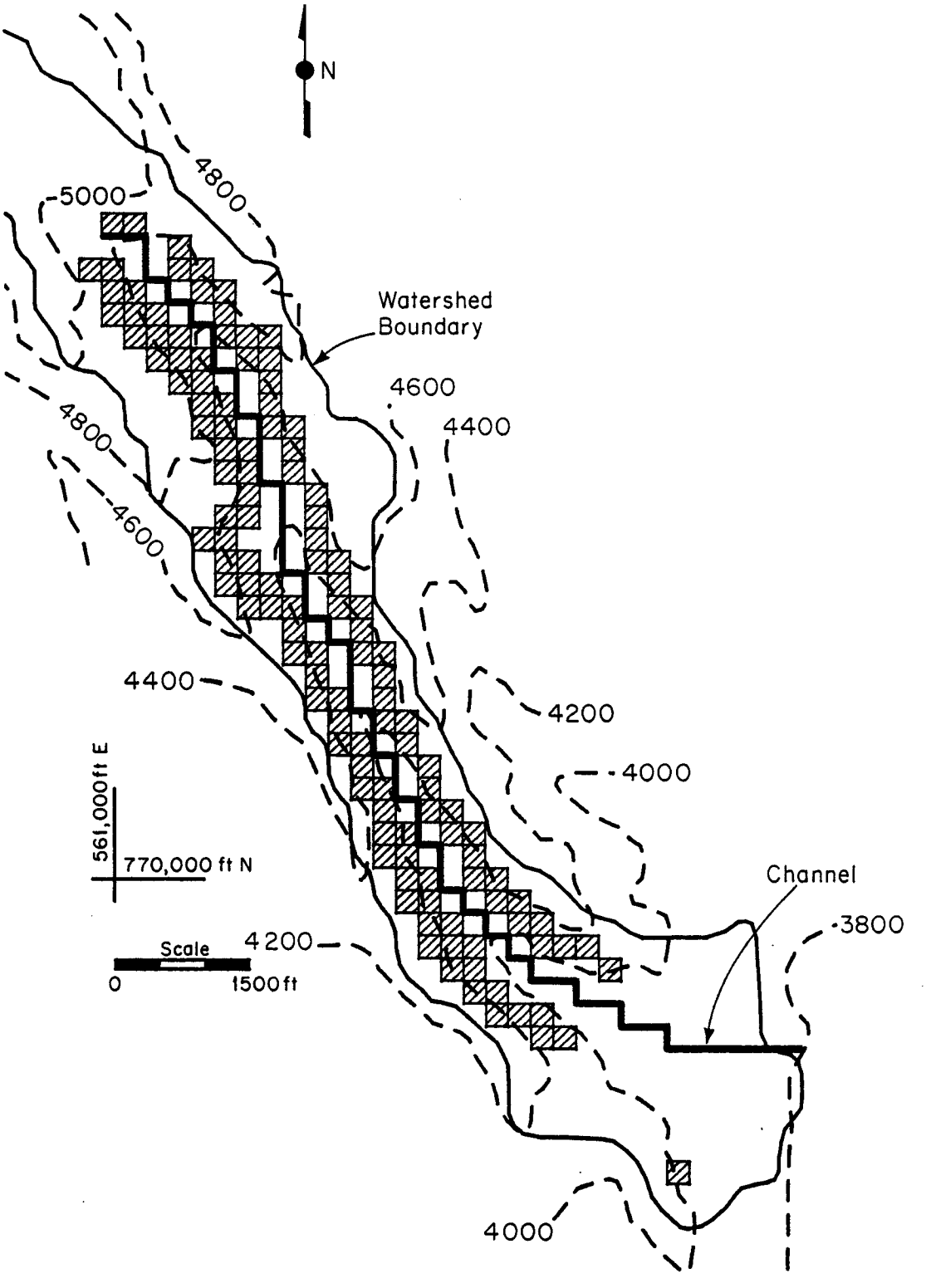

Figure 11. Grid cells used to represent channel and runoff source areas

$$dg = \exp(vg) \tag{13a}$$

$$vg = 0.01(g \cdot pg + d \cdot pd + t \cdot pt + y \cdot yp) \tag{13b}$$

$$g = \ln\left(\frac{d1 + g1}{2}\right) \tag{13c}$$

$$d = \ln\left(\frac{t1 + d1}{2}\right) \tag{13d}$$

$$t = \ln\left(\frac{y1 + t1}{2}\right) \tag{13e}$$

$$y = \ln\left(\frac{y1}{2}\right) \tag{13f}$$

where pg is the mass percent gravel, pd is the mass percent sand, pt is the mass percent silt, py is the mass percent clay, g1 is the upper size limit for gravel, d1 is the upper size limit for sand, t1 is the upper size limit for silt, and y1 is the upper size limit for clay. The maximum particle size was usually less than the 75.0 mm limit for gravel. Therefore, the smallest sieve size which allowed the complete sample to pass was used as the upper limit in the calculations for dg and sd. The geometric standard deviation is given by

$$sd = \exp((vr - vg^2)^{1/2}) \tag{14}$$
$$\text{where } vr = 0.01(g^2 \cdot pg + d^2 \cdot pd + t^2 \cdot pt + y^2 \cdot py)$$

Saturated hydraulic conductivity, ks, was estimated using an empirical equation in Campbell (1985)

$$ks = C \exp(-6.9 \cdot py/100 - 3.7 \cdot pt/100) \tag{15}$$

where C is a constant (3.9×10^{-5} m/s).

The unsaturated hydraulic properties were also estimated using dg, sd, and the air entry potential, ψ_e. The air entry potential is the potential at which the largest water filled pores drain (Campbell, 1985). The air entry potential is calculated using

$$\psi_e = -0.5 dg^{-1/2} \tag{16}$$

where the units for ψ_e are J/kg. The water release curve is controlled by the variable b1 which is calculated using

$$b1 = -2\psi_e + 0.2sd \tag{17}$$

Matric potential, ψ, is given by

$$\psi = \psi_e\left(\frac{f}{\theta}\right)^{b1} \tag{18}$$

where θ is the volumetric water content, and f is the soil's porosity. The estimated water release curves for the upland soils and alluvium are in Figure 12. The b1 parameters for the tuffs were obtained using linear regression of the logarithmic transformed data (Figure 13). The exponent for the unsaturated conductivity function, n, is given by

$$n = 2 + 3/b1 \tag{19}$$

The unsaturated hydraulic conductivity function is

$$k(\theta) = ks\left(\frac{f}{\theta}\right)^{n} \tag{20}$$

where k is given in m/s. The estimated hydraulic conductivity curves for the upland soils and alluvium are in Figure 14. Linear regression based on equations 18 and 20 was used with logarithmic transformed laboratory measurements to obtain the tuff samples' hydraulic parameters (Figure 15).

Unsaturated flow was predicted using Richards equation

$$\frac{\partial\theta}{\partial t} = \frac{\partial}{\partial z}\left[k(\theta)\left\{\frac{\partial\psi}{\partial z} + 1\right\}\right] \tag{21}$$

Campbell's (1985) solution to Richards equation is based on the "matric flux potential" (MFP), ϕ, as a driving force for flow

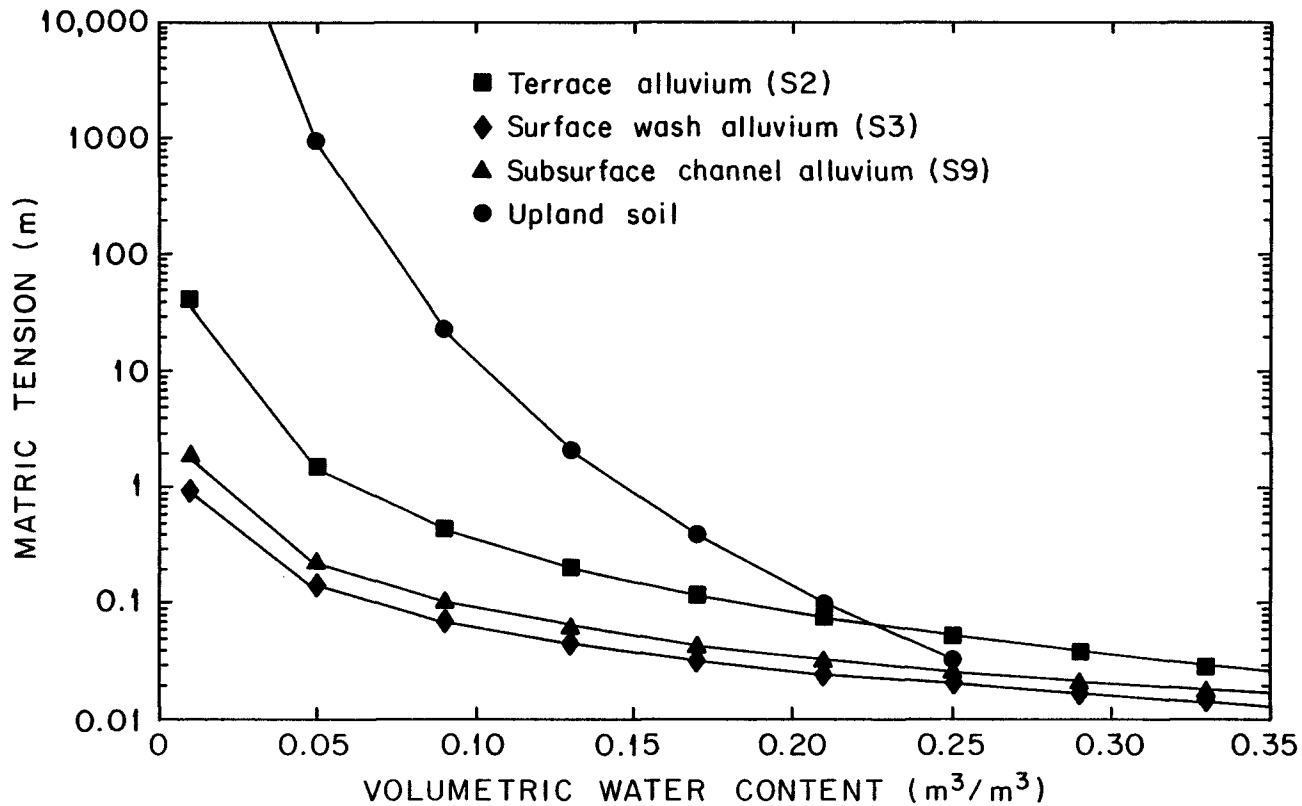

Figure 12. Estimated water release curves for upland soils and alluvium

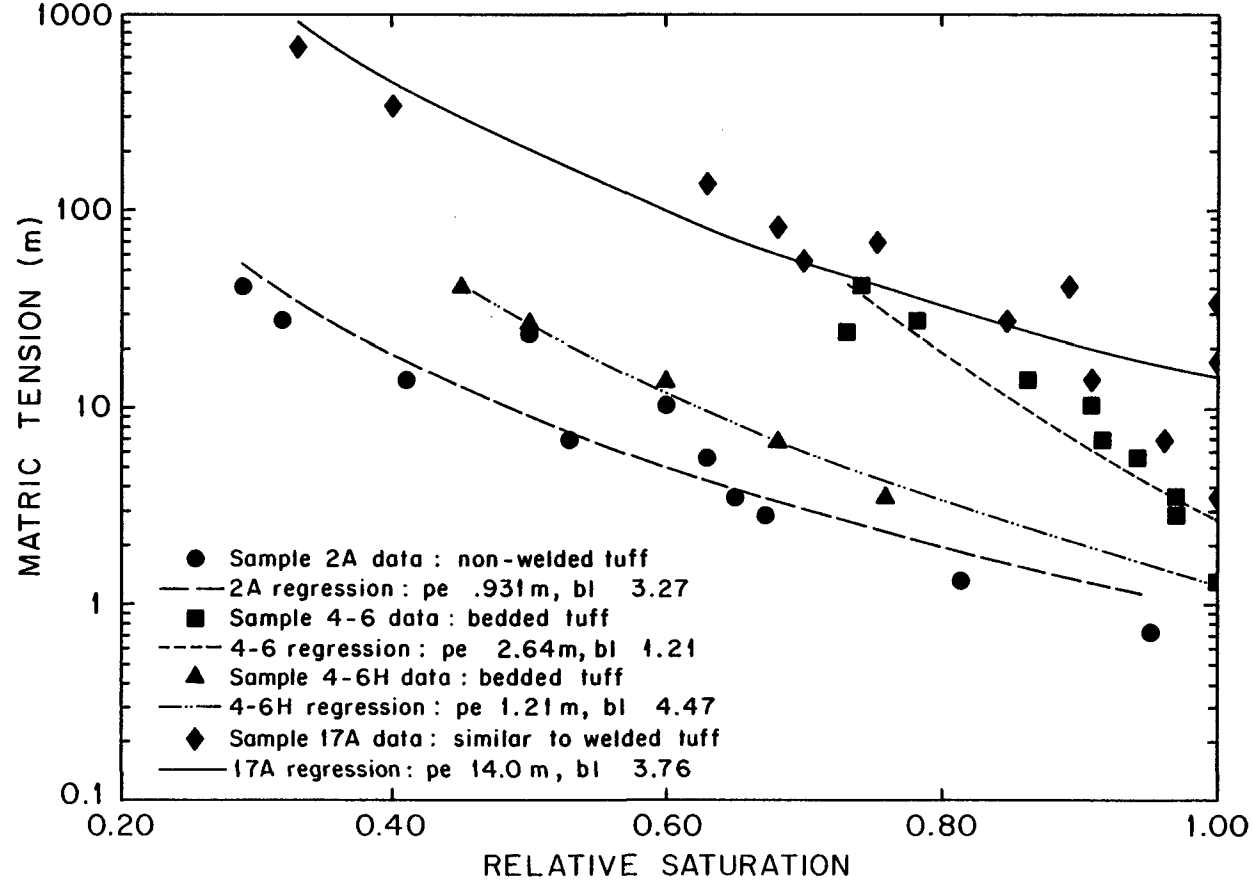

Figure 13. Measured water release curves for tuffs

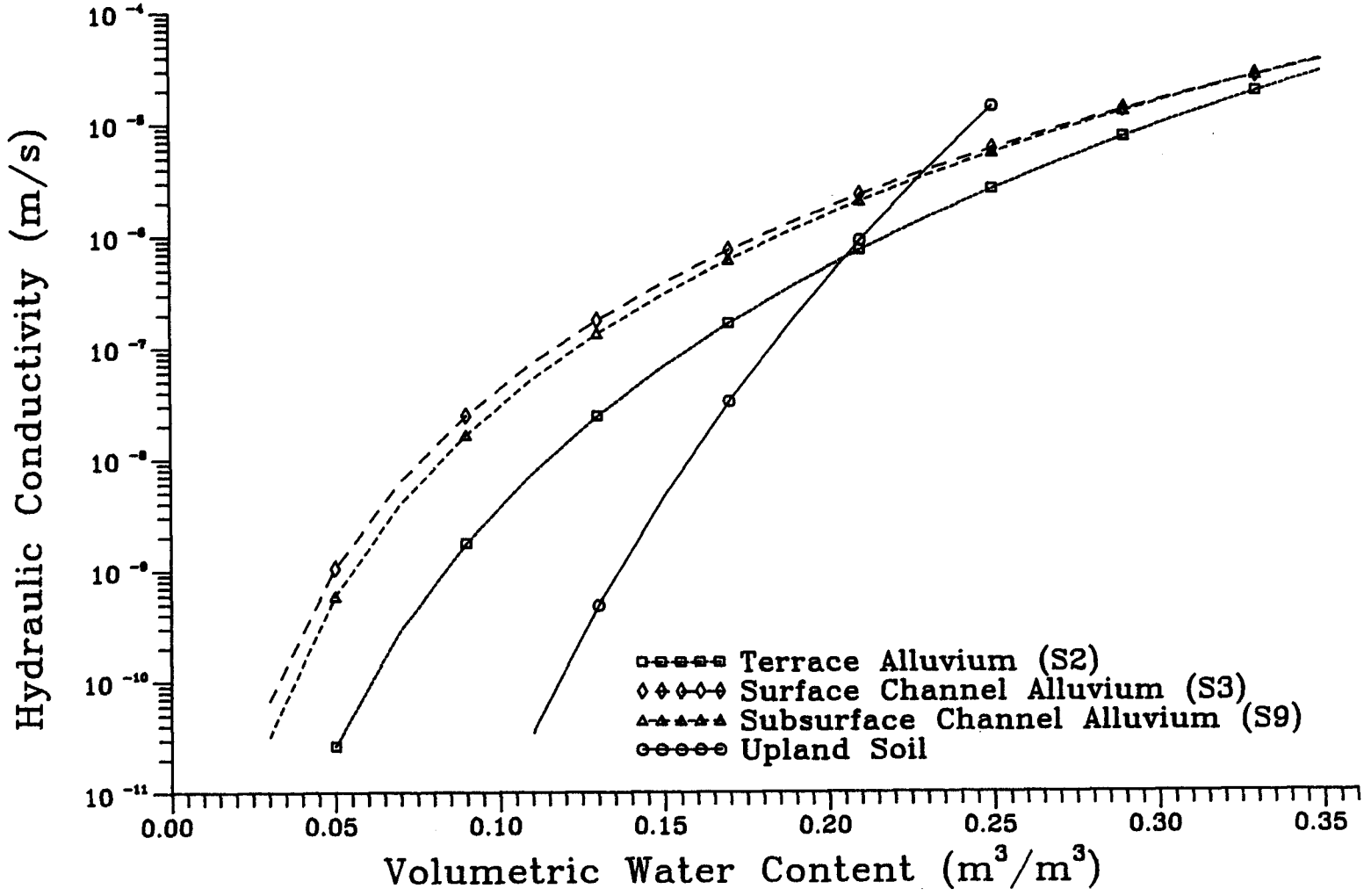

Figure 14. Estimated unsaturated hydraulic conductivity curves for upland soils and alluvium

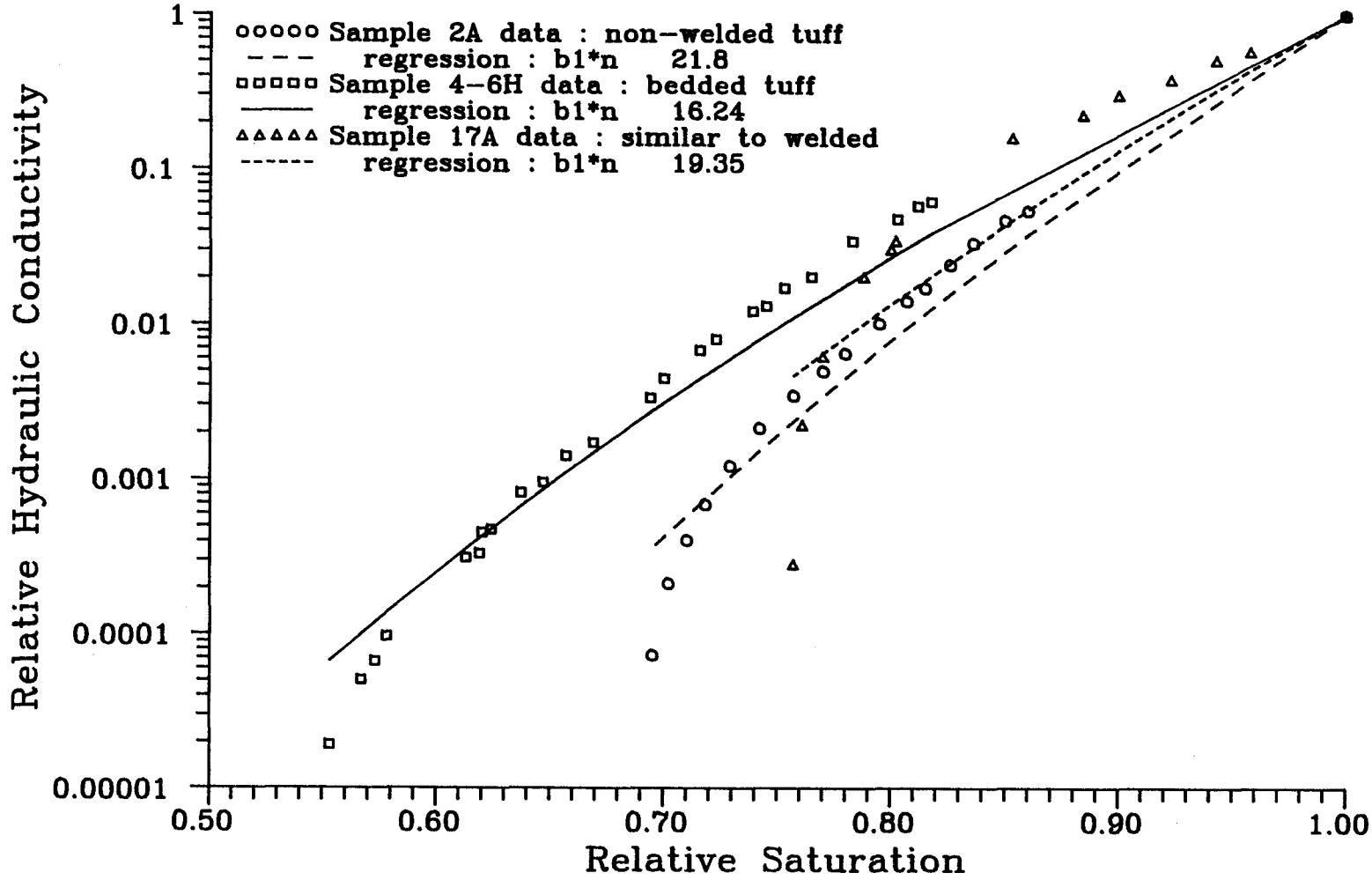

Figure 15. Measured unsaturated hydraulic conductivity for tuffs

$$\phi = \int_{-\infty}^{\psi} k(\psi)d\psi \tag{22}$$

Solving equation 18 for θ and substituting into equation 20 and performing the integration in equation 22 (assuming $\psi <= \psi_e$) yields

$$\phi = \frac{k\psi}{(1-n)} \tag{23}$$

A limitation of solutions based on matric flux potential is that MFP is not continuous across boundaries between materials having different properties. Rewriting Richards equation using ϕ gives

$$\frac{\partial\theta}{\partial t} = \frac{\partial}{\partial z}\left[\frac{1}{1-n}\left(\frac{\partial(k(\theta)\psi)}{\partial z}\right) + k(\theta)\right] \tag{24}$$

Assumptions and Limitations

The main assumptions of this study are given in this following section. Hystersis effects are assumed not to be siginificant for the coarse-textured soils in this study. The potential ET diurnal cycle can be approximately described by a sine-wave function beginning at 6:00, peaking at 12:00, and ending at 18:00. Soil heat flux, G, is assumed negligible over a day. It is assumed that the equivilent hydraulic conductivity for the boundary between the two soil layers can be described by $k_{eq} = 2k_1k_2/(k_1+k_2)$ where k_1 is the hydrualic conductivity of the soil just above the boundary and k_2 is the hydraulic conductivity of the soil just below the boundary. Finally, it is assumed that the matric flux potential is a valid describing unsaturated flow.

The major limitations of this study are given in this following section. The two-layer soil boundary only allows water to flow downward across it. The model cannot converge to a solution once the bottom soil element of a layer becomes saturated. The current program is limited to isothermal conditions. Vapor flow is not included in the soil water transport when evaporative demand does not exist at the surface. A positive head for water ponding at the surface and a matric potential greater than the air entry potential is not included.

MODEL CALIBRATION AND SENSITIVITY ANALYSIS

Model Calibration in Channel Alluvium

Water content data for neutron-access hole (NAH) N-7 were used to calibrate the model in the channel alluvium. Simulation execution began on August 14, 1984, the day of the first major precipitation event, and ended after the August 29 N-7 logging time (Figure 8). Water in addition to precipitation was added to the surface storage element; 3.02 cm (1.19 in) on August 14 and 17.86 cm (7.03 in) on August 19, 1984. All simulations used a uniform initial volumetric water content equal to 0.1 m^3/m^3.

Simulations were run using the surface channel alluvium parameters for the upper layer (Table 3).

Table 3. Properties of upland soils and alluvium

	Upland Soil	Terrace Alluvium (S2)	Surface Channel Alluvium (S3)	Subsurface Channel Alluvium (S9)
mean particle diameter, dg (mm)	2.35	3.89	13.4	9.73
geometric standard deviation, σ_g	28.6	7.84	4..57	5..10
saturated hydraulic conductivity, k_s(m/s)	1.41×10^{-5}	2.88×10^{-5}	3.61×10^{-5}	3.69×10^{-5}

Parameters for the lower layer are from tuff sample 17A (Lori Flint, U.S. Geological Survey, personal communication, 1990) which is believed to be representative of the welded Tiva Canyon unit that underlies this part of the watershed. The tuff-alluvium contact in N-7 for the simulations is 12.5 m (41.3 ft). An assumed logging time of 12:00 was used for the August 17, 22, and 29 moisture data retrieval. Because the August 20 moisture logging for N-7 was so close to the previous days major precipitation event, an output file was generated at the actual recording time, 12:30. The results were plotted along with the actual data for comparison.

Model Calibration in Terrace Alluvium

Data from NAH N-9 was used to calibrate the model in the terrace alluvium. Simulated moisture data was written to output files at 12:00 for August 17 and 21, and October 21 after which the simulation was concluded. The initial water content was set at 0.067 m^3/m^3 (average for upper 6 m, 19.8 ft). The tuff-alluvium contact was at 12.5 m (41.3 ft). The underlying tuff parameter were those obtained from tuff sample 17A. Only precipitation was added to the surface storage element for this simulation. Simulation output was plotted with actual data for comparison.

Runoff Event Simulation

The model was used to simulate runoff from the upland soils using assumed water contents. Simulation of the runoff event was performed using the actual precipitation. The underlying tuff parameters for this simulation were also those from tuff sample 17A. Thicknesses for the upland soil in these simulations was varied between 10, 15, and 30 cm (3.9, 5.9, and 12 in). Although arbitrarily chosen, the thicknesses are believed to be somewhat representative of the actual upland conditions. The variation of depths allows for a relative evaluation of upland soil thickness in relation to runoff. A porosity of 0.25 was used with a initial moisture content of 0.125 m^3/m^3 (50% saturation). The residual water content for ET, wr, was set at 0.07 m^3/m^3. The surface flux and remaining surface storage were recorded after each precipitation event. With the runoff event, it was assumed that any remaining water in surface storage would be moved off the grid cell by overland flow. To simulate the runoff event, the surface storage element, stor#(s), was set to zero after infiltration occurred. To evaluate the effect of antecedent moisture conditions, the simulations were duplicated, however, this time only the precipitation on August 19 was used. The results of both sets of simulations were presented together for comparison.

Sensitivity Analysis

Simulations involving variation of four model parameters were performed to evaluate the model's sensitivity to those parameters. The four parameters evaluated were the mean particle diameter, dg, the geometric standard deviation, sd, the saturated hydraulic conductivity, ks, and the porosity, ws. The standard set of parameters to which the sensitivity analysis was evaluated include dg = 1.0 mm (0.039 in), sd = 10, ks = 1.0×10^{-5} m/s (3.3×10^{-5} ft/s), and ws = 0.35. The standard set of parameters were arbitraily selected with values near those obtained from the soil samples used in this study. Simulations did not use precipitation input but added 20.0 cm (7.87 in) of water to the surface storage element at 15:00 of the first simulation day (August 14). Moisture date was written to files 24 hours, 72 hours, and 1 week after the surface storage was filled. The mean particle diameter was changed to 0.10 mm (0.0039 in) and 10 mm (0.39 in) for evaluation. The geometric standard deviation was changed to 5 and 15 for evaluation. The saturated hydraulic conductivity was changed to 1×10^{-6} m/s (3.3×10^{-6} ft/s) and 1×10^{-4} m/s (3.3×10^{-4} ft/s) for evaluation. Finally, the porosity was changed to 0.25 and 0.45. The residual water content for ET and uniform initial water content for porosity evaluation were scaled based on the potential corresponding to the standard set porosity and its initial conditions. The initial water contents were set to 0.0714 and 0.127 m^3/m^3 for the 0.25 and 0.45 porosity simulations, respectively. The residual water contents for ET were set at 0.0286 and 0.0514 m^3/m^3, respectively.

RESULTS AND DISCUSSION

Channel Alluvium Model Calibration

Results from simulating a two layer soil profile with the tuff-alluvium contact at 12.5 m (41.3 ft) show the water pulse from the storm events moving down much more rapidly than measured (Figure 16). The cumulative mass balance error for this simulation was -3.17×10^{-7} m (-1.0×10^{-6} ft) of water, approximately 6.1% of the maximum allowable error. The initial simulation of the wash alluvium shows water accumulating above the lower tuff layer. The cumulative flow into the tuff layer was 4.53×10^{-6} m (1.5×10^{-5} ft) of water. The calculated flux of water into the tuff is questionable due to the simulation's poor ability to duplicate the water content data for August 22 and 29. The results of this simulation do suggest however, the need for accurate saturated hydraulic conductivity data for the alluvium and the tuff. Total ET was 6.3 mm (0.25 in).

The saturated hydraulic conductivity of the wash alluvium was increased to two and three times the initial value for additional simulations. The results for the August 20 logging time are shown with actual data for comparison (Figure 17). Water accumulation above the tuff increases with increasing values of saturated hydraulic conductivity. Because higher conductivities increase the rate of flow into the soil profile, less water is available at the surface for ET. The cumulative ET on August 20 decreased from 5.4 mm (0.21 in) of water for the initial value of saturated hydraulic conductivity to 4.6 mm (0.18 in) for a value of saturated hydraulic conductivity that was three times larger.

The N-7 water content profiles show peak values near a depth of about 2.2 m (7.3 ft) (Figure 16a). This would suggest the presence of a layer below this depth that has a small hydraulic conductivity. To explore this concept, the bottom node of the upper layer was raised to 2.25 m (7.43 ft). The upper layer properties were set to those calculated for the surface channel alluvium sample (S3), the lower layer properties were set to those calculated for the subsurface channel alluvium sample (S9) with a reduced conductivity. The lower layer's conductivity was determined by adjusting the value of conductivity until a match was obtained with the water content data. A value of hydraulic conductivity for the lower layer equal to 1/20th of that for the upper layer was selected. The computed and observed water contents agreed very well for August 20 (Figure 18).

As the simulation progressed, the agreement between the computed and observed water contents decreased (note the August 29 profiles, Figure 18). One

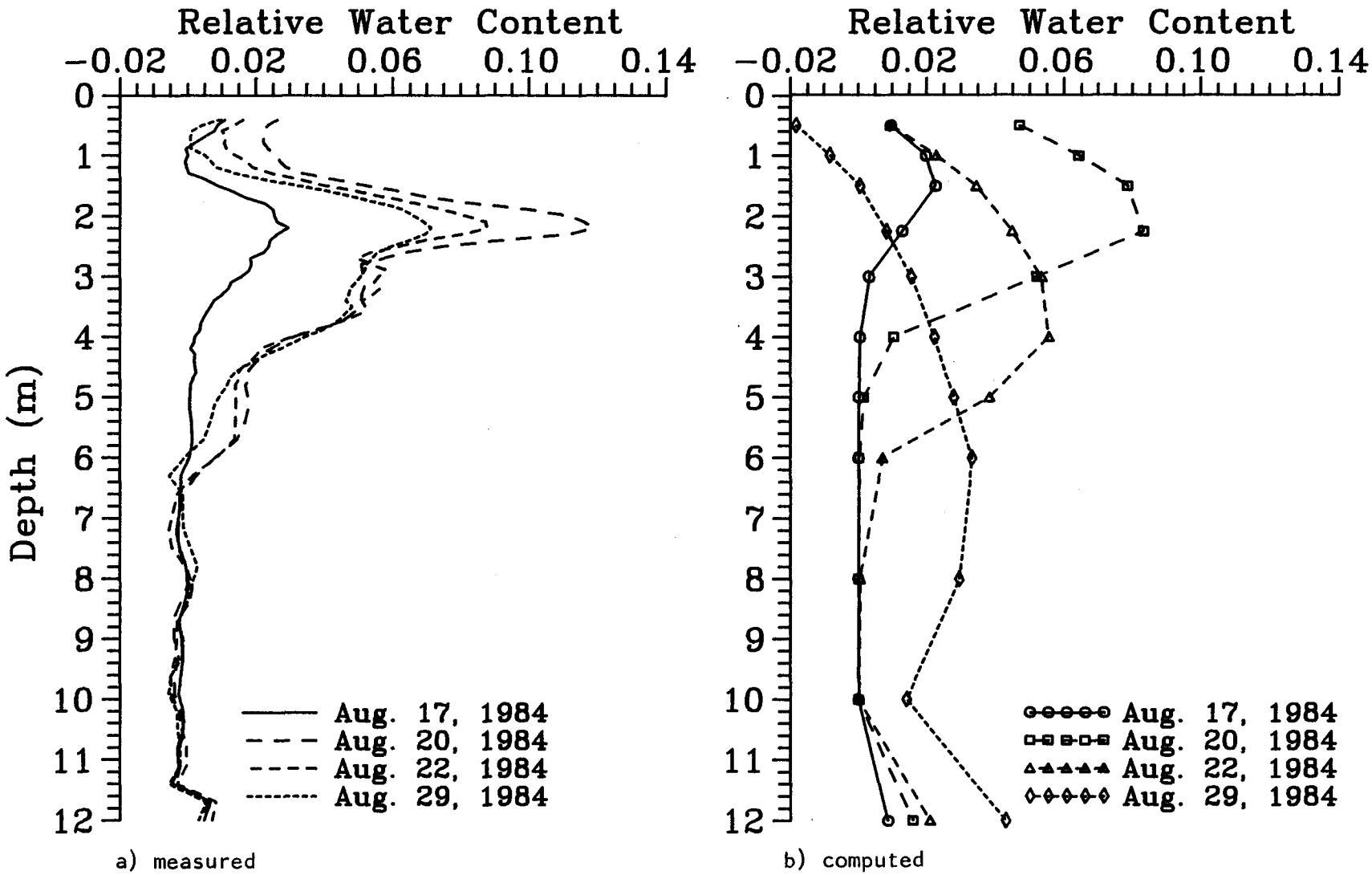

Figure 16. NAH N-7 simulation

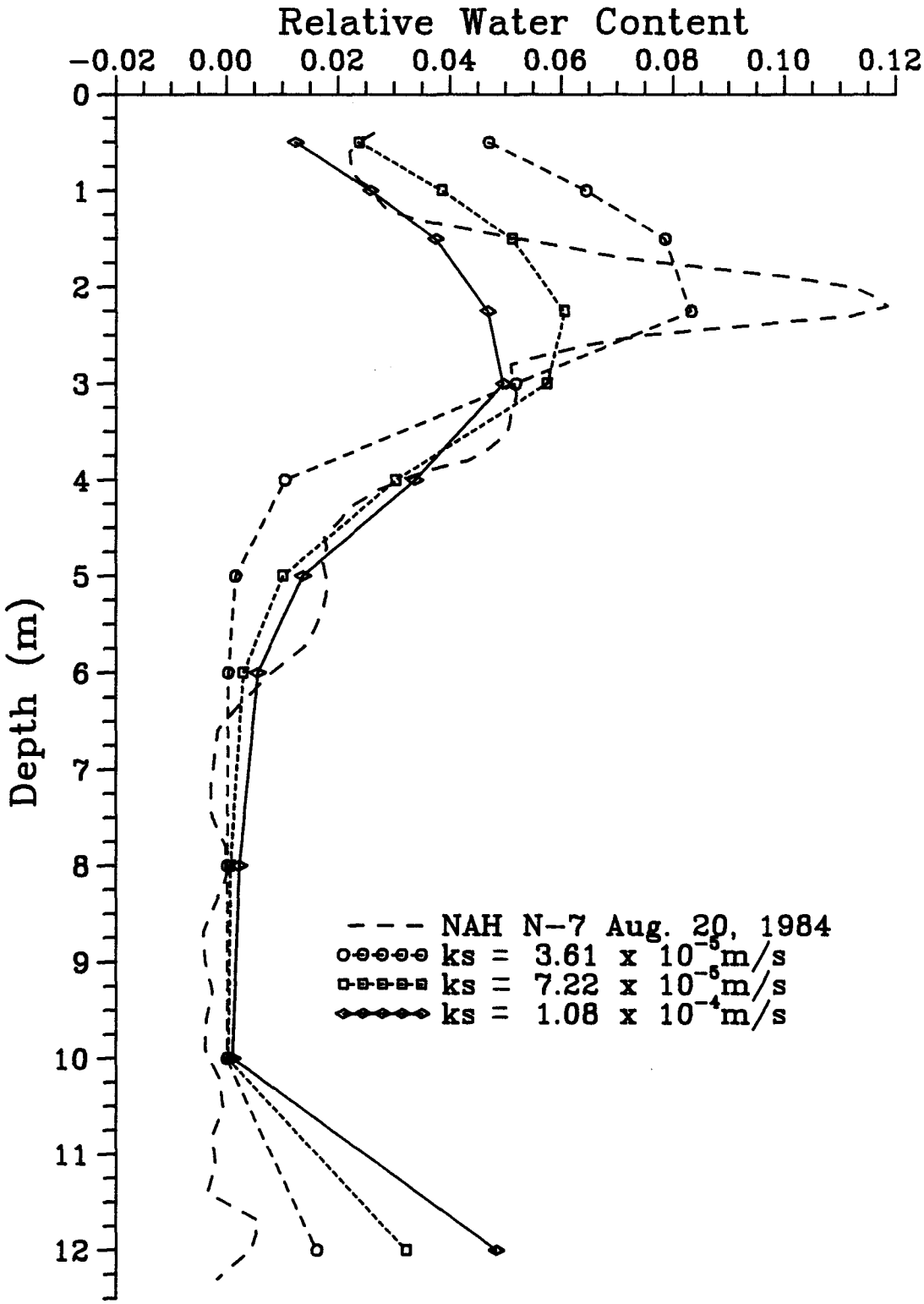

Figure 17. NAH N-7 simulation; increased saturated hydraulic conductivity

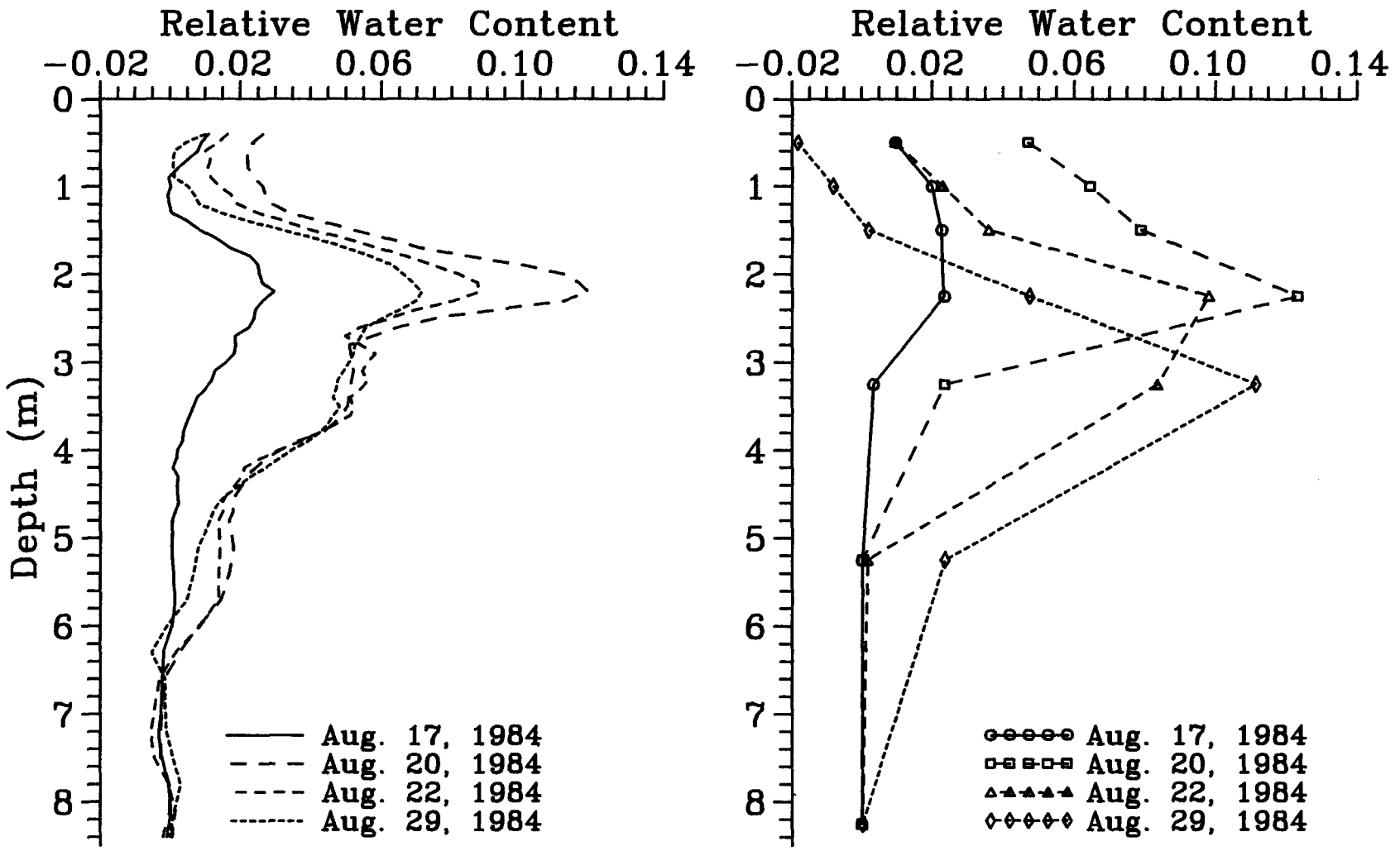

a) measured

b) computed

Figure 18. NAH N-7 simulation; 2.25 m upper alluvium layer

reason for this is that the actual soil profile contains more than two layers. Additional layers may be present at depths of about 4 and 6 m (13.2 and 19.8 ft) (see Figure 18a). Another reason is that the estimated parameters for the lower layer are in error.

The measured water content profiles indicate that most changes in water content occur within the upper 2.2 m (7.3 ft) (Figure 18a). This may be explained by thermally induced vapor and liquid flow (Cary, 1966, Hillel, 1982).

Additional simulations were performed for the wash alluvium by increasing the upper layer saturated hydraulic conductivity to 1.5 times the initial value, and decreasing the lower layer's saturated hydraulic conductivity to 1/30th of the upper layer's initial value. The computed and observed water contents agreed very well for both August 17 and 20 (Figure 19).

Terrace Alluvium Model Calibration

The purpose of this exercise was mainly to see how the model would perform using only the limited precipitation for a position outside the channel. The simulation output seems to match the data fairly well except with the last logging time where the model moves the water much further down (Figure 20). This can be possibly be due to two main factors. One factor is there may be several layers in the terrace as there were with the channel alluvium. This however does not seem very likely unless the layer is very near the surface. The more likely reason is the same expressed concerning the wash alluvium, ET can not be completely described without including flow due to soil thermal gradients.

Runoff Event Simulation

The results obtained from this simulation exercise tend to support the conceptual model for overland and channel flow (Table 4a). The runoff as described in the conceptual model occurred on two occasions, August 14 and August 19. This is exactly what was demonstrated from these simulations. The model also shows how antecedent moisture conditions are important to the runoff event.

Running these simulations again including only the precipitation event on August 19 allowed the ET process to remove more water from the soil. This increases the upper layer's water storage capacity resulting in less overland flow for the same date (Table 4b).

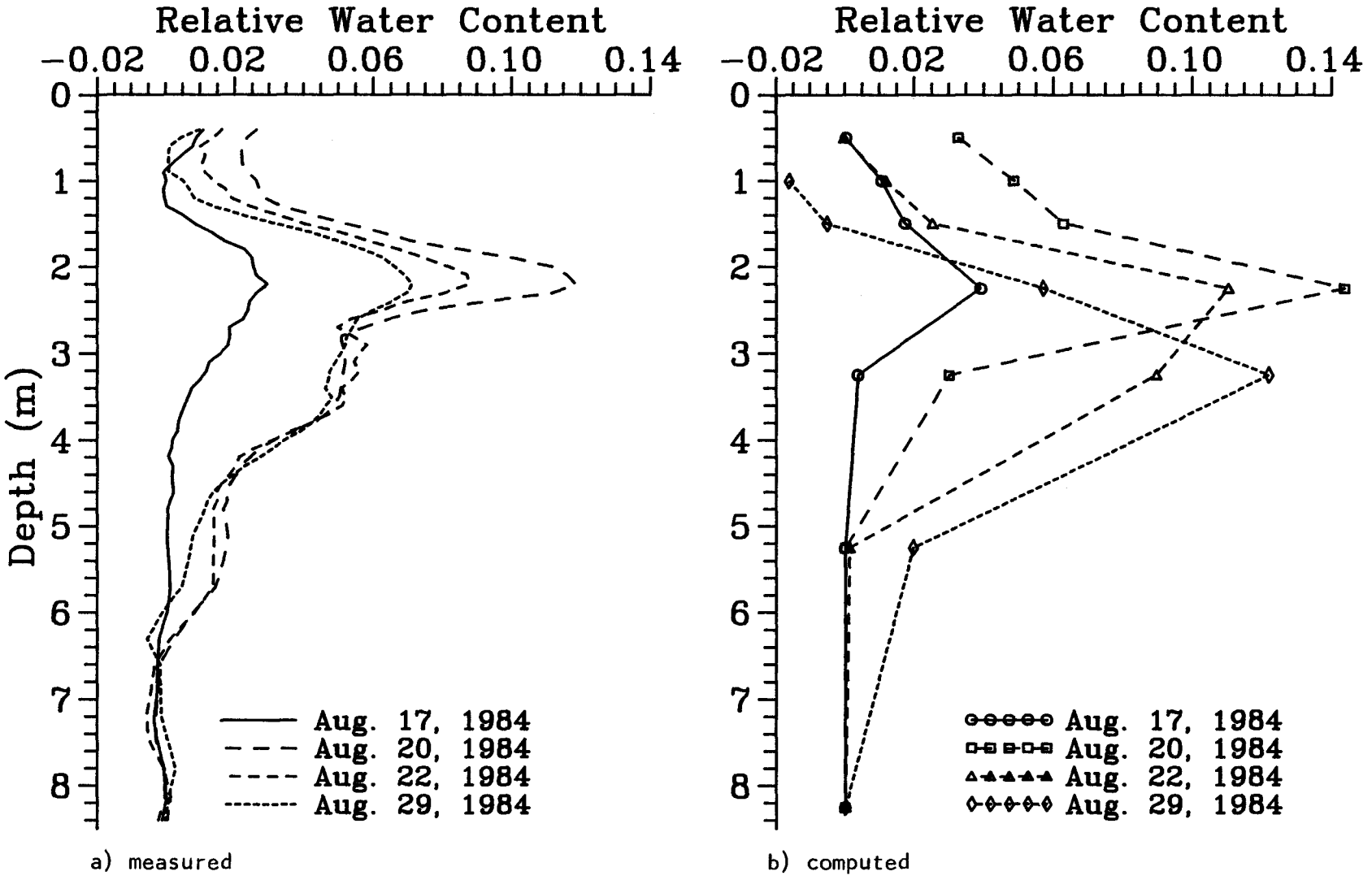

a) measured

b) computed

Figure 19. NAH N-7 simulation; 2.25 m upper alluvium layer, increased upper conductivity

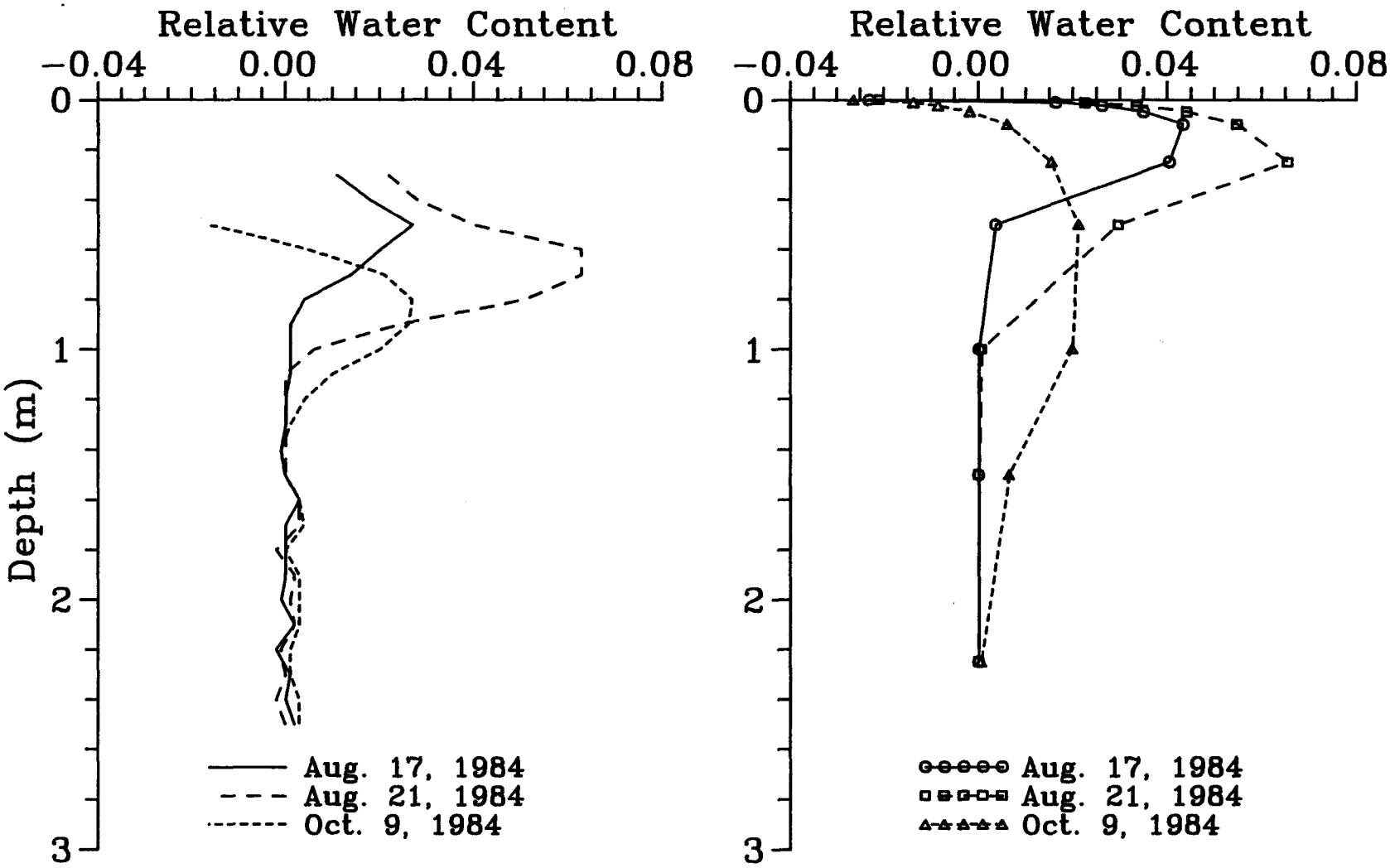

Figure 20. NAH N-9 simulation; terrace alluvium

Table 4a. Results of runoff simulation

Date	Time	Thickness = 10 cm Infiltration / Overland flow (mm)	(mm)	Thickness = 15 cm Infiltration / Overland flow (mm)	(mm)	Thickness = 30 cm Infiltration / Overland flow (mm)	(mm)
8/14	15:00	6.07	6.52	6.01	6.58	6.01	6.58
8/15	15:00	4.98	0.00	4.98	0.00	4.98	0.00
8/16	15:00	3.20	0.00	3.20	0.00	3.20	0.00
8/18	15:00	0.15	0.00	0.15	0.00	0.15	0.00
8/19	15:00	5.82	6.78	5.74	6.86	5.74	6.86
8/19	15:15	3.00	4.27	3.14	4.13	3.15	4.12

Table 4b. Results of runoff simulation; August 19 precipitation only

Date	Time	Thickness = 10 cm Infiltration / Overland flow (mm)	(mm)	Thickness = 15 cm Infiltration / Overland flow (mm)	(mm)	Thickness = 30 cm Infiltration / Overland flow (mm)	(mm)
8/19	15:00	6.38	6.21	6.31	6.29	6.28	6.32
8/19	15:15	3.66	3.61	3.40	3.87	3.38	3.89

Sensitivity Analysis

The sensitivity analysis showed that varying the model's parameters can significantly affect the simulation output. Variation of the mean particle diameter influenced model flow (Figure 21). Variation in the geometric standard deviation also significantly influenced model flow. The greater the distribution of particle size, that is the greater the value of sd, the slower the water in the profile moved (Figure 22). The saturated conductivity appeared to have the most significance with respect to model sensitivity (Figure 23). The saturated hydraulic conductivity is also the most poorly known of all the texturally-derived parameters. Finally, the porosity variation appeared to have the least influence on the model's performance (Figure 24).

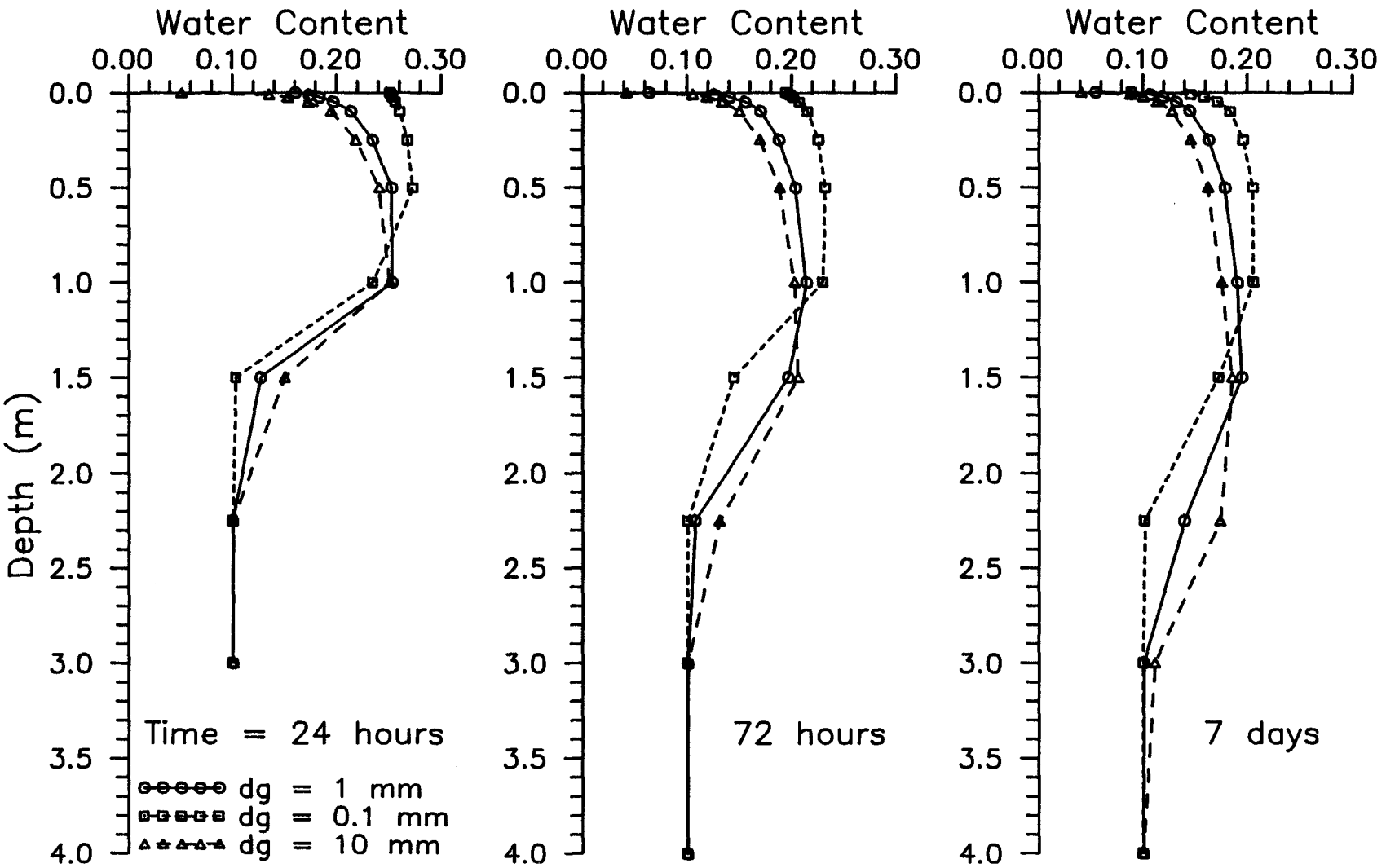

Figure 21. Results of sensitivity analysis; mean particle diameter variation

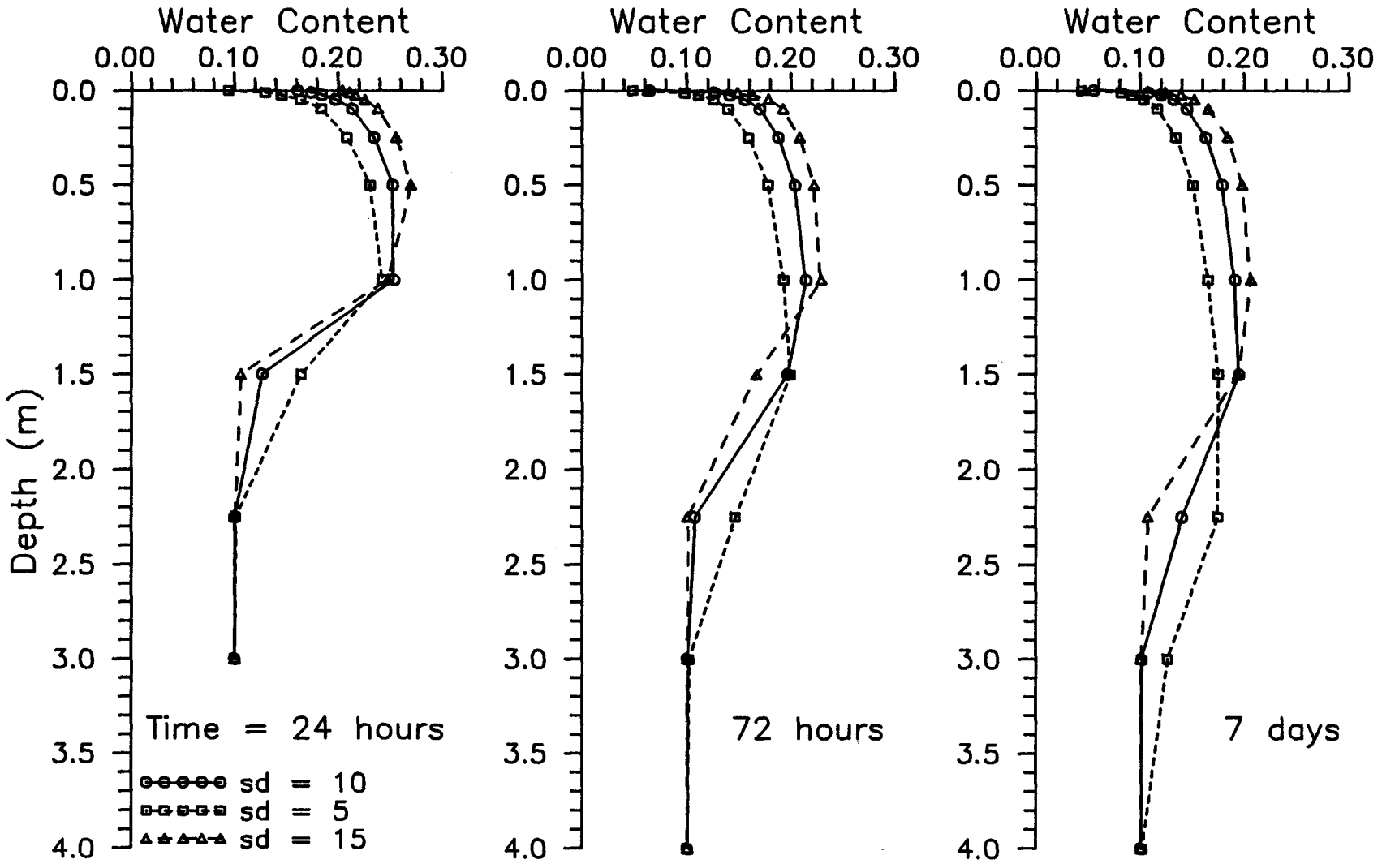

Figure 22. Results of sensitivity analysis; geometric standard deviation variation

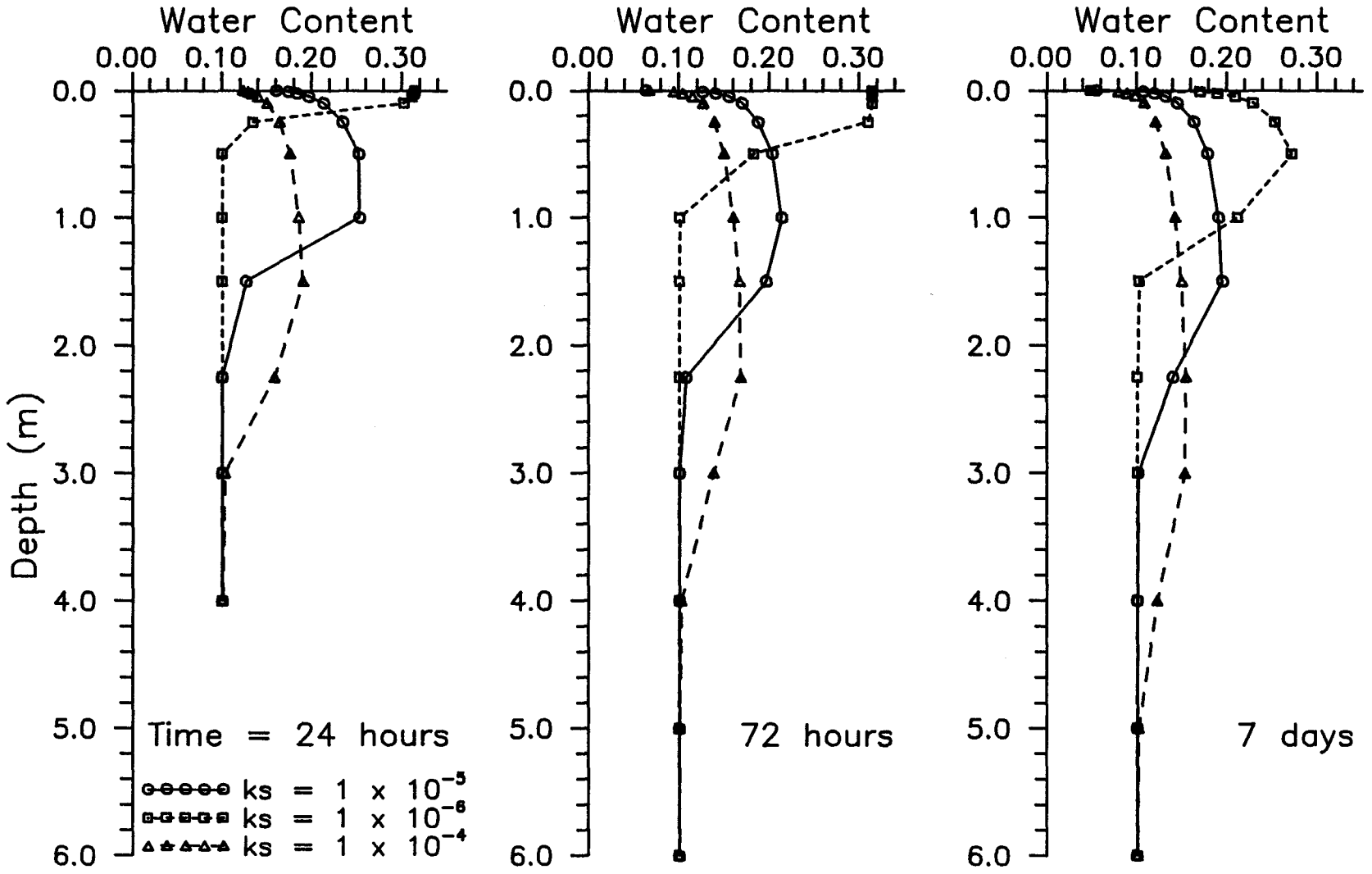

Figure 23. Results of sensitivity analysis; saturated hydraulic conductivity variation

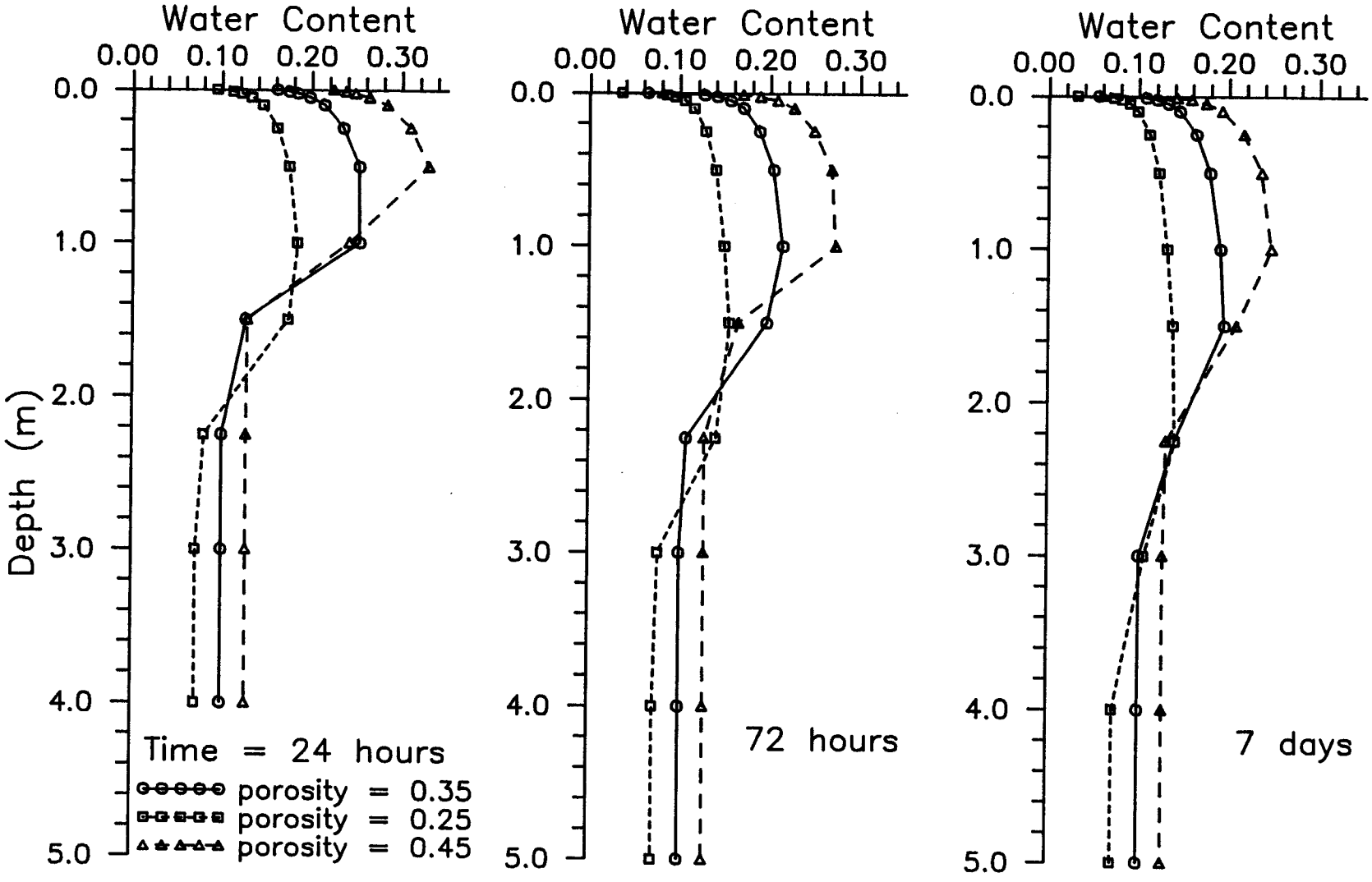

Figure 24. Results of sensitivity analysis; porosity variation

CONCLUSIONS

The computer program QBINFIL is an effective means of describing and linking the hydrologic processes considered in this study. The program has demonstrated very good mass balance accountability. Description of the soils' unsaturated flow characteristics based on texturally-derived parameters and using matric flux potential appears to work very well.

The computer program QBINFIL can be used to model vertical flow in the three surface soils in the study area using a two-layer soil profile. Because the soil profile in the channel alluvium is believed to be a multilayer, heterogenous system, the current version of the program cannot be used to model the complete profile from the channel surface to the underlying tuff including all the heterogeneous layers.

Computer simulation demonstrated that antecedent soil water content is important to runoff and overland flow.

RECOMMENDATIONS FOR FURTHER STUDY

The numerical model developed in this study was intended to provide only a partial representation of hydrologic processes. As these processes become better understood (possibly through additional simulations with this model) and as more accurate data becomes available during site characterization, further refinement of the model is expected. Based on the understanding and insight obtained through the development of this model and study of the watershed, four areas are addressed with recommendations. The first area concerns interpretation of current data and obtaining additional data. Water content data should be further investigated to try to determine soil layer stratification. Sampling with depth to obtain grain-size information would help in evaluation of soil layer stratification. Because changes in hydraulic conductivity appear to affect the model significantly, the parameters and equations involved should be further investigated for the watershed's soils and tuffs.

The second area of recommendations relates to the ET processes. The empirical equations for ET should be verified. The inclusion of thermal gradients should be explored. The evaporation module should be examined to see if a quicker solution can be attained.

The third area of recommendations relates to program modification. The program could be modified to include additional layers. Overland flow could be incorporated into the program by linking grid surface features. A channel flow component could be developed using the same solution algorithm as that was used in unsaturated flow.

The final area of recommendations concerns additional implementation of this model. The program could be used to model the complete unsaturated zone, allowing for different surface flux conditions to evaluate their significance.

BIBLIOGRAPHY

Campbell, G.S. 1977. An introduction to environmental biophysics. Springer-Verlag, New York, 159p.

Campbell, G.S. 1985. Soil physics with basic transport models for soil-plant systems. Develop. in Soil Sci. 14. Elsevier, New York.

Cary, J.W. 1966. Soil moisture transport due to thermal gradients: Practical aspects. Soil Science Society of America, Proceedings 30: 428-433.

Czarnecki, J.B. 1984. Simulated effects of increased recharge on the ground-water flow system of Yucca Mountain and vicinity, Nevada-California: U.S. Geological Survey Water-Resources Investigations Report 84-4344, 33 p.

Dettinger, M.D. 1989. Reconnaissance estimates of natural recharge to desert basins in Nevada, U.S.A., by using chloride-balance calculations. Journal of Hydrology, v. 106, p. 55-78.

Flint, A.L. and S.W. Childs. 1987. Modification of the Priestly-Taylor evaporation equation for soil water limited conditions, in 18th Conference on Agricultural and Forest Meteorology, W. Lafayette, Indiana, September, 1987. Pp. 70-73.

Flint, L.E. and A.L. Flint . 1990. Preliminary permeability and moisture retention data from non-welded and bedded tuff, Yucca Mountain area, Nye County, Nevada: U.S. Geological Survey Open-File Report (in preparation).

Freeze, R.A. and J.A. Cherry. 1979. Groundwater. Prentice-Hall, New Jersey. p. 67.

French, R.H. 1983. Precipitation in southern Nevada: Journal of Hydraulic Engineering, v. 109, no. 7, July, p. 1023-1036.

Gee, G.W. and J.W. Bauder. 1986. Particle Size Analysis 15-5, p.404-408, in Methods of Soil Analysis, Part 1, America Society of Agronomy, Madison, Wisconsin.

Green, W.A. and G.A. Ampt. 1911. Studies on soil physics: 1. The flow of air and water through soils. J. Agric. Sci. 4:1-24.

Haverkamp, R., M. Kutilek, J.-Y. Parlange, L. Rendon, and M. Krejca. 1988. Infiltration under ponded conditions: 2. Infiltration equations tested for parameter time-dependence and predictive use. Soil Science, 145: 317-329.

Hevesi, J.A., A.L. Flint, and J.D. Istok. In Press. Precipitation estimation in mountainous terrain using multivariate geostatistics--1.Structural Analysis

Hillel, D. 1982. Introduction to Soil Physics. Academic Press, Inc. San Diego, California.

Justus, P.S. and N.K. Stablein. 1989. Geoscientists help make 10,000-year decisions--U.S. Nuclear Regulatory Commission: Geotimes, January, p. 14-15.

Linsley, R.K. and J.B. Franzini. 1979. Water Resources Engineering, third edition. McGraw-Hill, Inc.

Linsley, R.K., M.A. Kohler, and J.L.H. Paulhus. 1982. Hydrology for Engineers, third edition. McGraw-Hill, Inc.

Maxey, G.B. and T.E. Eakin 1949. Ground water in White River Valley, White Pine, Nye, and Lincoln Counties, Nevada. Nev., State Eng., Water Resour. Bull., No.8, 59pp. (prepared in cooperation with U.S. Dep. Inter., U.S. Geol. Surv.).

Montazer, P. and W.E. Wilson. 1984. Conceptual hydrologic model of flow in the unsaturated zone, Yucca Mountain, Nevada: U.S. Geological Survey Water-Resources Investigations Report 84-4345, 55 p.

Nichols, W.D. 1987. Geohydrology of the unsaturated zone at the burial site for low-level radioactive waste near Beatty, Nye County, Nevada: U.S. Geological Survey Water-Supply Paper 2312, 52 p.

Priestly, C.H.B and R.J. Taylor. 1972. On the Assessment of Surface Heat Flux and Evaporation Using Large-Scale Parameters. Monthly Weather Rev. 100(2): 81-92.

Roseboom, E.H. 1983. Disposal of high-level nuclear waste above the water table in arid regions: U.S. Geological Survey Circular 903, 21p.

Rush, F.E. 1970. Regional ground-water system in the Nevada Test Site area, Nye, Lincoln, and Clark Counties,Nevada: Nevada Department of Conservation and Natural Resources Reconnaissance Series Report 54, 25 p.

Schmidt, M.R. 1988. Classification of Upland Soils by Geomorphic and Physical Properties Affecting Infiltration at Yucca Mountain, Nevada: Masters Thesis, Colorado School of Mines.

Scott, R.B., R.W. Spengler, S. Diehl, A.R. Lappin, and M.P. Chornack. 1983. Geologic character of tuffs in the unsaturated zone at Yucca Mountain, southern Nevada, in Mercer, J.W., P.S.C. Rao, and I.W. Marine, eds., Role of the unsaturated zone in radioactive and hazardous waste disposal: Ann Arbor, Mich., Ann Arbor Science, p. 289-335.

Scott,R.B.and J. Bonk. 1984. Preliminary geologic map of Yucca Mountain with geologic sections, Nye County, Nevada: U.S. Geological Survey Open-File Report 84-494, scale 1:12,000.

Shirazi, M.A. and L. Boersma. 1984. A unifying quantitative analysis of soil texture. Soil Sci. Soc. Am. J. 48:142-147.

Watson, P., P. Sinclair, and R. Waggoner. 1976. Quantitative evaluation of a method for estimating recharge to the desert basins of Nevada: Journal of Hydrology, v. 31, p. 335-357.

Weber, I.P. and S.D. Wiltshire. 1985. The Nuclear Waste Primer, A Handbook for Citizens: The League of Women Voters Education Fund.

Winograd, I.J. 1981. Radioactive waste disposal in thick unsaturated zones: Science, v. 212, no. 4502, p. 1457-1464.

Winograd, I.J. and W. Thordarson. 1975. Hydrogeologic hydrochemical framework, south-central Great Basin, Nevada-California, with special reference to the Nevada Test Site: U.S. Geological Survey Professional Paper 712-C, 126 p.

APPENDICES

APPENDIX A
QBINFIL description

COMPUTER PROGRAM

Introduction

A computer program was written to implement the numerical model. The current version of the program contains procedures for precipitation, ET (with isothermal vapor flow and liquid flow), infiltration through the full range of surface conditions, and redistribution in the unsaturated zone for a two layer soil profile (Figure 25). The program can currently run these simulations for numerous grid cells (limited by available computer memory). The movement of water, however, is only vertical ; there is no subsurface exchange of water between adjacent cells.

The computer program was written using a modular design. This permits the separate development and testing of individual program modules. This design also allows for enhancement of the program to include additional processes.

The program was written using QuickBasic version 4.5. This programming language provides many useful editing and debugging features. The screen color graphics were also appreciated and useful in presenting simulation output.

The program is readily adaptable to receive input from either the keyboard or ASCII data files. The program is currently configured so that the parameters remain constant between consecutive runs unless changed within the code itself. The code could very easily be adapted to allow user variation of the parameters by keyboard entry prior to each run.

Program output is written to the screen and to ASCII files. Screen output includes both text and color graphics displays. Screen text displays execution time, total mass balance error, surface water storage, total evaporation, and total water flow between the two layer soil profile. The text can easily be altered to display additional information. Graphic displays include the collection of grid cells used to represent Pagany Wash Watershed; different colors are used to portray the slope of each cell. Within the total number of grid cells representing a watershed, it is assumed that many locations will behave hydrologically similarly. Therefore it would be appropriate to limit calculations to only a few representative grid cells. Computed soil moisture profiles for up to three grid cells are also displayed. Between the hours of 6:00 and 18:00 a graph above each soil profile displays potential and actual ET. Information written to output files includes the coordinates for the grid cells, the simulation time, computed water contents, total mass balance error, total flux between the two unsaturated layers, and total ET.

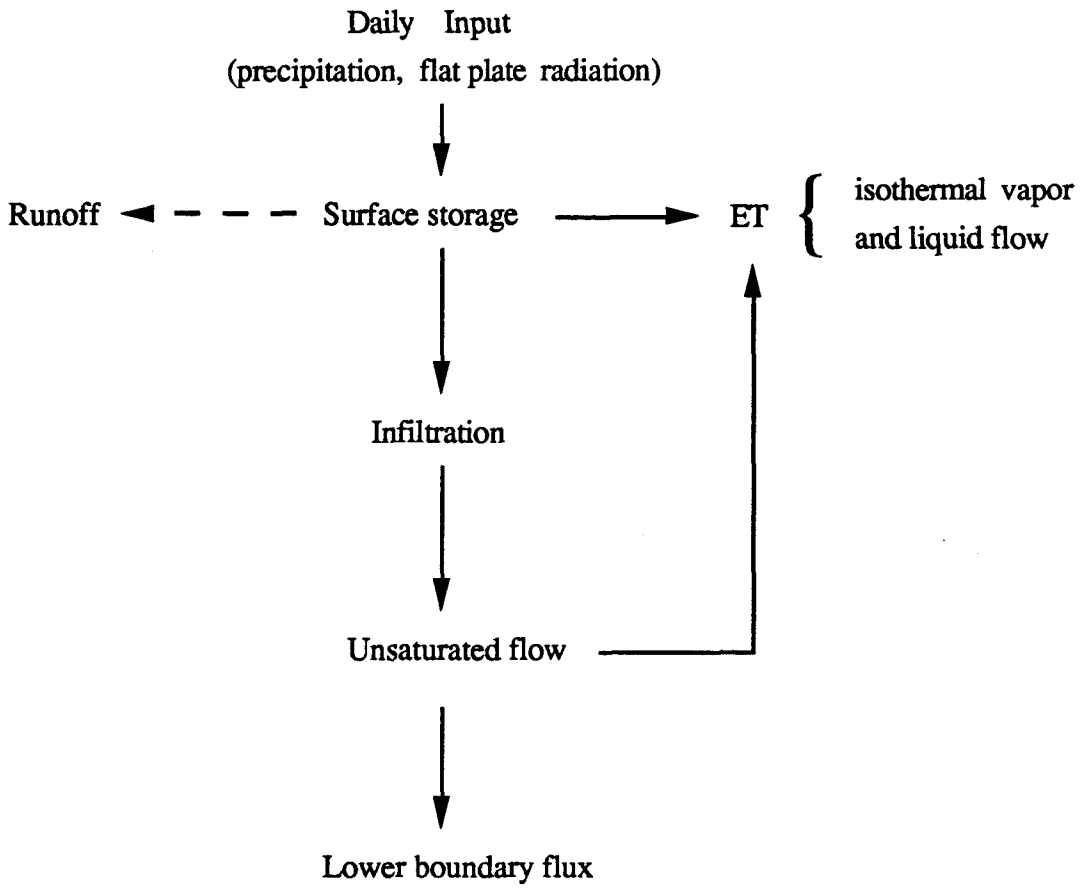

Figure 25. Hydrologic processes considered in computer program QBINFIL

Code Structure

A main program, QBINFIL, controls execution of the individual modules. Grid cells to be simulated are selected within the main program. Dimensioning of variables, initialization, and setting constants also occurs within the main module. The simulation time algorithm is also controlled from within the main program (Figure 26). Modules called before the time loop and simulation begin include TOPO, SOILS, SETUP, and GRAPH. During program execution within the time loop, PREC, INFIL, GRAPH and OUTFILES modules are called. Within the INFIL module, BOTITRN is called and either UNSAT or EVAP and EVAPPIC, depending on evaporative demand.

TOPO Module

The TOPO module performs all topographic feature calculations (i.e., grid cell slope and aspect). The topographic data are read into the program, the cell topographic features are calculated, and a color graphics representation of the computed topographic features are displayed on the screen (Figure 27).

The available elevation data were obtained as an ASCII file containing the easting, northing, and elevation for each grid cell. A geographic information system (GIS) program, ARCINFO, was used to plot the points and elevations. Locations of the neutron-access holes (NAHs) were also plotted to help indicate the watershed location. Beginning at the watershed's outlet, individual slope vectors at each point were calculated by hand to the extent that a grid cell's general direction of slope was indicated (simple comparison of adjacent elevations in a given vector direction). At each point an arrow on the plot was drawn to indicate the general direction in which surface flow would be expected to occur. Points which indicated any possible flow toward the assumed channel location were included as part of the Pagany Wash watershed. Those grid points with slopes directed away from the channel were discarded. In this way, a watershed boundary was drawn. The roughly sketched basin boundary was digitized into the computer using ARCINFO. The digitized boundary was superimposed over the elevation points to generate a file, PAGANY.XY, containing the easting and northing coordinates of the points within the basin boundary. This is the first data file read by the TOPO module. As the data are being read, the grid cells are displayed on right portion of the screen.

The other data file required within the TOPO module, PAGANY.XYZ, contains a rectangular grid of the elevation points that completely encompasses the collection of

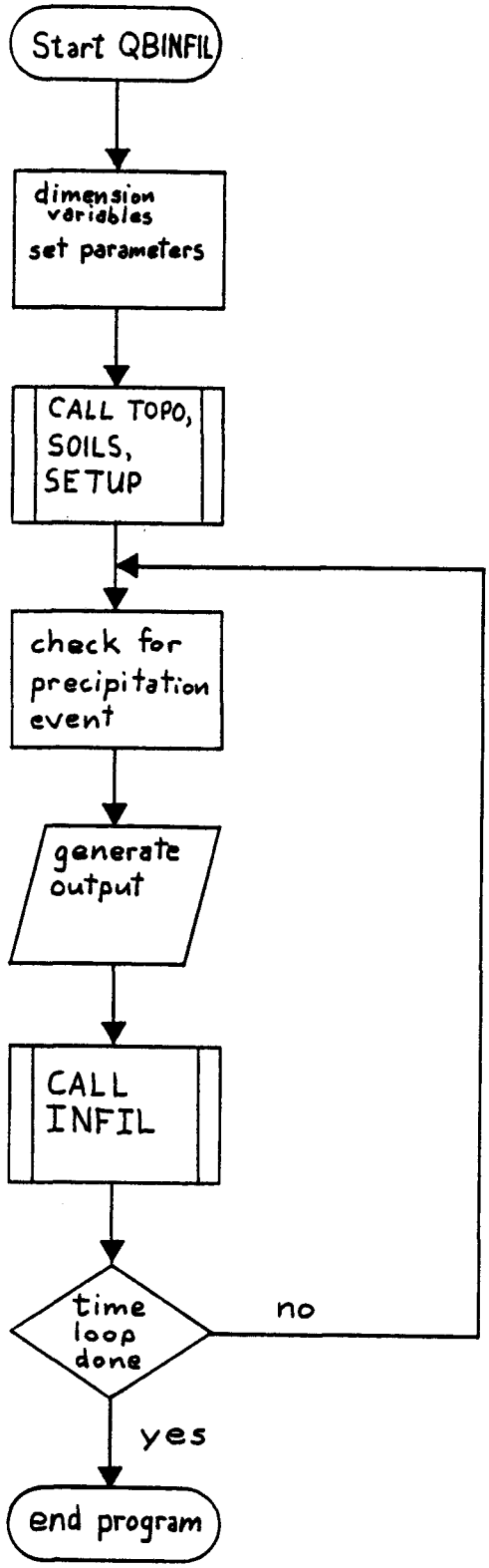

Figure 26. Flowchart for program QBINFIL

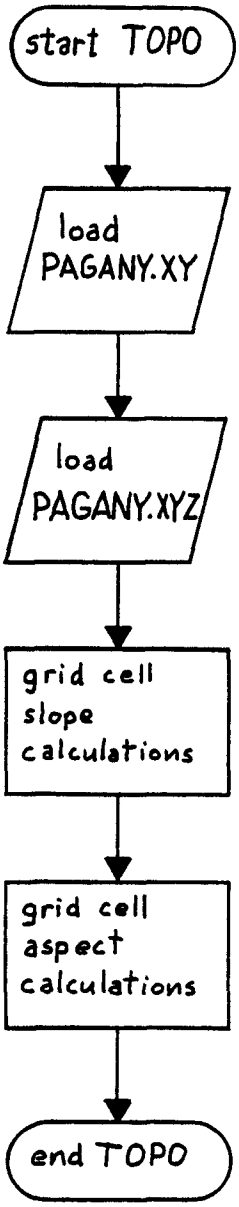

Figure 27. Flowchart for TOPO module

grid cells used to define Pagany Wash Watershed. This file contains the northing, easting, and elevation data for each point. Elevation data for points outside and adjacent to the watershed boundary are used in slope and aspect calculations for the grid cells along the watershed boundary.

Slope calculations are performed by computing the slope component in each coordinate direction. The slope component for the east-west direction, easting, is computed using

$$\text{slopex} = \frac{(z(x+1,y) - z(x-1,y))}{(2*dx)} \tag{25}$$

where dx is the grid cell spacing in the x-direction (75.7 m or 250 ft). The slope component for the north-south direction is computed using

$$\text{slopey} = \frac{(z(x,y+1) - z(x,y-1))}{(2*dy)} \tag{26}$$

Once both slope components are calculated the resultant slope angle is computed using

$$\text{ang}(g) = (\tan^{-1}((\text{slopex}^2 + \text{slopey}^2)^{1/2})) * \frac{180}{\pi} \tag{27}$$

where g is the grid cell number (1 to 477) and the units are degrees.

The grid cell aspect calculations are next performed. If the computed slope is zero, a value of zero is assigned to the aspect, otherwise aspect is assigned as previously explained (north = 360 degree, positive in clockwise direction). The aspect calculation is performed using the grid cell's slope components. Aspect for the four coordinate direction and a horizontal plane is assigned as follows:

asp(g) = 360 (for slopex = 0 and slopey < 0)

asp(g) = 180 (for slopex = 0 and slopey > 0)

asp(g) = 0 (for slopex = 0 and slopey = 0, no aspect)

asp(g) = 90 (for slopex < 0 and slopey = 0)

asp(g) = 270 (for slopex > 0 and slopey = 0)

The cell's in which both slope components are non-zero base aspect calculations on the slope component magnitudes using the variable angle, as given by

angle = ATN(ABS(slopey/slopex)) * 180 / pi

where pi = 3.14159. The remaining aspect are computed as follows:

asp(g) = 90 - angle (for slopex < 0 and slopey < 0)

asp(g) = 90 + angle (for slopex < 0 and slopey > 0)

asp(g) = 270 - angle (for slopex > 0 and slopey > 0)

asp(g) = 270 + angle (for slopex > 0 and slopey < 0)

The computed slopes for each grid cell are displayed on the screen using a color scheme; each color represents a specified range of slope values. Finally, selected grid cells were identified on the screen using different colors. In this way, it was possible to adapt the grid cell display to portray different types of information.

SOILS Module

The SOILS module sets model depth parameters and reads grid cell soil depths for each grid cell (Figure 28).

Calculations for unsaturated flow (described below) require a set of nodes spaced vertically within the soil column. Each node represents a soil element. In this way the soil profile is discretized into a set of soil elements. The soil elements are represented by the variable d(i), where i is and whole number from 0 to 20. Node d(1) represents the soil surface. The specified node depths are 0, 0.0125, 0.025, 0.05, 0.1, 0.25, 0.5, 1, 1.5, 2.25, 3, 4, 5, 6, 8, 10, 12, 16, 20, and 24 m. Node spacing is initially small and increases with depth to allow the greatest detail to be located at the surface where the greatest changes in water content occur (Figure 29). If there were a large node spacing at the top of the layer, the infiltration rate would remain constant until the first few nodes wet (Campbell, 1985).

Two ASCII data files are required in the SOILS module. The first file, SOIL1.DAT, contains the easting, northing, and depth in meters for the grid cells designated as channel alluvium. The second file, SOIL2.DAT, contains the easting, northing, and soil depth in meters for the grid cells designated as terrace alluvium.

The soil depths for grid cells not designated as alluvium are estimated using the grid cell slope and upland soil depth data from Schmidt (1984). Grid cells with slopes greater than 35 degrees were assigned a depth of 0.1 meters. Grid cells with slopes less than 5 degrees were assigned a depth of 1.0 meters. The remaining grid cells were assigned depths based on a linear distribution of soil depth ranging between 0.1 and 1.0 meters as a function the cell's slope.

The final procedure within the SOILS module matches the actual soil depth to the nearest node greater than or equal to the actual soil depth for each grid cell. This is done by determining the deepest soil node, the maximum i-variable in the d(i) term. The deepest soil node is represented by the variable m(g) where g is a whole number

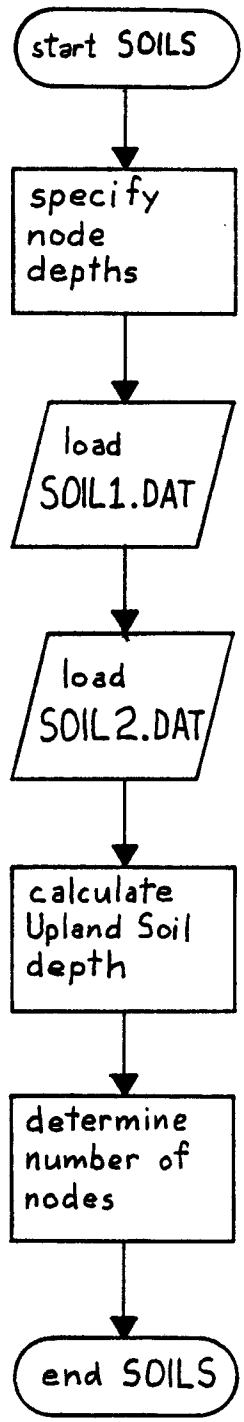

Figure 28. Flowchart for SOILS module

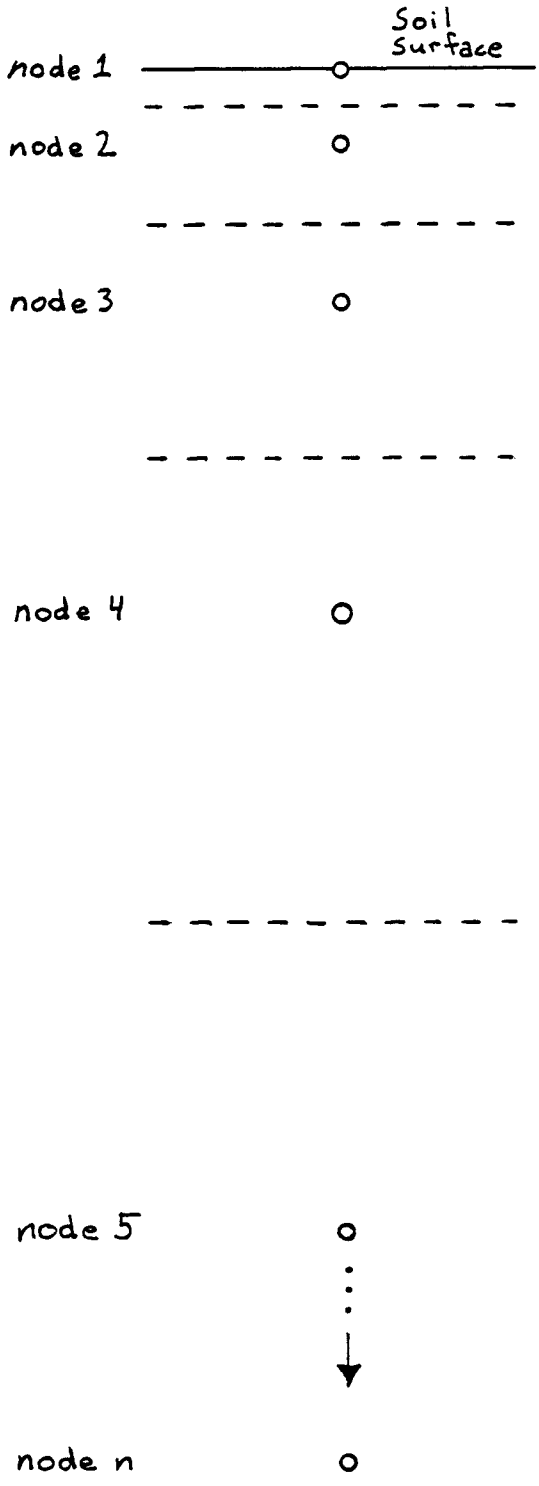

Figure 29. Soil nodes

representing the grid cell number (1 to 477). In some simulations, it may be desired to specify the depth of the interface between the two unsaturated layers. This can be done by specifying a particular maximum node element within the node matching loop (e.g. m(g) = 15).

SETUP Module

The SETUP module procedures include specification and calculation of different soil parameters, soil element calculations, setting initial water contents, and loading precipitation and solar radiation data from ASCII files (Figure 30).

The first procedure within SETUP specifies the four main parameters for the three types of surface soils included in this study (soil(g) = 1 for wash alluvium, soil(g) = 2 for terrace alluvium, and soil (g) = 3 for upland soil). The four parameters are the mean particle diameter, dg(i) in mm, the geometric standard deviation, sd(i) in percent, the saturated hydraulic conductivity, cond(i) in m/s, and the porosity, por(i) as a decimal fraction. The i term represents which of the three soil types is being specified.

To minimize computations, calculations are only performed for the grid cells selected for simulation. The variable used to identify the selected grid cells is sm(s) where s is a whole number representing the grid cell. The SETUP module contains a loop to match the simulation coordinates with grid cell coordinates to specify which grid cell number, g, to match with each simulation location (e.g., sm(1) = 376). During calculations it is often necessary to change node depths for various reasons at a simulation location. A variable related to the node depth, d(i), was introduced to accommodate this change, nd(s,i). This variable allows changing the node depths at each simulation location, s, without changing the values of the initial distribution of node depths given by d(i). Using the nd(s,i) variable, node depths for the lower soil layer are specified within SETUP.

Upper layer soil variables are specified or calculated next. These variables include ws(s,i), the porosity; ks(s,i), the saturated hydraulic conductivity; pe(s,i), the air entry potential (equation 16.); b1(s,i), the exponent for calculating matric potential (equation 17); b2(s,i), the inverse of b1(s,i); n(s,i), the exponent for calculating unsaturated hydraulic conductivity (equation 19); n1(s,i), one minus n(s,i); w#(s,i), the volumetric water content for a node at the beginning of the time step; wn#(s,i), the volumetric water content at the end of the time step; and a variable representing the thickness of a soil element, v(s,i), given by

$$v(s,i) = (nd(s,i+1) - nd(s,i-1))/2 \qquad (28)$$

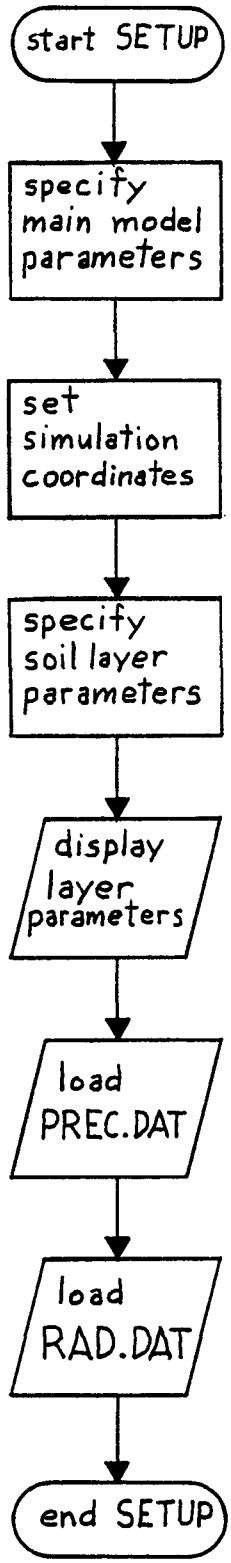

Figure 30. Flowchart for SETUP module

The lower soil layer variables are specified or calculated somewhat differently than the upper soil layer variables. When the lower layer is designated as tuff, the mean particle diameter, dg, and geometric standard deviation, sd, are not used. Instead a regression was performed to obtain hydrologic properties for the different types of tuff. Except for the water content, the remaining variable specifications are similar to that used for the upper soil layer.

Within the SETUP module, the surface storage variable for each simulation location, stor#(s), is set to zero. If different initial storage conditions are desired, the variable could be set either at this location in the program or in the main program module.

Two ASCII data files are loaded into the program in the SETUP module. The first file, PREC.DAT, is a file containing the Julian day number and the precipitation data, in inches, for that day. The other file, RAD.DAT, contains the Julian day number and the flat plate soil radiation data, $k\downarrow$, in MJ/m^2.

An additional procedure included in the SETUP module is screen output of the variables and parameters that were specified for each simulation location. The module SIMSTAT is called from within SETUP to display the output. This output permits the user to monitor the computations and verify the parameters prior to execution of the actual watershed simulation. The screen output can also be sent to the printer to get a hard copy of the information. The choice of parameters to be displayed on the screen can be easily modified.

PREC Module

The PREC module's function is to transfer water from the precipitation storage term, prec(s,day), to each simulated grid cell's surface storage element, stor#(s) (Figure 31). Daily computer model precipitation is released beginning at 15:00. Precipitation is applied during a time step is subtracted from the total amount stored. Remaining precipitation applied at the beginning of subsequent time steps using the greatest allowable intensity (currently 5.1 cm/hr or 2.0 in/hr) until the storage is deleted.

GRAPH Module

The GRAPH module displays the soil profile water content curves during program execution. The procedures performed within the graph module include illustration of soil moisture movement and surface water storage conditions at a

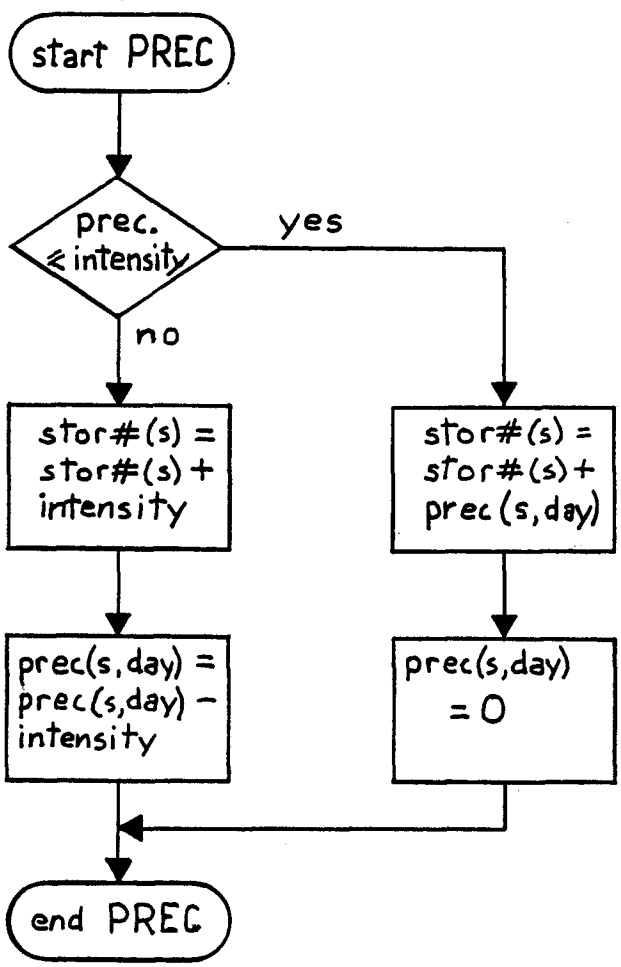

Figure 31. Flowchart for PREC module

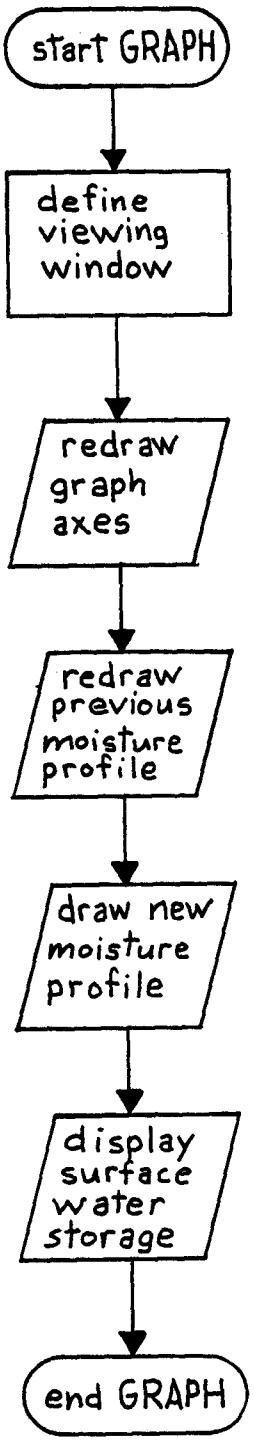

Figure 32. Flowchart for GRAPH module

simulation location (Figure 32). As currently configured, the screen output can accommodate up to three soil profiles being simultaneously displayed.

A soil profile is represented on the screen by a graph with the vertical axis being the soil depth (m), and the horizontal axis the volumetric water content (m^3/m^3). A red line is used to connect the soil water contents at each node at the end of each time step. A yellow line is used to show the water contents at each node for the previous time step. Both lines change as the simulation progresses. By this means, the movement of the soil moisture profile can be viewed as program execution proceeds.

The boundary between the two soil layers is represented on the screen by a horizontal line at the appropriate depth. The depth of the profile illustrated on the screen can be changed by altering the WINDOW.

An additional area is designated above each profile to show surface water storage (stor#(s) > 0). When a precipitation event or runoff fills a grid cell's surface storage element, the amount is displayed by filling solid a portion of the area on the screen to represent the event. This display feature is useful for showing infiltration and the soil water content profile response to infiltration. When soil profiles with different hydraulic properties are simulated, this display feature is useful for comparison of relative infiltration capacities.

INFIL Module

The INFIL module controls the movement of water through the two layer unsaturated flow system, from surface storage of water to flow out of the bottom of the simulated soil profile. The INFIL module contains procedures for computing rates of ET, volume of surface storage, rates of infiltration, soil water redistribution, fluxes of water between the two soil layers, computing water contents and total mass balance errors, and producing screen output of selected variables. The INFIL module uses three sub modules to simulate water flow within the soil profile. The first module, BOTITRN (BOTtem ITeRatioN), calculates the rate of water flow out of the bottom of the upper soil layer. The second module, UNSAT (UNSATurated flow), computes rates of unsaturated flow and redistribution in both soil layers. The third module, EVAP (EVAPoration), computes rates of unsaturated flow and redistribution in the top layer when an evaporative demand exists at the soil surface. The EVAP module is nearly identical as the UNSAT module except for additional terms related to the ET process. Discussion of these three additional modules is presented later. The discussion that follows is facilitated using simplified flowcharts of the INFIL module's

procedures. Further understanding can be attained by examining source module's code in the appendix.

The INFIL module begins by calculating the potential at each node based on the nodes initial water content, w#(s,i). Profile simulation starts with the upper soil layer. To help impose the desired boundary condition, the depth of the top node of the lower layer is set to a very large number (Figure 33a). The BOTITRN module is called to set the initial conditions at the top node of the lower layer to give the desired flux at the bottom of the upper layer. Surface flux conditions are then calculated. The maximum infiltration rate into the soil profile due to flow from surface water storage is given by the variable, flux# (m/s) as described by

$$\text{flux\#} = \text{stor\#(s)}/dt \tag{29}$$

where stor#(s) is the depth of water contained in the surface storage element (measured in meters), s is a whole number representing the simulation location being specified, and dt is the model time step, 900 seconds (15 minutes). The maximum infiltration rate into the soil profile due to matrix potential gradients at the beginning of the time step (infiltration capacity) is given by

$$\text{flamax\#} = \frac{\text{p\#(s,1)}*\text{k\#(s,1)}-\text{p\#(s,2)}-\text{k\#(s,2)}}{(\text{nd(s,2)}-\text{nd(s,1)})\text{n1(s,1)}} + \text{k(s,1)} + \frac{(\text{wmx\#}-\text{w\#(s,1)})*\text{v(s,j)}}{dt} \tag{30}$$

where the node variable j equals 1 and wmx# is the maximum permissible water content for the surface node. The variable wmx# is given by

$$\text{wmx\#} = 0.9 * \text{ws(s,j)} \tag{31}$$

where ws(s,j) is the node porosity. The reason the actual porosity cannot be used relates to the mechanism for solving redistribution. From equation 30, it is seen that the infiltration capacity is a function of the moisture conditions at both the surface node (node 1) and the node beneath it (node 2). During an infiltration event, the water content at node 2 increases. The actual infiltration is calculated using the water contents at the end of the time step. If the infiltration capacity calculated using equation 30 is greater than the actual amount of water that can enter the soil, the program will not

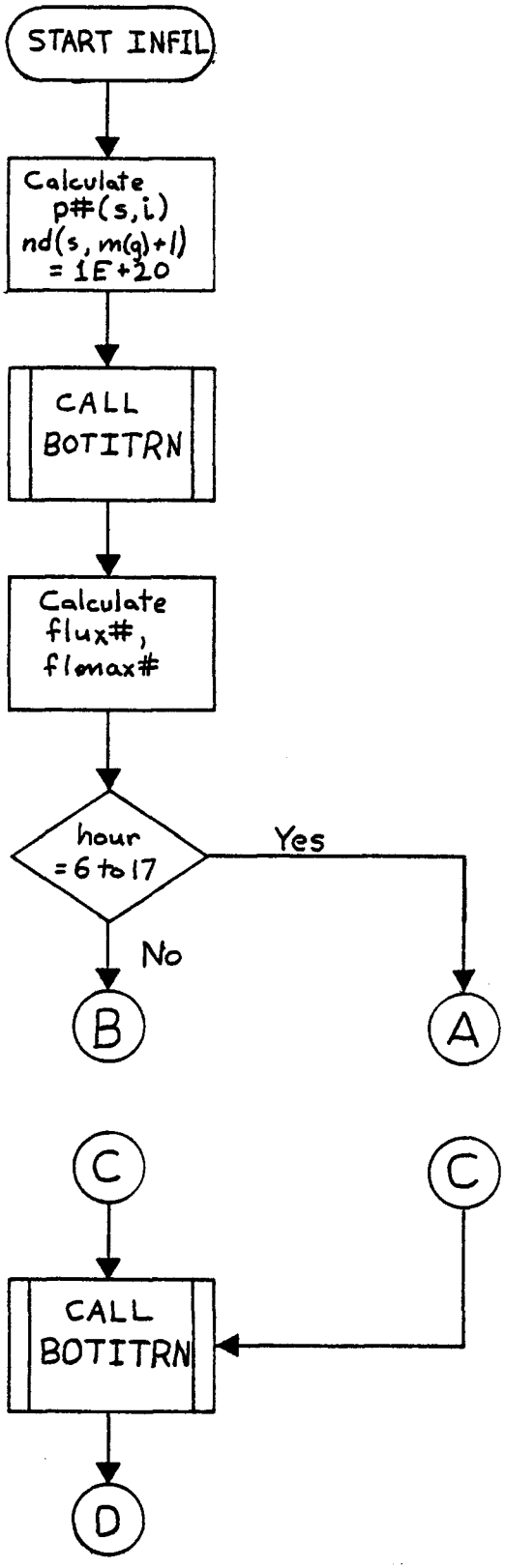

Figure 33a. Flowchart for INFIL module; initial calculations

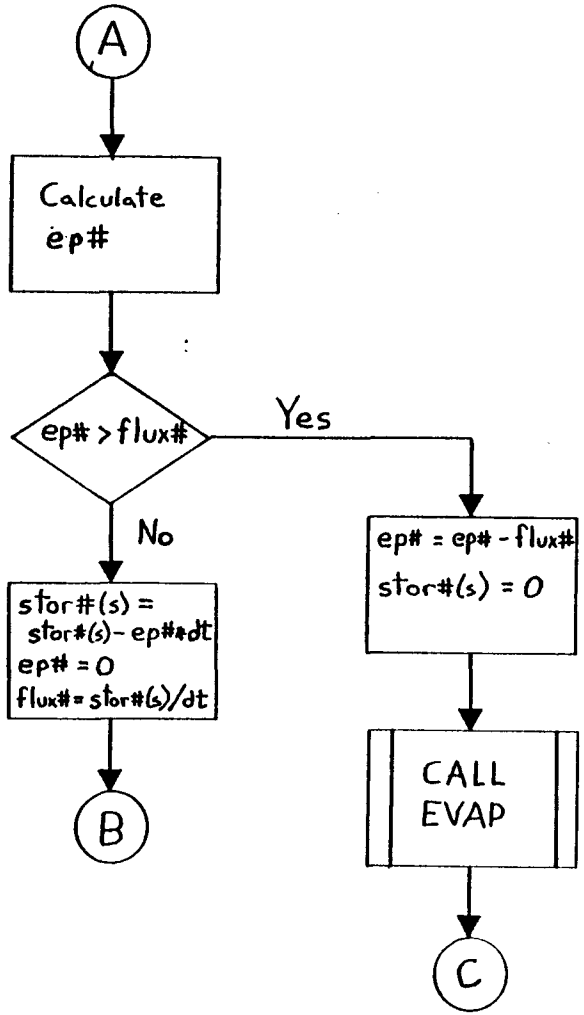

Figure 33b. Flowchart for INFIL module; upper layer ET calculations

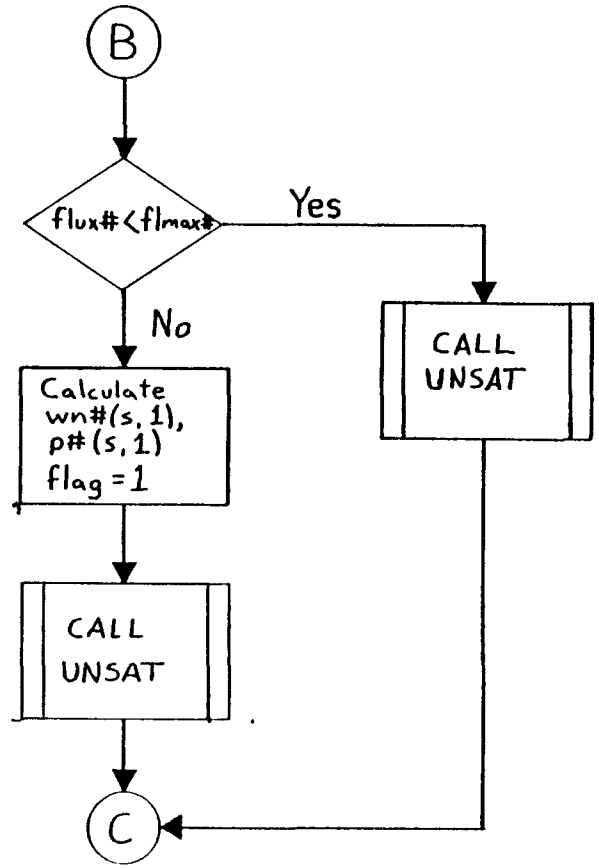

Figure 33c. Flowchart for INFIL module; upper layer unsaturated flow calculations

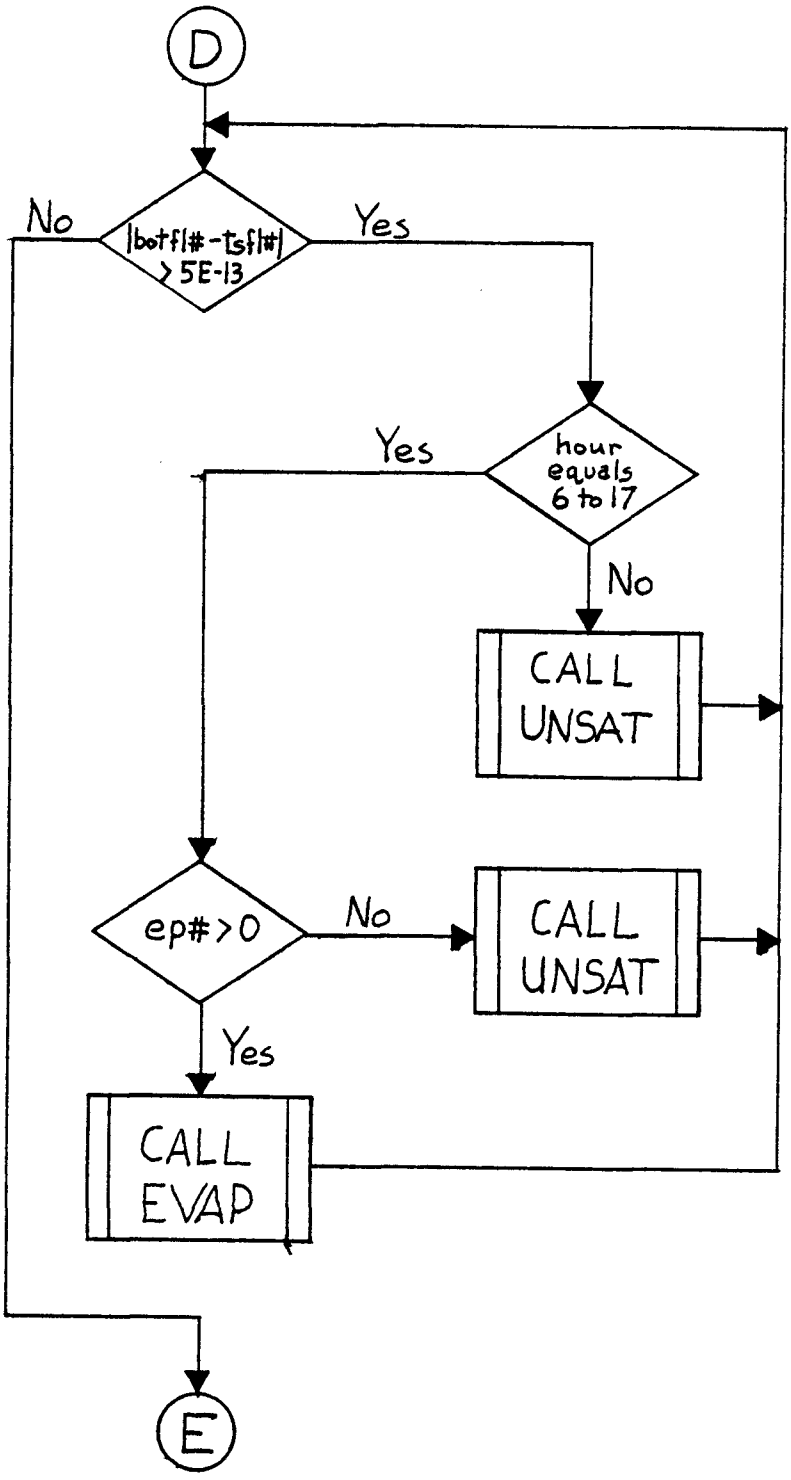

Figure 33d. Flowchart for INFIL module; matching flows between layers

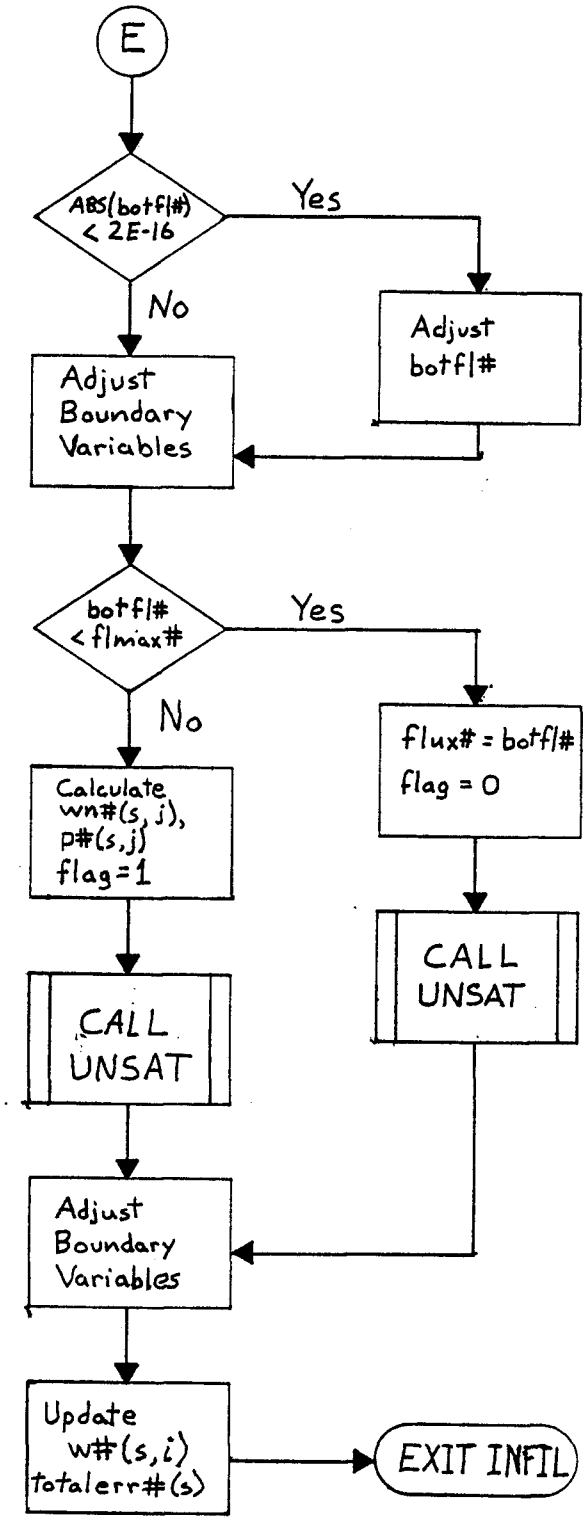

Figure 33e. Flowchart for INFIL module; lower layer unsaturated flow calculations

converge to a solution. The surface water content reduction is partially justified by the fact that in actual field conditions, water will not completely fill the empty soil pore volume due to a small amount of entrapped air.

The INFIL module also computes ET rates. If the time is between 6:00 and 18:00, the potential ET for the current time step described by the variable ep#, and is given by

$$\text{ep\#} = 3.1428*\text{et(s,day)}/1000/86400 * \sin\left(0.2618*\left(\left(\text{hour}+\frac{\text{min}}{60}\right)-6\right)\right) \quad (32)$$

where et(s,day) is the potential calculated ET (mm) for the simulated grid location. Figure 33b shows the sequence of steps. If ep# is greater than flux# then the amount of water stored in the surface storage element is subtracted from ep# and the corrected evaporative flux is applied. If ep# is not greater than flux# then ep# is subtracted directly from the surface storage element, ep# is set to 0, flux# is recalculated, and the program continues execution (Figure 33c).

The flowchart shown in Figure 33c demonstrates the two different conditions for applying a boundary condition at the soil surface. If flux# is less than the calculated infiltration intensity, flmax#, then specified infiltration rate, flux#, is added to node 1's mass balance term in the UNSAT module which converges to the solution. If flux# is not less than the calculated infiltration intensity, then a second boundary condition is applied to the UNSAT module for solution iteration. The second boundary condition is a specified matric potential at node 1. This boundary condition is applied by first calculating the water content at node 1 using the same procedure as in equation 31, calculating the potential at node 1 based on that water content, specifying the proper value for the switch variable, flag, and calling the UNSAT module.

The BOTITRN module recalculates the bottom flux from the upper soil layer using the most recently computed water contents.

The fluxes between the two soil layers are matched using the most recently computed water contents (Figure 33d). At this section of the code, all surface flux values have been set, allowing simple routing based on the time and the value of ep# (Figure 33d). Iteration is continued until the absolute value of the difference between the bottom flow of the upper layer, botfl#, to the top flow of the lower layer, tsfl#, must be within the convergence criterion (5×10^{-13} m/s).After the convergence criterion has been achieved, the program prepares for simulating the redistribution within the lower layer (Figure 33e). Due to the nature of the solution scheme and the convergence

criterion within the UNSAT module, if the value of the top flux into the lower layer (botfl# at this point) is less than 2×10^{-16} m/s, unacceptable mass balance errors occur. The algorithm used to compute water contents for the lower layer is the same as that used for the upper layer except that the reduction for the water content at the top node of the lower layer (when maximum infiltration conditions exist) is 98% of the porosity instead of 90% used for the upper layer. With the slower hydraulic properties in the tuff, the maximum water content does not need to be reduced as much as the with the alluvium during maximum infiltration conditions.

Once calculations for the lower layer are completed, the initial water content at each node for the next time step is set to the ending water content at each node for this time step. The total mass balance error, ttlerr#(s) (meters of water), is given by

$$\text{totalerr\#(s)} = \text{totalerr\#(s)} + \text{er\#} + \text{ter\#} + (\text{tsfl\#}-\text{botfl\#})*dt \qquad (33)$$

where er# is the mass balance error for the upper layer during the current time step, ter# is the mass balance error for the lower layer during the current time step, and (tsfl# - botfl#) * dt is the error from flow matching between the two layers.

At the end of each time step INFIL module displays the values for the surface storage element, the water content at node 1, the cumulative flow between layers, the cumulative mass balance error, and the cumulative amount of water that has been removed by ET.

BOTITRN Module

The BOTITRN module matches the flow between the two layers of this model. To simplify matters, the variable k is set equal to the bottom node element of the upper layer, m(g) (Figure 34). The flow capacity, flmax#, is calculated for the top of the lower layer. The potential at node k, p#(s,k), is calculated using the latest value of the water content at that node, wn#(s,k).

The concept for matching potentials across the boundary is used to solve for the initial water content of the lower layer. This is done by solving for the matric potential of the bottom element of the upper layer using equation 18 and resolving this equation to determine the water content for the top element of the lower layer using the upper layer's parameters so that the desired flux is achieved. If the calculated water content for the lower layer is greater than its porosity, ws(s,i), then the water content is reduced to 98% saturation. The reduction to less than saturation is necessary to allow program convergence. The BOTITRN module attempts to match boundary matric potentials as

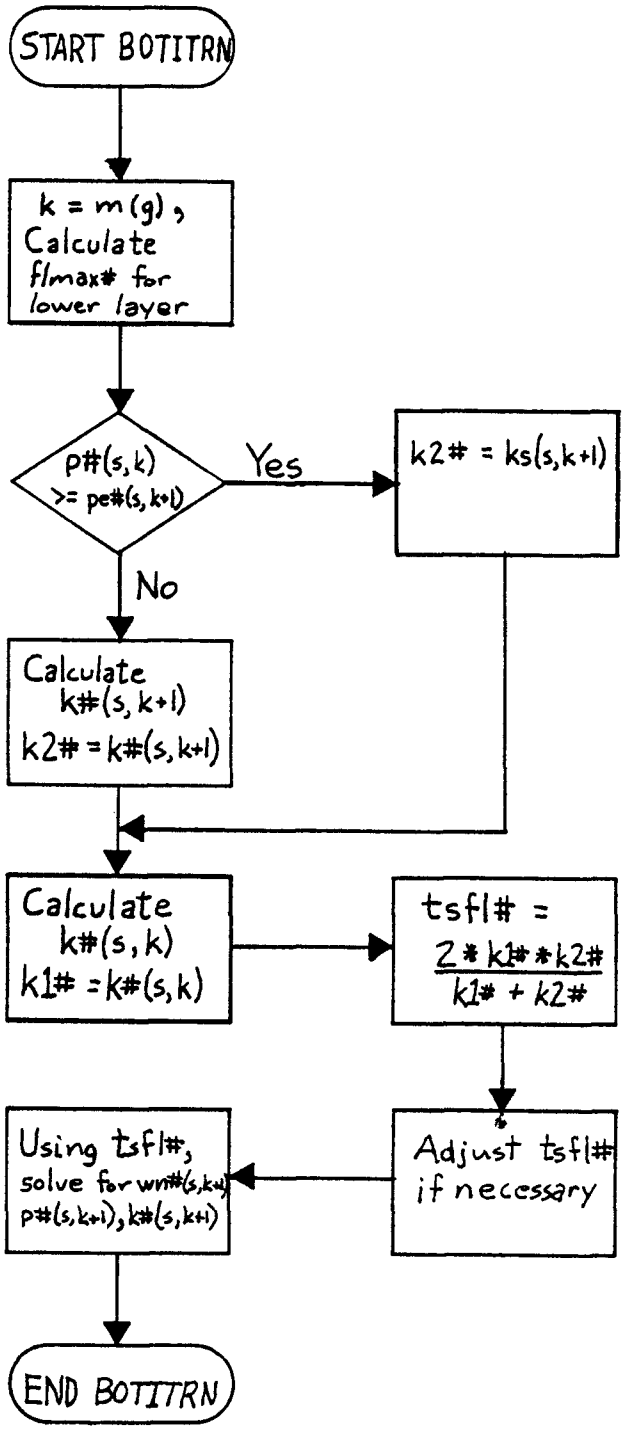

Figure 34. Flowchart for BOTITRN module

closely as possible and calculates the conductivity for each of the adjacent boundary nodes based on their calculated matric potentials. If the calculated potential at node k is greater than or equal to the air entry potential of the node immediately beneath it, pe#(s,k+1), then a new variable, k2#, is set equal to the saturated conductivity of the lower layer. This is done because the potential at node k+1 cannot be greater than its air entry potential. If the calculated potential at node k is less than the air entry potential at node k+1, then k2# is set equal to a calculated hydraulic conductivity for node k+1 using the potential at node k. Another new variable, k1#, is set equal to the calculated value for the hydraulic conductivity at node k. Using these two new variables, k1# and k2#, the equivalent hydraulic conductivity is calculated using

$$tsfl\# = 2 * k1\# * k2\# / (k1\# + k2\#) \quad (34)$$

where tsfl# is the flow into the top of the lower soil layer (m/s). If the magnitude of tsfl# is less than 2×10^{-16}, then its magnitude is set equal to 2×10^{-16} for computational purposes. If tsfl# is greater than flmax# then it is set equal to flmax#. Using the updated value for tsfl#, the mass balance equation at node k+1 is solved for the water content that would give the desired flux using, however, the parameters from the upper layer. This may create unrealistic values for the node k+1 since they are based on the node k parameters, but it allows convergence to the desired flux. The BOTITRN module matches the layers' flows until within the tolerance specified in the INFIL module (5×10^{-13} m/s). It is much more difficult to control a flux at the bottom of a profile than it is at the top of a profile using the current solution scheme in UNSAT. UNSAT applies the most recently computed value of tsfl# to the top of the lower layer and converge to a more accurate solution quicker, ensuring better mass balance. Parameters for node k+1 are later set to their normal values in the INFIL module.

UNSAT Module

UNSAT solves Richards' equation using a finite difference scheme developed by Campbell (1985). UNSAT first sets the convergence variable, se#, equal to one to cause the program to enter the solution loop. Then the iterative loop is begun and continues until se# less than 1×10^{-16} m/s (Figure 35). Prior to each run within the loop, se# is reset to 0 and the hydraulic conductivities at each node are calculated using equation 20.

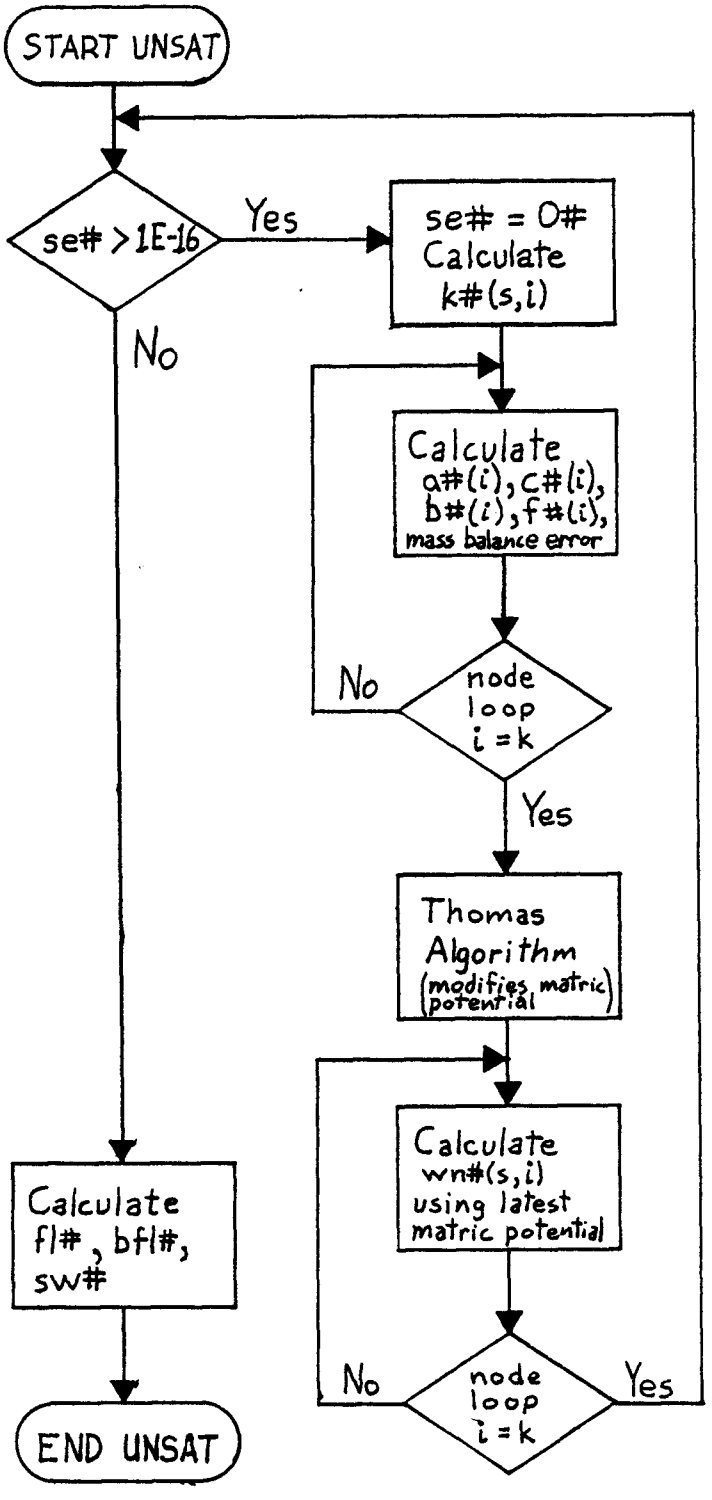

Figure 35. Flowchart for UNSAT module

The module relies on the Newton-Raphson method to obtain a solution (Campbell, 1985). Four variables are calculated for each node. The mass balance at each node, f#(i), is calculated by

$$f\#(i) = \frac{p\#(s,i)*k\#(s,i) - p\#(s,i-1)*k\#(s,i-1)}{(nd(s,i) - nd(s,i-1))*n1(s,i)} - \frac{p\#(s,i+1)*k\#(s,i+1) - p\#(s,i)*k\#(s,i)}{(nd(s,i+1) - nd(s,i)*n1(s,i)} + \frac{v(s,i)*(wn\#(s,i) - w\#(s,i))}{dt} - k\#(s,i-1) + k\#(s,i) \quad (35)$$

Writing equation 35 for each node using the Newton-Raphson method results in a tridiagonal matrix system of equations. The variable on the subdiagonal, a#(i), is given by

$$a\#(i) = \frac{-k\#(s,i-1)}{(nd(s,i) - nd(s,i-1))} + \frac{n(s,i-1)*k\#(s,i-1)}{p\#(s,i-1)} \quad (36)$$

where a#(i) is the derivative of f#(i) with respect to p#(i-1). The superdiagonal variable, c#(i), is next calculated as given by

$$c\#(i) = \frac{-k\#(s,i+1)}{(nd(s,i+1) - nd(s,i))} \quad (37)$$

where c#(i) is the derivative of f#(i) with respect to p#(i+1). The central-diagonal variable, b#(i), is given by

$$b\#(i) = \frac{k\#(s,i)}{(nd(s,i) - nd(s,i-1))} + \frac{k\#(s,i)}{(nd(s,i+1 - nd(s,i))} - \frac{n(s,i)*k\#(s,i)}{p\#(s,i)} - \frac{v(s,i)*wn\#(s,i)}{(b1(s,i)*p\#(s,i)*dt)} \quad (38)$$

where b#(i) is the derivative of f#(i) with respect to p#(i). If the current node is the top node of the profile and the variable flag equals zero, then the desired upper flux, flux#, is added to the mass balance term for the top node, f#(1). If the current node is not the top node and variable flag equals one, then the mass balance term is calculated by

$$se\# = se\# + ABS(\ f\#(i)\ ) \quad (39)$$

where ABS means absolute value. If the variable flag equals zero, the mass balance term is also calculated using equation 39, except that the top node is included in the calculation.

Immediately following this loop, the variables f#(1) and c#(1) are set equal to zero if the variable flag equals one. In this way the upper soil element potential can be set to a specified value. If the variable flag equals zero, the upper boundary condition is specified flux and the values of f#(1) and c#(1) remain unchanged.

The Thomas Algorithm is used to compute the potentials at each node; water contents for each node are calculated using these potentials.

Once the mass balance criterion is satisfied, the program calculates mass balance error for the profile. The actual flux that occurred at the surface, fl#, as given by

$$fl\# = \frac{(p\#(s,1)*k\#(s,1)-p\#(s,2)*k\#(s,2))}{((nd(s,2)-nd(s,1)*n1(s,1))} + k\#(s,1) + \frac{(wn\#(s,1)-w\#(s,1))*v(s,1)}{dt} \quad (40)$$

which is based on solving for the upper flux from the mass balance calculations at node 1, f#(1). The bottom flux, bfl#, is also required and is given by

$$bfl\# = \frac{(p\#(s,m(g))*k\#(s,m(g))-p\#(s,m(g)+1)*k\#(s,m(g)+1))}{((nd(s,m(g)+1)-nd(s,m(g)))*n1(s,m(g))+k\#(s,m(g))} \quad (41)$$

where bfl# is derived from the mass balance calculations for the bottom node, f#(m(g)). The change in water storage, sw#, is given by

$$sw\# = sw\# + v(s,i) * (wn\#(s,i) - w\#(s,i)) \quad (42)$$

where sw# is set equal to zero prior to calculation. Once these calculations have been performed, the UNSAT module procedure has been completed and the program returns to the INFIL module.

EVAP Module

The EVAP module is identical to the UNSAT module except that it includes additional procedures for computing changes in water content due to ET. The

flowchart for the UNSAT module (Figure 35) will be referred to in this discussion of the EVAP module with the additional procedures indicated.

Due to a greater difficulty in achieving convergence when ET is included, the mass balance tolerance has been relaxed slightly (solution converges when se# is less than or equal to 1×10^{-13} m/s). The next change comes after the hydraulic conductivities have been calculated and before the matrix calculations begin. The residual water content for the ET calculations, wr, is set at this point. A variable expressing the relative degree of saturation, theta, is calculated using

$$\text{theta} = (\text{wn\#(s,1)} - \text{wr})/(\text{ws(s,1)} - \text{wr}) \tag{43}$$

Based on the relative degree of saturation at the surface node, the actual flux leaving the surface at node 1 for the current time step is given by

$$\text{jv\#(0)} = 0.92*(1-\text{EXP}(-10*\text{theta}))*\text{ep\#} \tag{44}$$

where ep# is the potential ET for the current time step. The final additional variable calculated here is the derivative of jv#(0) with respect to p#(i), dj#(0). This variable is needed when calculating the central-diagonal matrix term.

The soil vapor conductivity, kv, is calculated by

$$\text{kv} = \frac{0.66*\text{dv}*\text{vp}*(\text{ws(s,i)}-(\text{wn\#(s,i)}-\text{wn\#(s,i+1)}))}{2*\text{gr}*(\text{nd(s,i+1)}-\text{nd(s,i)})} \tag{45}$$

where dv is vapor diffusivity term and vp is the saturation vapor concentration at soil temperature (Campbell, 1985). The variable for the gravitational constant, gr, was necessary for unit conversion. The vapor flux at a node, jv#(i), is given by

$$\text{jv\#(i)} = \text{kv} * (\text{h\#(i+1)} - \text{h\#(i)}) \tag{46}$$

where h#(i) is the relative humidity as calculated by equation 12. The first derivative of the vapor flow variable with respect to p#(i), dj#(i) is given by

$$\text{dj\#(i)} = \text{mw} * \text{h\#(i)} * \text{kv} / (\text{r} * \text{t}) \tag{47}$$

where mw is mass of a mole of water, r is the gas constant, and t is the Kelvin temperature (Campbell, 1985). The matrix diagonal variable a#(i) and c#(i) are unchanged between the UNSAT and EVAP modules. The central diagonal variable, b#(i), is changed slightly by adding the vapor derivatives as given by:

$$b\#(i) = (b\#(i) \text{ from UNSAT}) + dj\#(i-1) + dj\#(i) \tag{48}$$

The node mass balance variable, f#(i), is also altered slightly to include vapor flow as given by:

$$f\#(i) = (f\#(i) \text{ from UNSAT}) + jv\#(i-1) - jv\#(i) \tag{49}$$

The conditions that require routing to the EVAP module also require that it would be a flux controlled boundary with the upper flux equal to jv#(0). The mass balance convergence variable, se#, is calculated as discussed for the flag equals zero option in then UNSAT module.

The Thomas Algorithm remains unchanged from the UNSAT module. In addition to calculating the new water contents after the matric potentials have been updated, the node relative humidity, h#(i), is also updated.

The flux calculations are the same except for inclusion of the vapor flow terms. The calculated surface flux, fl# for UNSAT, is modified in EVAP by subtracting jv#(1). The calculated bottom flux, bfl# from UNSAT, is modified in EVAP by subtracting jv#(m(g)). Calculating the change in the soil water storage is the same. Once all these procedures have been completed, program control is returned to INFIL.

APPENDIX B
Source code listing for QBINFIL

```
'=========================================================
'      QBINFIL version 1.0 - This program is a watershed
'      model that includes precipitation,
'      evapotranspiration,infiltration, and redistribution
'      in a two-layer soil profile.  Model parameters are
'      derived from textural analysis.
'                by Michael J. Britch
'                    July 6, 1990
'=========================================================
DECLARE SUB EVAPPIC () : DECLARE SUB EVAP ()
DECLARE SUB UNSAT () : DECLARE SUB BOTITRN ()
DECLARE SUB SOILS () : DECLARE SUB TOPO ()
DECLARE SUB SETUP () : DECLARE SUB GRAPH ()
DECLARE SUB PRECIP () : DECLARE SUB INFIL ()
DECLARE SUB SURFLW () : DECLARE SUB OUTFILES ()
DECLARE SUB SIMSTAT ()
'~~~~~~~~~~~~~~~~~~ QBINFIL Program ~~~~~~~~~~~~~~~~~~~~~~
CLS
'******** define simulation locations ********
sim = 1: REM sim = number of grids for simulation
DIM sm(sim), xsm(sim), ysm(sim)
 xsm(1) = 566250: ysm(1) = 768750
' xsm(2) = 566000: ysm(2) = 768500
' xsm(3) = 562750: ysm(3) = 775000
'******** dimension variables ********
DIM a#(24), b#(24), c#(24), cp#(24), d(24), dj#(24),
DIM dp#(24), v(sim, 24), f#(24), h#(24), jv#(24),
DIM k#(sim, 24), p#(sim, 24), nd(sim, 24),
DIM wold#(sim, 24), ang(477), asp(477), soil(477),
DIM kd(366), b1(sim, 24), b2(sim, 24), depth(477),
DIM stor#(sim), ws(sim, 24), ks(sim, 24), m(477)
DIM n(sim, 24), n1(sim, 24), pe(sim, 24), et(sim, 366)
DIM x(477), y(477), w#(sim, 24), wn#(sim, 24), z(42, 55)
DIM prec(sim, 366), sd(3), dg(3), cond(3), por(3),
DIM oldpet#(3) oldaet#(3)
'******** performing initial procedures ********
xmax = 568750#: xmin = 558250#: ymax = 779750#
ymin = 766000# dx = 250!: dy = 250!
maxx = (xmax - xmin) / dx: maxy = (ymax - ymin) / dy
dt = 900: gr = 9.8: ttlit = 0
tol# = 4.78E-09 * dt * .001: intensity = .5: 'inches/dt
mw = .018: t = 293: r = 8.310001: dv = .000024: vp = .017
SCREEN 9: COLOR 11, 0: PRINT "      QBINFIL Simulation"
clock$ = " Day ### : hour ## : min ##"
CALL TOPO: CALL SOILS: CALL SETUP: CALL GRAPH
FOR s = 1 TO sim
 ttler#(s) = 0#: ttlbf#(s) = 0#
 ttlaet#(s) = 0#: ttlpet#(s) = 0#
 ttlevap#(s) = 0#: aet#(s) = 0#: pet#(s) = 0#
NEXT s
```

```
'******** time loop ********
FOR day = 227 TO 235
 at# = -.9729 + 20.98 * (day / 360 * 3.1416)
     - 2.0396 * (day / 360 * 3.1416) ^ 3
 ssg# = -44.957 - .13318 * (at# + 273.15)
      + 4.9452 * (at# + 273.15) ^ .5
 FOR s = 1 TO sim
  g = sm(s)
  rc# = 8.597 + (.024 * kd(day) ^ 2)
      - (.001 * (TAN(ang(g) / 180 * 3.1416) * asp(g)))
  rn# = ((rc# / .0009) * .58889 - 42.4394) * .0009
  et(s, day) = .4 * ssg# * rn#
 NEXT s
FOR hour = 0 TO 23
FOR min = 0 TO 45 STEP dt / 60
'******** precipitation and surface flow *******
  IF hour >= 15 AND prec(1, day) > 0 THEN CALL PRECIP
  IF day = 227 AND hour = 15 AND min = 0 THEN stor#(1) =
stor#(1) + .0302#
  IF day = 232 AND hour = 15 AND min = 0 THEN stor#(1) =
stor#(1) + .1786#
'******** main modules ********
  CALL GRAPH
  CALL OUTFILES
  CALL INFIL
  LOCATE 1, 52: PRINT USING clock$; day; hour; min
NEXT min: NEXT hour: NEXT day
CLS : PRINT "PROGRAM COMPLETE"
END
```

```
'~~~~~~~~~~~~~~~~~~ BOTtem ITeRatioN Module ~~~~~~~~~~~~~~~
SUB BOTITRN
SHARED nd(), k#(), p#(), w#(), wn#(), v(), sm(), m(), s,
SHARED g, flmax#, ks(), pe(), ws(), b1(), b2(), n(), n1(),
SHARED dt, tsfl#
 k = m(g): w1# = wn#(s, k)
'******** Calculate Maximum Flux ********
 wmx# = ws(s, k + 1) * .98
 k#(s, k + 2) = ks(s, k + 2) * (pe(s, k + 2)
/ p#(s, k + 2))^ n(s, k + 2)
 p#(s, k + 1) = pe(s, k + 1) * (ws(s, k + 1) / wmx#)
^ b1(s, k + 1)
 k#(s, k + 1) = ks(s, k + 1) * (pe(s, k + 1)
/ p#(s, k + 1))^ n(s, k + 1)
 flmax# = (p#(s, k + 1) * k#(s, k + 1) - p#(s, k + 2)
* k#(s, k + 2)) / ((nd(s, k + 2) - nd(s, k + 1))
* n1(s, k + 1)) + k#(s, k + 1)
+ (wmx# - w#(s, k + 1)) * v(s, k + 1) / dt
'******** Solve for Boundary Flow ********
 p1# = pe(s, k) * (ws(s, k) / w1#) ^ b1(s, k)
 IF p1# >= pe(s, k + 1) THEN
   k2# = ks(s, k + 1)
 ELSE
   k2# = ks(s, k + 1) * (pe(s, k + 1) / p1#) ^ n(s, k + 1)
 END IF
 k1# = ks(s, k) * (pe(s, k) / p1#) ^ n(s, k)
 tsfl# = 2 * k1# * k2# / (k1# + k2#)
 IF ABS(tsfl#) < 2E-16 THEN tsfl# = tsfl# / ABS(tsfl#) *
2E-16
 IF tsfl# > flmax# THEN tsfl# = flmax#
 p2k2# = (k1# - tsfl#) * (nd(s, k + 1) - nd(s, k))
* n1(s, k) + p1# * k1#
 w2# = ws(s, k) * (p2k2# / (pe(s, k) * ks(s, k)))
^ (1 / (b1(s, k) * n(s, k) - b1(s, k)))
 p#(s, k + 1) = pe(s, k) * (ws(s, k) / w2#) ^ b1(s, k)
 k#(s, k + 1) = ks(s, k) * (pe(s, k) / p#(s, k + 1))
^ n(s, k)
END SUB
```

```
'~~~~~~~~~~~~~~~~~~ EVAPoration Module ~~~~~~~~~~~~~~~~~
SUB EVAP
SHARED m(), d(), p#(), w#(), wn#(), ks(), pe(), stor#,
SHARED ws(), b1(), n(), mw, r, b2(), n1(), dt, eit, dp#(),
SHARED fl#, bfl#, ep#, nd(), k, gr, sw#, s, a#(), b#(),
SHARED c#(), v(), dj#(), f#(), jv#(), h#(), k#(), dv, vp,
SHARED sm(), t, soil(), g
eit = 0: p#(s, 0) = p#(s, 1): k#(s, 0) = 0
FOR i = j TO k: h#(i) = EXP(mw * p#(l, i) * gr / (r * t))
NEXT i
h#(k + 1) = h#(k): se# = 1
DO WHILE se# > 1E-13
se# = 0: eit = eit + 1
FOR i = 1 TO k
  k#(s, i) = ks(s, i) * (pe(s, i) / p#(s, i))^ n(s, i)
NEXT i
k#(s, k + 1) = ks(s, k) * (pe(s, k) / p#(s, k + 1))^n(s,k)
wr = .04
theta = (wn#(s, 1) - wr) / (ws(s, 1) - wr)
 jv#(0) = .92 * (1 - EXP(-10 * theta)) * ep#
 dj#(0) = -.92 * ep# * EXP(-10 * theta) * -10
/ (ws(s, 1) - wr) * -b2(s, 1) / p#(s, 1) * wn#(s, 1)
FOR i = 1 TO k
 kv = .66 * dv * vp / gr * (ws(s, i) - (wn#(s, i)
+ wn#(s, i + 1)) / 2) / (nd(s, i + 1) - nd(s, i))
 jv#(i) = kv * (h#(i + 1) - h#(i))
 dj#(i) = mw * h#(i) * kv / (r * t)
 a#(i) = -k#(s, (i - 1)) / (nd(s, i) - nd(s, i - 1))
+ n(s, (i - 1)) * k#(s, (i - 1)) / p#(s, (i - 1))
 c#(i) = -k#(s, (i + 1)) / (nd(s, i + 1) - nd(s, i))
 b#(i) = k#(s, i) / (nd(s, i) - nd(s, i - 1)) + k#(s, i)
/ (nd(s, i + 1) - nd(s, i)) - n(s, i) * k#(s, i)
/ p#(s, i) - v(s, i) * wn#(s, i) / (b1(s, i)
* p#(s, i) * dt) + dj#(i - 1) + dj#(i)
 f#(i) = ((p#(s, i) * k#(s, i) - p#(s, (i - 1))
* k#(s, (i - 1))) / (nd(s, i) - nd(s, i - 1))
- (p#(s, (i + 1)) * k#(s, (i + 1)) - p#(s, i)
* k#(s, i)) / (nd(s, i + 1) - nd(s, i))) / n1(s, i)
+ v(s, i) * (wn#(s, i) - w#(s, i)) / dt - k#(s, i - 1)
+ k#(s, i) + jv#(i - 1) - jv#(i)
 se# = se# + ABS(f#(i))
NEXT i
FOR i = 1 TO k - 1
  c#(i) = c#(i) / b#(i): f#(i) = f#(i) / b#(i)
  b#(i + 1) = b#(i + 1) - a#(i + 1) * c#(i)
  f#(i + 1) = f#(i + 1) - a#(i + 1) * f#(i)
NEXT i
dp#(k) = f#(k) / b#(k): p#(s, k) = p#(s, k) - dp#(k)
IF p#(s, k) > pe(s, k) THEN p#(s, k) = pe(s, k)
```

```
FOR i = k - 1 TO 1 STEP -1
  dp#(i) = f#(i) - c#(i) * dp#(i + 1)
  p#(s, i) = p#(s, i) - dp#(i)
  IF p#(s, i) > pe(s, i) THEN p#(s, i) =
     (p#(s, i) + dp#(i) + pe(s, i)) / 2
NEXT i
FOR i = 1 TO k
 wn#(s, i) = ws(s, i) * (pe(s, i) / p#(s, i)) ^ b2(s, i)
 h#(i) = EXP(mw * p#(s, i) * gr / (r * t))
NEXT i
LOOP
fl# = (p#(s, 1) * k#(s, 1) - p#(s, 2) * k#(s, 2))
/ ((nd(s, 2) - nd(s, 1)) * nl(s, 1)) + k#(s, 1)
+ (wn#(s, 1) - w#(s, 1)) * v(s, 1) / dt - jv#(1)
bfl# = (p#(s, k) * k#(s, k) - p#(s, k + 1) * k#(s, k + 1))
/ ((nd(s, k + 1) - nd(s, k)) * nl(s, k)) + k#(s, k)
- jv#(k)
sw# = 0#
FOR i = 1 TO k
  sw# = sw# + v(s, i) * (wn#(s, i) - w#(s, i))
NEXT i
END SUB
```

```
'~~~~~~~~~~~~~~~~~~ EVAPoration PICture Module ~~~~~~~~~~~~
SUB EVAPPIC
SHARED s, aet#(), pet#(), hour, min, dt, oldpet#(),
SHARED oldaet#()
IF s <= 3 THEN
 VIEW (s * 160 + 18, 66)-((s + 1) * 159 - 22, 145), , 11
 WINDOW (0, 0)-(48, 160)
 IF hour = 6 AND min = 0 THEN
   oldpet#(s) = 0#: oldaet#(s) = 0#
   LINE (0, 0)-(48, 160), 0, BF
 FOR x = 4 TO 44 STEP 4: LINE (x, 0)-(x, 160), 7: NEXT x
 FOR y = 20 TO 140 STEP 20: LINE (0, y)-(48, y), 7: NEXT y
 END IF
   x = INT((hour - 6) * 4 + min / 15)
   y1 = INT(pet#(s) * 1000000! * dt)
   y2 = INT(aet#(s) * 1000000! * dt)
   LINE (x - 1, oldpet#(s))-(x, y1), 13
   LINE (x - 1, oldaet#(s))-(x, y2), 10
   oldpet#(s) = y1: oldaet#(s) = y2
END IF
END SUB
```

```
'~~~~~~~~~~~~~~~~~~ GRAPH Module ~~~~~~~~~~~~~~~~~~~~~~~~
SUB GRAPH
SHARED w#(), wold#(), m(), sm(), sim, stor#(), nd()
last = sim
IF sim > 3 THEN last = 3
FOR s = 1 TO last
g = sm(s) : VIEW (s * 160, 150)-((s + 1) * 159, 349)
WINDOW (-10, -1200)-(60, 200)
contact = -(nd(s, m(g)) + nd(s, m(g) + 1)) * 40
LINE (1, -2)-(50, contact), 8, BF
LINE (1, contact)-(50, -1200), 6, BF
LINE (1, contact)-(50, contact), 11, BF
FOR y = -80 TO -1120 STEP -80
  LINE (1, y)-(50, y), 11, , &H1111
NEXT y
FOR x = 10 TO 40 STEP 10
  LINE (x, -2)-(x, -1200), 11, , &H1111
NEXT x
FOR i = 1 TO m(g) - 1
  x1 = INT(wold#(s, i) * 100): x2 = INT(wold#(s, i + 1) *
100)
  LINE (x1, -INT(nd(s, i) * 80))-(x2, -INT(nd(s, i + 1) *
80)), 14
NEXT i
i = m(g)
  x1 = INT(wold#(s, i) * 100): x2 = INT(wold#(s, i + 1) *
100)
  LINE (x1, -INT(nd(s, i) * 80))-(x1, contact), 14
  LINE (x1, contact)-(x2, contact), 14
  LINE (x2, contact)-(x2, -INT(nd(s, i + 1) * 80)), 14
FOR i = m(g) + 1 TO m(g) + 2
  x1 = INT(wold#(s, i) * 100): x2 = INT(wold#(s, i + 1) *
100)
  LINE (x1, -INT(nd(s, i) * 80))-(x2, -INT(nd(s, i + 1) *
80)), 14
NEXT i
LINE (0, 0)-(50, 400), 0, BF
water = INT(stor#(s) * 2000)
IF stor#(s) > .00001 THEN LINE (0, 2)-(50, water), 9, BF
LINE (0, 0)-(50, 0), 7: LINE (0, 0)-(0, -1200), 11
FOR i = 1 TO 18: LINE (-2, -i * 80)-(0, -i * 80), 11: NEXT
i
FOR i = 1 TO m(g) - 1
  LINE (INT(w#(s, i) * 100), -INT(nd(s, i) *
80))-(INT(w#(s, i + 1) * 100), -INT(nd(s, i + 1) * 80)),
12
  wold#(s, i) = w#(s, i)
NEXT i
i = m(g)
LINE (INT(w#(s, i) * 100), -INT(nd(s, i) * 80))-(INT(w#(s,
i) * 100), contact), 12
```

```
LINE (INT(w#(s, i) * 100), contact)-(INT(w#(s, i + 1) *
100), contact), 12
LINE (INT(w#(s, i + 1) * 100), contact)-(INT(w#(s, i + 1)
* 100), -INT(nd(s, i + 1) * 80)), 12
wold#(s, i) = w#(s, i)
FOR i = m(g) + 1 TO m(g) + 2
  LINE (INT(w#(s, i) * 100), -INT(nd(s, i) *
80))-(INT(w#(s, i + 1) * 100), -INT(nd(s, i + 1) * 80)),
12
  wold#(s, i) = w#(s, i)
NEXT i
wold#(s, m(g) + 3) = w#(s, m(g) + 3)
NEXT s
END SUB
```

```
'~~~~~~~~~~~~~~~~~~ INFILtration Module ~~~~~~~~~~~~~~~~~~
SUB INFIL
SHARED nd(), k#(), p#(), v(), w#(), wn#(), flux#, stor#(),
SHARED ttler#(), m(), dt, ks(), pe(), gr, ws(), b1(), n(),
SHARED b2(), n1(), sw#, d(), a#(), b#(), c#(), dp#(),
SHARED f#(), iit, x(), y(), ttlit, sim, sm(), flmax#, ep#,
SHARED et(), ttlevap#(), ttlbf#(), h#(), jv#(), tsfl#, mw,
SHARED dv, vp, flag, kd(), asp(), ttlaet#(), tol#, bfl#,
SHARED fl#, day, hour, min, g, j, k, r, s, t, soil(),
SHARED ttlpet#(), aet#(), pet#()
COLOR 12, 0: LOCATE 2, 7: PRINT "INFIL Module "
LOCATE 3, 1: PRINT "Simulation Execution"
VIEW PRINT 4 TO 25
FOR s = 1 TO sim
 g = sm(s): flag = 0: iit = 0
 FOR i = 1 TO m(g) + 3: p#(s, i) = pe(s, i) * (ws(s, i)
        / w#(s, i)) ^ b1(s, i): NEXT i
 p#(s, m(g) + 4) = p#(s, m(g) + 3): p#(s, 0) = p#(s, 1)
 k#(s, m(g) + 4) = ks(s, (m(g) + 3)) * (pe(s, (m(g) + 3))
       / p#(s, m(g) + 4)) ^ n(s, m(g) + 3)
 nd(s, m(g) + 1) = 1E+20
'******** Solving for potential boundary ********
 CALL BOTITRN
'******** Upper layer unsaturated flow ********
 sc# = .9
 flux# = stor#(s) / dt: j = 1: k = m(g)
 wmx# = ws(s, j) * sc#
 k#(s, j + 1) = ks(s, j + 1) * (pe(s, j + 1)
/ p#(s, j + 1)) ^ n(s, j + 1)
 p#(s, j) = pe(s, j) * (ws(s, j) / wmx#) ^ b1(s, j)
 k#(s, j) = ks(s, j) * (pe(s, j) / p#(s, j)) ^ n(s, j)
 flmax# = (p#(s, j) * k#(s, j) - p#(s, j + 1)
* k#(s, j + 1)) / ((nd(s, j + 1) - nd(s, j)) * n1(s, j))
+ k#(s, j) + (wmx# - w#(s, j)) * v(s, j) / dt
SELECT CASE hour
CASE 6 TO 17
  ep# = 3.1428 * et(s, day) / 1000 / 86400 * SIN(.2618
      * ((hour + min / 60) - 6))
  pet#(s) = ep#
  IF ep# > flux# THEN
    IF ABS(stor#(s)) > .0001 THEN
     ep# = ep# - flux#: stor#(s) = 0#
    END IF
    CALL EVAP
    aet#(s) = flux# - fl#
  ELSE
    stor#(s) = stor#(s) - ep# * dt: ep# = 0#
    flux# = stor#(s) / dt
    aet#(s) = pet#(s)
    IF flux# < flmax# THEN
      CALL UNSAT
    ELSE
```

```
      wn#(s, 1) = ws(s, 1) * sc#
    p#(s, 1) = pe(s, 1) * (ws(s, 1) / wn#(s, 1)) ^ b1(s,1)
      flag = 1: CALL UNSAT
    END IF
  END IF
CASE IS < 6, IS > 17
    IF flux# < flmax# THEN
      CALL UNSAT
    ELSE
      wn#(s, 1) = ws(s, 1) * sc#
    p#(s, 1) = pe(s, 1) * (ws(s, 1) / wn#(s, 1)) ^ b1(s,1)
      flag = 1: CALL UNSAT
    END IF
END SELECT
topfl# = fl#: botfl# = bfl#
er# = fl# * dt - sw# - bfl# * dt
'******** Matching fluxes between layers ********
'******** upper flux ********
CALL BOTITRN
DO WHILE ABS(botfl# - tsfl#) > 5E-13
 CALL BOTITRN
 SELECT CASE hour
 CASE 6 TO 17
  IF ep# > 0 THEN CALL EVAP
  IF ep# <= 0 THEN CALL UNSAT
 CASE IS < 6, IS > 17
  CALL UNSAT
 END SELECT
 topfl# = fl#: botfl# = bfl#
  er# = fl# * dt - sw# - bfl# * dt
LOOP
IF ABS(botfl#) < 2E-16 THEN botfl# = botfl# / ABS(botfl#)
* 2E-16
'******** lower flux ********
 nd(s, m(g) + 1) = d(m(g)) + 1: 'make sure this matches
with SETUP
 j = m(g) + 1: k = m(g) + 3: k#(s, j - 1) = 0#
 nd(s, j - 1) = -1E+30
 p#(s, j) = pe(s, j) * (ws(s, j) / w#(s, j)) ^ b1(s, j)
 IF botfl# < flmax# THEN
   flux# = botfl#
   flag = 0: CALL UNSAT
 ELSE
   wn#(s, j) = ws(s, j) * .98
   p#(s, j) = pe(s, j) * (ws(s, j) / wn#(s, j)) ^ b1(s, j)
   flag = 1: CALL UNSAT
 END IF
 nd(s, j - 1) = d(j - 1)
 k#(s, j - 1) = ks(s, j - 1) * (pe(s, j - 1)
/ p#(s, j - 1)) ^ n(s, j - 1)
 tsfl# = fl#: tbfl# = bfl#
 ter# = fl# * dt - sw# - bfl# * dt
```

```
'******** mass balance and updating water contents ******
FOR i = 1 TO m(g) + 3: w#(s, i) = wn#(s, i): NEXT i
ttler#(s) = ttler#(s) + er# + ter# + (tsfl# - botfl#) * dt
IF ep# = 0 THEN stor#(s) = stor#(s) - topfl# * dt
IF hour > 5 AND hour < 18 THEN CALL EVAPPIC
ttlit = ttlit + iit
ttlbf#(s) = ttlbf#(s) + tsfl# * dt
ttlaet#(s) = ttlaet#(s) + aet#(s) * dt
ttlpet#(s) = ttlpet#(s) + pet#(s) * dt
ttlevap#(s) = ttlevap#(s) + aet#(s) * dt
aet#(s) = 0#: pet#(s) = 0#
IF hour = 0 AND min = 0 THEN
  ttlaet#(s) = 0#: ttlpet#(s) = 0#
END IF
COLOR 14, 0: PRINT "Simulation Number"; s: COLOR 11, 0
PRINT " stor#  ="; : PRINT USING "##.#^^^^"; stor#(s)
PRINT " wn#(1) ="; : PRINT USING "##.#####"; wn#(s, 1)
PRINT " bdyfl  ="; : PRINT USING "##.#^^^^"; ttlbf#(s)
PRINT " error  ="; : PRINT USING "##.#^^^^"; ttler#(s)
PRINT " evap(m)="; : PRINT USING "##.##^^^^"; ttlevap#(s)
PRINT " et(day)="; : PRINT USING "##.##^^^^"; et(s, day) /
1000
NEXT s
VIEW PRINT
END SUB
```

```
'~~~~~~~~~~~~~~~~~~ OUTFILES Modules ~~~~~~~~~~~~~~~~~~~~~
SUB OUTFILES
SHARED day, hour, min, xsm(), ysm(), m(), sm(), nd(),
SHARED wn#(), ttler#(), ttlbf#(), ttlevap#(), sim
IF day = 230 AND hour = 12 AND min = 0 THEN
   OPEN "D:\MJB\PROFILE.DAT" FOR OUTPUT AS #1
   PRINT #1, "  x ="
   PRINT #1, "  y ="
   PRINT #1, " day ="
   PRINT #1, "hour ="
   PRINT #1, " min ="
   FOR i = 1 TO m(sm(1)) + 3
     PRINT #1, USING " ##.####"; nd(1, i)
   NEXT i
   PRINT #1, "error ="
   PRINT #1, "bdyfl ="
   PRINT #1, "ttlET ="
   CLOSE #1
 END IF
 IF day = 230 AND hour = 12 AND min = 0 THEN
   OPEN "D:\MJB\07840817.DAT" FOR OUTPUT AS #1
   PRINT #1, xsm(1): PRINT #1, ysm(1): PRINT #1, day
   PRINT #1, hour: PRINT #1, min
   FOR i = 1 TO m(sm(1)) + 3: PRINT #1, USING " ##.####";
    wn#(1, i): NEXT i
   PRINT #1, ttler#(1): PRINT #1, ttlbf#(1)
   PRINT #1, ttlevap#(1)
   CLOSE #1
 END IF
 IF day = 233 AND hour = 12 AND min = 30 THEN
   OPEN "D:\MJB\07840820.DAT" FOR OUTPUT AS #1
   PRINT #1, xsm(1): PRINT #1, ysm(1): PRINT #1, day
   PRINT #1, hour: PRINT #1, min
   FOR i = 1 TO m(sm(1)) + 3: PRINT #1, USING " ##.####";
    wn#(1, i): NEXT i
   PRINT #1, ttler#(1): PRINT #1, ttlbf#(1)
   PRINT #1, ttlevap#(1)
   CLOSE #1
 END IF
 IF day = 235 AND hour = 12 AND min = 0 THEN
   OPEN "D:\MJB\07840822.DAT" FOR OUTPUT AS #1
   PRINT #1, xsm(1): PRINT #1, ysm(1): PRINT #1, day
   PRINT #1, hour: PRINT #1, min
   FOR i = 1 TO m(sm(1)) + 3: PRINT #1, USING " ##.####";
      wn#(1, i): NEXT i
   PRINT #1, ttler#(1): PRINT #1, ttlbf#(1)
   PRINT #1, ttlevap#(1)
   CLOSE #1
 END IF
 IF day = 242 AND hour = 12 AND min = 0 THEN
   OPEN "D:\MJB\07840829.DAT" FOR OUTPUT AS #1
   PRINT #1, xsm(1): PRINT #1, ysm(1): PRINT #1, day
```

```
    PRINT #1, hour: PRINT #1, min
    FOR i = 1 TO m(sm(1)) + 3: PRINT #1, USING " ##.####";
       wn#(1, i): NEXT i
    PRINT #1, ttler#(1): PRINT #1, ttlbf#(1)
    PRINT #1, ttlevap#(1) : CLOSE #1
 END IF
END SUB
```

```
'~~~~~~~~~~~~~~~~~~ PRECIPitation Module ~~~~~~~~~~~~~~~~~~
SUB PRECIP
SHARED stor#(), dt, prec(), intensity, sim, day
FOR s = 1 TO sim
IF prec(s, day) <= intensity THEN
  stor#(s) = stor#(s) + prec(s, day) * .0254
  prec(s, day) = 0#
ELSE
  stor#(s) = stor#(s) + intensity * .0254
  prec(s, day) = prec(s, day) - intensity
END IF
NEXT s
END SUB
```

```
'~~~~~~~~~~~~~~~~~~ SETUP Module ~~~~~~~~~~~~~~~~~~~~~~~~
SUB SETUP
SHARED d(), k#(), p#(), v(), w#(), wn#(), pe(), soil(),
SHARED nd(), ang(), m(), dt, ks(), gr, ws(), b1(), n(),
SHAED b2(), n1(), depth(), s, g, stor#(), sim, xsm(),
SHARED ysm(), sm(), x(), y(), prec(), kd(), asp(), dg(),
SHARED sd(), cond(), por()
LOCATE 2, 7: PRINT "SETUP Module        "
dg(1) = 13.4: dg(2) = 3.89: dg(3) = 2.35
sd(1) = 4.57: sd(2) = 7.84: sd(3) = 28.6
cond(1) = .0000361: cond(2) = .0000288: cond(3) = .0000142
por(1) = .35: por(2) = .35: por(3) = .25
FOR s = 1 TO sim
  i = 0
  WHILE x(i) <> xsm(s) OR y(i) <> ysm(s): i = i + 1: WEND
  sm(s) = i
NEXT s
FOR s = 1 TO sim: g = sm(s): nd(s, 0) = 0
    nd(s, m(g) + 1) = d(m(g)) + 1
    nd(s, m(g) + 2) = d(m(g)) + 2
    nd(s, m(g) + 3) = d(m(g)) + 4
    nd(s, m(g) + 4) = d(m(g)) + 8
    FOR i = 1 TO m(g): nd(s, i) = d(i): NEXT i
    FOR i = 1 TO m(g)
      ws(s, i) = por(soil(g)): ks(s, i) = cond(soil(g))
      pe(s, i) = -.5 * dg(soil(g)) ^ (-.5)
      b1(s, i) = -2 * pe(s, i) + .2 * sd(soil(g))
      pe(s, i) = pe(s, i) / gr
      n(s, i) = 2 + 3 / b1(s, i): b2(s, i) = 1 / b1(s, i)
      n1(s, i) = 1 - n(s, i)
      w#(s, i) = .1#: wn#(s, i) = w#(s, i)
      v(s, i) = (nd(s, i + 1) - nd(s, i - 1)) / 2
    NEXT i
      k#(s, 0) = 0#: nd(s, 0) = -1E+20
      v(s, m(g) + 1) = (nd(s, m(g) + 2) - nd(s, m(g))) / 2
      v(s, m(g) + 2) =
          (nd(s, m(g) + 3) - nd(s, m(g) + 1)) / 2
      v(s, m(g) + 3) =
          (nd(s, m(g) + 4) - nd(s, m(g) + 2)) / 2
      p# = pe(s, m(g)) * (ws(s, m(g)) / w#(s, m(g)))
     ^ b1(s, m(g))
    FOR i = m(g) + 1 TO m(g) + 3
      ws(s, i) = .1: ks(s, i) = 5E-12: pe(s, i) = -14
      b1(s, i) = 3.76: b2(s, i) = 1 / b1(s, i)
      n(s, i) = 5.15: n1(s, i) = 1 - n(s, i)
      w#(s, i) = ws(s, i) * (p# / pe(s, i)) ^ -b2(s, i)
    IF w#(s, i) > ws(s, i) THEN w#(s, i) = ws(s, i) * .98
      wn#(s, i) = w#(s, i)
    NEXT i
    stor#(s) = 0#
CALL SIMSTAT
NEXT s
```

```
OPEN "D:\MJB\PREC.DAT" FOR INPUT AS #1
 WHILE NOT EOF(1)
  INPUT #1, day, rain: FOR s = 1 TO sim
  prec(s, day) = rain: NEXT s
 WEND
CLOSE #1
OPEN "D:\MJB\RAD.DAT" FOR INPUT AS #2
 WHILE NOT EOF(2)
  INPUT #2, day, rad: kd(day) = rad
 WEND
CLOSE #2
END SUB
```

```
'~~~~~~~~~~~~~~~~~~ SIMSTAT Module ~~~~~~~~~~~~~~~~~~~~~~~
SUB SIMSTAT
SHARED s, g, ang(), asp(), xsm(), ysm(), dg(), sd(),
SHARED soil(), b1(), n(), nd(), depth(), pe(), ws(), ks(),
SHARED m()
VIEW PRINT 3 TO 25
COLOR 14, 0: PRINT "      Simulation Grid Cell
Information"
COLOR 11, 0: PRINT "      simulation location no.    ="; s
PRINT "       grid cell number           ="; g
PRINT "       grid cell slope (degrees)  ="; ang(g)
PRINT "       grid cell aspect           ="; asp(g)
PRINT "       cell x-location (easting)  ="; xsm(s)
PRINT "       cell y-location (northing) ="; ysm(s)
COLOR 14, 0: PRINT "      Simulation Soil Information"
COLOR 12, 0: PRINT "                                 Layer 1
Layer 2"
COLOR 11, 0: PRINT "       mean diameter (mm)     ";
dg(soil(g))
PRINT "       geom. std. dev.      "; sd(soil(g))
PRINT "       sat.hydr.cond.(m/s) "; : PRINT USING "
##.##^^^^"; ks(s, 1); ks(s, m(g) + 1)
PRINT "       porosity             "; : PRINT USING "
##.###   "; ws(s, 1); ws(s, m(g) + 1)
PRINT "       air entry pot. (m)   "; : PRINT USING
"###.####  "; pe(s, 1); pe(s, m(g) + 1)
PRINT "       b1(s,i)              "; : PRINT USING
"###.####  "; b1(s, 1); b1(s, m(g) + 1)
PRINT "       n(s,i)               "; : PRINT USING
"###.####  "; n(s, 1); n(s, m(g) + 1)
PRINT "       soil depth (m)       "; : PRINT USING
"###.####  "; depth(g)
PRINT "       layer thickness (m) ";
PRINT USING "###.####  "; (nd(s, m(g)) + nd(s, m(g) + 1))
/ 2; ((nd(s, m(g) + 4) + nd(s, m(g) + 3)) / 2)
   - ((nd(s, m(g)) + nd(s, m(g) + 1)) / 2)
PRINT "       nd(s,m(g)) ="; nd(s, m(g)); "  :
nd(s,m(g)+1) ="; nd(s, m(g) + 1)
COLOR 14, 0: PRINT "      press PRINT SCREEN for hard
copy"
COLOR 15, 0: PRINT "      press any other key to continue"

DO: LOOP UNTIL INKEY$ <> ""
CLS 2
VIEW PRINT
END SUB
```

```
'~~~~~~~~~~~~~~~~~~ SOILS Module ~~~~~~~~~~~~~~~~~~~~~~~~~~
SUB SOILS
SHARED grids, soil(), depth(), x(), y(), ang(), d(), m()
LOCATE 2, 7: PRINT "SOILS Module       "
d(0) = 0: d(1) = 0: d(2) = .0125: d(3) = .025: d(4) = .05
d(5) = .1: d(6) = .25: d(7) = .5: d(8) = 1: d(9) = 1.5
d(10) = 2.25: d(11) = 3: d(12) = 4: d(13) = 5: d(14) = 6
d(15) = 8: d(16) = 10: d(17) = 12: d(18) = 16: d(19) = 20
d(20) = 24
OPEN "D:\MJB\SOIL1.DAT" FOR INPUT AS #1
WHILE NOT EOF(1)
  INPUT #1, a, b, c: g = 0
  WHILE x(g) <> a OR y(g) <> b: g = g + 1: WEND
  soil(g) = 1: depth(g) = c
WEND
CLOSE #1
OPEN "D:\MJB\SOIL2.DAT" FOR INPUT AS #2
WHILE NOT EOF(2)
  INPUT #2, a, b, c: g = 0
  WHILE x(g) <> a OR y(g) <> b: g = g + 1: WEND
  soil(g) = 2: depth(g) = c
WEND
CLOSE #2
FOR g = 1 TO grids
  IF soil(g) = 0 THEN
    soil(g) = 3
    SELECT CASE ang(g)
      CASE IS > 35: depth(g) = .1
      CASE IS < 5: depth(g) = 1!
      CASE ELSE: depth(g) = ((35 - ang(g)) / 30) * .9 + .1
      END SELECT
  END IF
NEXT g
FOR g = 1 TO grids
  i = 4
  WHILE d(i) < depth(g): i = i + 1: WEND
  m(g) = i
'  m(g) = 16: 'specifying desired depth
NEXT g
END SUB
```

```
'~~~~~~~~~~~~~~~~~~~ SURface FLoW Module ~~~~~~~~~~~~~~~~~~
SUB SURFLW
 '
 'Route surface flow
 '
END SUB
```

```
'~~~~~~~~~~~~~~~~~~ TOPO Module ~~~~~~~~~~~~~~~~~~~~~~~~~~
SUB TOPO
SHARED x(), y(), z(), dx, dy, xmax, xmin, ymax, ymin
SHARED ang(), asp(), grids, sim, xsm(), ysm()
VIEW (403, 49)-(638, 348), 8, 2
WINDOW (558000, 766000)-(569000, 780000)
COLOR 12, 0: PRINT "      TOPO Module         "
LOCATE 2, 52: PRINT "Pagany Wash Watershed"
LOCATE 3, 52: PRINT "(250 ft sq grid cells)"
OPEN "D:\MJB\PAGANY.XY" FOR INPUT AS #1
g = 0
WHILE NOT EOF(1)
  g = g + 1
  INPUT #1, a, b: x(g) = a: y(g) = b
  LINE (a - 125, b - 125)-(a + 125, b + 125), 11, B
WEND
grids = g
CLOSE #1
OPEN "D:\MJB\PAGANY.XYZ" FOR INPUT AS #2
WHILE NOT EOF(2)
     INPUT #2, a, b, c
     z((a - xmin) / dx, (b - ymin) / dy) = c
WEND
CLOSE #2
pi = 3.14159
FOR g = 1 TO grids
xx = (x(g) - xmin) / dx: yy = (y(g) - ymin) / dy
slopex = (z(xx + 1, yy) - z(xx - 1, yy)) / (2 * dx)
slopey = (z(xx, yy + 1) - z(xx, yy - 1)) / (2 * dy)
slope = SQR(slopex ^ 2 + slopey ^ 2)
 ang(g) = ATN(slope) * 180 / pi
     SELECT CASE slopex
      CASE 0
          IF slopey < 0 THEN asp(g) = 360
          IF slopey > 0 THEN asp(g) = 180
          IF slopey = 0 THEN asp(g) = 0
      CASE ELSE
          angle = ATN(ABS(slopey / slopex)) * 180 / pi
          IF slopex < 0 AND slopey = 0 THEN asp(g) = 90
          IF slopex > 0 AND slopey = 0 THEN asp(g) = 270
          IF slopex < 0 AND slopey < 0 THEN asp(g) = 90
                - angle
          IF slopex < 0 AND slopey > 0 THEN asp(g) = 90
                + angle
          IF slopex > 0 AND slopey > 0 THEN asp(g) = 270
                - angle
          IF slopex > 0 AND slopey < 0 THEN asp(g) = 270
                + angle
      END SELECT
IF ang(g) <= 10 THEN LINE (x(g) - 50, y(g) - 50)-(x(g) +
50, y(g) + 50), 14, BF
```

```
IF ang(g) > 10 AND ang(g) <= 20 THEN LINE (x(g) - 50, y(g)
- 50)-(x(g) + 50, y(g) + 50), 10, BF
IF ang(g) > 20 AND ang(g) <= 30 THEN LINE (x(g) - 50, y(g)
- 50)-(x(g) + 50, y(g) + 50), 12, BF
IF ang(g) > 30 THEN LINE (x(g) - 50, y(g) - 50)-(x(g) +
50, y(g) + 50), 4, BF
NEXT g
FOR s = 1 TO sim
  LINE (xsm(s) - 125, ysm(s) - 125)-(xsm(s) + 125, ysm(s)
+ 125), 1, B
NEXT s
COLOR 11, 0
LOCATE 19, 53: PRINT "Slope Angles"
LOCATE 20, 54: PRINT "<= 10 deg.s": LINE (558500,
769500)-(558600, 769600), 14, BF
LOCATE 21, 54: PRINT "> 10, <= 20": LINE (558500,
768850)-(558600, 768950), 10, BF
LOCATE 22, 54: PRINT "> 20, <= 30": LINE (558500,
768200)-(558600, 768300), 12, BF
LOCATE 23, 54: PRINT "> 30 deg.s ": LINE (558500,
767500)-(558600, 767600), 4, BF
COLOR 14, 0
LOCATE 3, 7: PRINT "press any key to continue"
LOCATE 4, 7: PRINT "(display will be erased)": COLOR 12, 0
DO: LOOP UNTIL INKEY$ <> ""
LOCATE 3, 7: PRINT "                              "
LOCATE 4, 7: PRINT "                              "
VIEW (403, 1)-(638, 349), 0, 0
END SUB
```

```
'~~~~~~~~~~~~~~~~~~ UNSATurated flow Module ~~~~~~~~~~~~~~~
SUB UNSAT
SHARED nd(), k#(), p#(), v(), w#(), wn#(), flux#, fl#,
SHARED bfl#, flmax#, m(), dt, ks(), pe(), gr, ws(), bl(),
SHARED n(), b2(), nl(), sw#, flag, a#(), b#(), c#(),
SHARED dp#(), f#(), iit, s, g, j, k, sim, sm(), d()
se# = 1
DO WHILE se# > 1E-16 :iit = iit + 1: se# = 0#
FOR i = j TO k
  k#(s, i) = ks(s, i) * (pe(s, i) / p#(s, i)) ^ n(s, i)
NEXT i
k#(s, k + 1) = ks(s, k) * (pe(s, k) / p#(s, k + 1))^n(s,k)
'============== Matric Manipulation ======================
FOR i = j TO k
  a#(i) = -k#(s, i - 1) / (nd(s, i) - nd(s, i - 1))
+ n(s, (i - 1)) * k#(s, i - 1) / p#(s, i - 1)
  c#(i) = -k#(s, (i + 1)) / (nd(s, i + 1) - nd(s, i))
  b#(i) = k#(s, i) / (nd(s, i) - nd(s, i - 1)) + k#(s, i)
/ (nd(s, i + 1) - nd(s, i)) - n(s, i) * k#(s, i)
/ p#(s, i) - v(s, i) * wn#(s, i) / (bl(s, i)
* p#(s, i) * dt)
  f#(i) = ((p#(s, i) * k#(s, i) - p#(s, (i - 1))
* k#(s, (i - 1))) / (nd(s, i) - nd(s, i - 1))
- (p#(s, (i + 1)) * k#(s, (i + 1)) - p#(s, i)
* k#(s, i)) / (nd(s, i + 1) - nd(s, i))) / nl(s, i)
+ v(s, i) * (wn#(s, i) - w#(s, i)) / dt - k#(s, (i - 1))
+ k#(s, i)
  IF i = j AND flag = 0 THEN f#(i) = f#(i) - flux#
  IF i > j AND flag = 1 THEN se# = se# + ABS(f#(i))
  IF flag = 0 THEN se# = se# + ABS(f#(i))
NEXT i
IF flag = 1 THEN f#(j) = 0#: IF flag = 1 THEN c#(j) = 0#
'============== Thomas Algorithm ==========================
FOR i = j TO k - 1
  c#(i) = c#(i) / b#(i): f#(i) = f#(i) / b#(i)
  b#(i + 1) = b#(i + 1) - a#(i + 1) * c#(i)
  f#(i + 1) = f#(i + 1) - a#(i + 1) * f#(i)
NEXT i
 dp#(k) = f#(k) / b#(k)
 p#(s, k) = p#(s, k) - dp#(k): IF p#(s, k) > pe(s, k) THEN
       p#(s, k) = pe(s, k)
FOR i = (k - 1) TO j STEP -1
  dp#(i) = f#(i) - c#(i) * dp#(i + 1)
  p#(s, i) = p#(s, i) - dp#(i)
  IF p#(s, i) > pe(s, i) THEN p#(s, i) = (p#(s, i) +
dp#(i) + pe(s, i)) / 2
NEXT i
'============== Water Content at End of Time Step ========
FOR i = j TO k
  wn#(s, i) = ws(s, i) * (pe(s, i) / p#(s, i)) ^ b2(s, i)
NEXT i
```

```
'============== Check Convergence ========================
LOOP
fl# = (p#(s, j) * k#(s, j) - p#(s, j + 1) * k#(s, j + 1))
      / ((nd(s, j + 1) - nd(s, j)) * n1(s, j)) + k#(s, j)
      + (wn#(s, j) - w#(s, j)) * v(s, j) / dt
bfl# = (p#(s, k) * k#(s, k) - p#(s, k + 1) * k#(s, k + 1))
      / ((nd(s, k + 1) - nd(s, k)) * n1(s, k)) + k#(s, k)
sw# = 0#
FOR i = j TO k
  sw# = sw# + v(s, i) * (wn#(s, i) - w#(s, i))
NEXT i
END SUB
```

APPENDIX C
List of variables for QBINFIL

LIST OF VARIABLES

Variable	Description	Units
a	input loading variable	-
a#(i)	subdiagonal matrix variable	s^{-1}
ang(g)	grid cell slope	degrees
asp(g)	grid cell aspect	degrees
at#	daily air temperature	°C
b	input loading variable	-
b#(i)	central-diagonal matrix variable	s^{-1}
b1(s,i)	moisture release curve power	-
b2(s,i)	1 - b1(s,i)	-
bfl#	flow out of bottom of upper layer	m/s
BOTITRN	Module for matching flows between layers	-
c	input loading variable	-
c#(i)	superdiagonal matrix variable	s^{-1}
cond(3)	saturated hydraulic conductivity for one of the 3 soil types	m/s
contact	display feature for drawing tuff-alluvium contact line on the screen	-
clock$	time display output format string	-
d(i)	node i placement depth	m
day	julian day number (1 - 366)	-
depth(g)	actual depth for grid cell g based on input file or calculated value	m
dg(3)	mean particle diameter size for one of the three soil types possible	m
dj#(0)	actual ET flux derivative at the surface	s^{-1}
dj#(i)	vapor flux derivative at node i	s^{-1}
dp#(i)	change in potential for node i	m
dx	grid cell spacing in x-direction (easting)	ft

dy	grid cell spacing in y-direction (northing)	ft
dt	model time step	s
dv	vapor diffusivity in soil	m^2/s
eit	evaporation iteration number count variable	-
ep#	time step potential ET	m/s
er#	total mass balance error within the upper soil layer	m
et(s,day)	daily total ET for simulation location s	mm
ev#	variable for summation of ET	m/s
EVAP	module for ET processes	-
EVAPPIC	module for ET screen display	-
f#(i)	node mass balance variable	m/s
fl#	actual calculated flux at the top of a soil layer	m/s
flag	variable for setting conditions for surface boundary conditions	-
flmax#	maximum calculated allowable flux for top of a soil layer using a reduced porosity	m/s
flux#	maximum possible flux for top of a soil based on surface storage	m/s
g	grid cell number (1 to 477)	-
gr	gravitation constant of acceleration	m/s
GRAPH	module for soil moisture and surface water storage screen display	-
grids	variable to count total number of grids during file data loading	-
h#(i)	relative humidity at a node	-
hour	hour of the day	
i	variable to represent node element	-

iit	iteration count variable for UNSAT module	-
INFIL	module to link surface and unsaturated flow processes for each grid cell	-
intensity	selected maximum precipitation per time step	in
j	node variable to represent top node element	-
jv#(0)	actual ET surface flux	m/s
jv#(i)	vapor flux at each node	m/s
k	node variable to represent bottom node element of a soil layer	-
k#(s,i)	hydraulic conductivity for simulation location s at node i	m/s
kd(day)	daily flat plate solar radiation	MJ/m^2
ks(s,i)	saturated hydraulic conductivity for simulation location s at node i	m/s
kv	soil vapor conductivity	m/s
m(g)	bottom node element number for upper soil layer at grid cell g	-
maxx	maximum number of nodes in the x-direction for the .XYZ file	-
maxy	maximum number of nodes in the y-direction for the .XYZ file	-
min	simulation minutes	minutes
mw	mass of a mole of water	J/mol.K
n(s,i)	hydraulic conductivity exponent	-
n1(s,i)	1 - n(s,i)	-
nd(s,i)	node depth at simulation location s for node i	m
p#	node boundary potential variable	m
p#(s,i)	matrix potential at simulation location s for node i	m

pe#(s,i)	air entry potential at simulation location s for node i	m
por(3)	porosity for one of the 3 soil types	m^3/m^3
prec(s,day)	precipitation at node location s for a given day	in
PRECIP	module to release precipitation	-
r	universal gas constant	J/mol.K
rc#	solar radiation corrected for slope and aspect	MJ/m^2
rad	input variable for loading flat plate solar radiation	MJ/m^2
rain	input variable for loading daily precipitation	in
rn#	net solar radiation	MJ/m^2
s	simulation location variable	-
sc#	multiplication scale factor for porosity in maximum surface flux calculations	-
sd(3)	geometric standard deviation for one of the three soil types	%
se#	soil layer iteration mass balance error	m/s
SETUP	module that specifies layer parameters and initial conditions	-
sim	number of grid cell locations to simulate	-
slope	grid cell slope variable	decimal
slopex	grid cell x-slope component	decimal
slopey	grid cell y-slope component	decimal
sm(s)	grid cell number of simulation location s	-
soil(g)	soil type for grid cell g	-

SOILS	module to specify depth parameters for grid cells	-
ssg#	s/s+gamma term for ET calculations	-
stor#(s)	surface water storage for simulation location s	m
sw#	change in water storage in a soil profile	m
t	soil temperature	°K
tbfl#	flow out of the bottom of the lower soil layer	m/s
ter#	total mass balance error within the lower soil layer	m
theta	relative water content for reduction of potential ET	-
tol#	allowable error per time step	m
topfl#	flow variable for reducing surface water storage	m/s
totalbf#(s)	total flow across boundary between the two soil layers	m
totevap#(s)	total simulation actual ET loss for simulation location s	m
totalerr#(s)	total mass balance error for simulation location s	m
totalit	total number of iterations in the UNSAT module for a simulation location during a time step	-
tsfl#	flux across the top of the lower soil layer	m/s
UNSAT	module to solve iteration process for unsaturated flow	-
v(s,i)	thickness at simulation location s for node element i	m
vp	saturation vapor concentration in air	g/m^3

w#(s,i)	initial volumetric water content at simulation location s for node i at beginning of time step	m^3/m^3
w1#	water content variable in BOTITRN	m^3/m^3
water	display variable for surface water storage	-
wmx#	maximum surface element water content for maximum flow calculations	m^3/m^3
wn#(s,i)	ending volumetric water content at simulation location s for node i at end of the time step	m^3/m^3
wold#(s,i)	variable for displaying previous time step moisture profile	m^3/m^3
wr	relative water content for ET surface reduction	m^3/m^3
ws(s,i)	soil porosity at simulation location s for node i	m^3/m^3
x(g)	x-coordinate of center of grid cell g (easting coordinate)	ft
xmax	maximum easting for .XYZ file	ft
xmin	minimum easting for .XYZ file	ft
xsm(s)	x-coordinate for simulation grid cell (easting coordinate)	ft
xx	x-node location variable	-
y(g)	y-coordinate for center of grid cell g (northing coordinate)	ft
ymax	maximum northing for .XYZ file	ft
ymin	minimum northing for .XYZ file	ft
ysm(s)	y-coordinate for simulation grid cell (northing coordinate)	ft
yy	y-node location variable	-
z(42,55)	elevation for rectangular node network from .XYZ file	ft